FLUID TRANSPORT AND ITS REGULATION BY CYCLIC 3′,5′-ADENOSINE MONOPHOSPHATE IN THE PORCINE CILIARY BODY EPITHELIUM

LAW CHEUNG SING

Ph.D

The Hong Kong Polytechnic University

2010

The Hong Kong Polytechnic University

School of Optometry

Fluid Transport and Its Regulation by Cyclic 3′,5′-Adenosine Monophosphate in the Porcine Ciliary Body Epithelium

Law Cheung Sing

A thesis submitted in partial fulfilment of the requirements for the degree of Doctor of Philosophy

December 2009

CERTIFICATE OF ORIGINALITY

I hereby declare that this thesis is my own work and that, to the best of my knowledge and belief, it reproduces no material previously published or written, nor material that has been accepted for the award of any other degree or diploma, except where due acknowledgement has been made in the text.

_____

Law Cheung Sing

Abstract

Glaucoma is the leading cause of irreversible blindness worldwide, frequently associated with elevated intraocular pressure (IOP). Currently, there is no cure for the disease, although its progression can be retarded by pharmacological reduction of IOP. Reducing IOP is the only medical treatment documented effective in delaying the onset and retarding the progression of visual loss. Anti-glaucoma drugs function to lower IOP by reducing the production of aqueous humour (AH). However, the transport mechanisms underlying AH formation are not yet fully understood, although many transporters are identified in the ciliary epithelium. Moreover, its regulation is of crucial importance for the development of novel pharmacological treatment of glaucoma.

In the present study, a modified Ussing-type fluid chamber for the simultaneous measurement of both fluid flow (FF) and electrical parameters across the whole annulus of porcine ciliary body epithelium (CBE) preparation has been constructed. The porcine CBE preparation transported fluid in the blood-to-aqueous direction at an average rate of ~2.75 µL/h per preparation. The standing transepithelial potential difference (PD) declined gradually, but subsisted for at least 4 hours. The aqueous-negative PD indicated a net anion transport across the CBE from blood to aqueous. The *in vitro* FF was largely dependent on Cl^- and HCO_3^-, to a lesser extent, indicating that the fluid movement was primarily driven by the transepithelial anion secretion across the preparation. Blocking Na^+,K^+-ATPase with ouabain remarkably reduced the FF (stromal ouabain nearly abolished the FF) and elicited a typical biphasic response across the CBE preparation, suggesting the fluid movement was active and derived from the Na^+,K^+-ATPase activity.

The effects of several Cl^- transport inhibitors on the FF rate and PD were examined. Blocking Cl^-/HCO_3^- and Na^+/H^+ antiporters with 4,4′-diisothiocyanatostilbene-2,2′-disulfonic acid (DIDS, 0.1 mM) and 5-(N,N-dimethyl)amiloride hydrochloride (DMA, 0.1 mM) applied on the stromal side respectively did not cause significant effects in both FF and PD across the CBE. However, the blockade of Na^+-K^+-$2Cl^-$ cotransporter with stromal bumetanide (0.1 mM) reduced the FF by 46%, and induced a slight depolarisation of PD, suggesting that Na^+-K^+-$2Cl^-$ cotransporter was the predominant Cl^- uptake pathway into the pigmented epithelium (PE), while the paired were less important. Heptanol, a blocker of gap junction, virtually abolished the PD and largely reduced the FF by nearly 80%, indicating that the FF was primarily driven by the transcellular Cl^- transport. The Cl^- channel blocker niflumic acid (1 mM), applied on aqueous-side bath, abolished the PD and markedly reduced the FF by 61%, suggesting that the Cl^- release by the non-pigmented epithelium (NPE) was mediated through niflumic acid-sensitive Cl^- channels.

In addition, the potential regulation of AH formation by the second messenger cyclic 3′,5′-adenosine monophosphate (cAMP) were investigated. Aqueous application of forskolin (10 μM) and 8-Br-cAMP (100 μM) elicited a tremendous hyperpolarisation of PD by 100% and 171% respectively, and a concomitant increase in FF by 42% and 54% respectively, suggesting that cAMP was able to modulate the *in vitro* ion and fluid transport. Aqueous application of 3-isobutyl-1-methylxanthine (IBMX, 1 mM) induced a slight hyperpolarisation of PD by 22%, but did not cause significant change in FF. The pre-treatment of protein kinase A (PKA) inhibitor H-89 (50 μM) effectively blocked the cAMP stimulated PD and FF by 65% and 52% respectively, implying that PKA activation was

essential, at least in part, for the cAMP-induced stimulation of ion and fluid transport.

These results support a major role of net Cl^- transport as the driving force for fluid formation across the ciliary epithelium. cAMP can stimulate the AH formation mainly via a PKA pathway.

Publications arising from the thesis

Publications:

Law, C. S., Candia, O. A. and To, C. H. (2009). Inhibitions of chloride transport and gap junction reduce fluid flow across the whole porcine ciliary epithelium. *Invest Ophthalmol Vis Sci* 50(3): 1299-306.

Candia, O. A., To, C. H. and Law, C. S. (2007). Fluid transport across the isolated porcine ciliary epithelium. *Invest Ophthalmol Vis Sci* 48(1): 321-7.

Presentation:

Law, C. S., Candia, O. A. and To, C. H. (2006). Transepithelial fluid transport and potential difference across porcine ciliary epithelium. *XVII International Congress of Eye Research*, Buenos Aires, Argentina. Nov 2006.

Abstracts:

Law, C. S., Candia, O. A. and To C. H. (2010). Cyclic 3′,5′-Adenosine Monophosphate Transiently Stimulates the *in vitro* Fluid Transport Across the Isolated Porcine Ciliary Body Epithelium via Protein Kinase A. *Invest Ophthalmol Vis Sci* 51: E-Abstract 161.

Law, C. S., Candia, O. A. and To C. H. (2006). Simultaneous Measurement of Fluid Transport and Transepithelial Potential Difference in Porcine Iris–Ciliary Body: Effects of Chloride Substitution and Ouabain**.** *Invest Ophthalmol Vis Sci* 47: E-Abstract 222.

Law, C., Chan, C. Y., Candia, O. A. and To, C. H. (2005). Fluid Transport Across Porcine Ciliary Body Epithelium. *Invest Ophthalmol Vis Sci* 46: E-Abstract 3682.

Acknowledgements

I would like to express my sincere thanks to Professor Chi-ho To, my supervisor, for his guidance and suggestions to my research study. He always shows his great enthusiasm and emphasises the significance of the present study in the field of transport physiology that has led me to the completion of my thesis. I would also like to thank Professor Oscar Candia, the collaborator of this project, for his generous provision of the chambers and his valuable comments on the study and critical review of the manuscripts.

I am grateful to the School of Optometry of The Hong Kong Polytechnic University for providing resourceful facilities in supporting the current study, particularly to the availability of a laboratory set up in Sheung Shui that makes this work possible. I would also like to express my gratitude to the research team members of the laboratory for their support and encouragement. They have also brought me plenty of warmth and fun that have brightened up my research life.

Most importantly, I have to express my heartfelt thank to Karen Shek, my wife and friend, for her care, patience, understanding and support throughout the period of my study. Lastly, I would like to thank my parents for their long-standing love and care. They would be so proud to see the completion of my doctoral thesis.

Law Cheung Sing

"The fear of the LORD is the beginning of wisdom, and

knowledge of the Holy One is understanding."

Proverbs 9:10

"If we become increasingly humble about how little we know,

we may be more eager to search."

Sir John Templeton

Table of Contents

List of figures

List of tables

List of abbreviations

8-Br-cAMP	8-bromoadenosine 3′,5′-cyclic monophosphate
AC	Adenylate cyclase
ADP	Adenosine 5′-diphosphate
AE	Cl^-/HCO_3^- anion exchanger
AH	Aqueous humour
AR	Adenosine receptor
ATP	Adenosine 5′-triphosphate
CA	Carbonic anhydrase
cAMP	Cyclic 3′,5′-adenosine monophosphate
CBE	Ciliary body epithelium
CE	Ciliary epithelium
cGMP	Cyclic 3′,5′-guanosine monophosphate
Cx	Connexin
DIDS	4,4′-diisothiocyanatostilbene-2,2′-disulfonic acid
DMA	5-(N,N-dimethyl)amiloride
DMSO	Dimethyl sulfoxide
Epac	Exchange protein directly activated by cAMP
ET	Endothelin
FC1/2	Fluid chamber configuration 1/2
FF	Fluid flow
HRP	Horseradish peroxidase
IBMX	3-isobutyl-1-methylxanthine
ICB	Iris-ciliary body
IOP	Intraocular pressure
I_{sc}	Short-circuit current
NHE	Na^+/H^+ exchanger
NO	Nitric oxide
NOS	Nitric oxide synthase

NPE	Non-pigmented epithelium
NPPB	5-Nitro-2-(3-phenylpropylamino)-benzoic acid
PD	Potential difference
PE	Pigmented epithelium
pH_i	Intracellular pH
PKA	Protein kinase A or cAMP-dependent protein kinase
PKC	Protein kinase C
PKG	Protein kinase G
R_t	Tissue resistance
RT-PCR	Reverse transcriptase polymerase chain reaction
sGC	Soluable guanylate cyclase
TM	Trabecular meshwork
TNF-α	Tumour necrosis factor-alpha
VIP	Vasoactive intestinal peptide

CHAPTER 1

INTRODUCTION

1.1 Background

Glaucoma is the leading cause of irreversible blindness worldwide (Quigley, 1996). It is frequently associated with elevated intraocular pressure (IOP) of the eye, typically attributed to increased resistance to the drainage of aqueous humour from the eye (Brubaker, 1998). Glaucoma is sometimes referred to "silent blinder" because no noticeable symptoms are detected in its early stage (Coleman, 1999). People are unaware that they have the disease until substantial visual loss has occurred, in which the visual impairment is irreversible. Currently, there is no cure for the disease, although its progression can be retarded by pharmacological reduction of IOP. Reducing IOP is the only medical treatment documented effective in delaying the onset and retarding the progression of visual loss (Collaborative Normal-Tension Glaucoma Study Group, 1998b; Collaborative Normal-Tension Glaucoma Study Group, 1998a; The AIGS Investigators, 2000).

IOP is the measure of the dynamic balance between the secretion (inflow) and the drainage (outflow) of aqueous humour (AH). AH is a transparent fluid circulating inside the eye. It is continuously secreted by the ciliary epithelium lining on the ciliary body into the posterior chamber, then flows through the pupil into the anterior chamber. It drains away from the anterior chamber mainly through the trabecular meshwork (TM) in the anterior angle, and to a lesser extent, through the uveoscleral outflow pathway. The circulation of AH inside the anterior segment of the eye provides several important functions (Krupin and Civan, 1996; Civan, 1998):

1. inflation of the eyeball and bathing the tissues inside the eye, maintaining structural and optical integrity for normal functioning of the eye;
2. transport of the substrates to, and removal of the metabolic wastes from, the avascular tissues inside the anterior segment (cornea, crystalline lens, and TM);
3. transport of ascorbate at high concentration to the anterior segment to provide antioxidant and free radical scavenging functions; and
4. involvement of the local immune responses during inflammation and infection.

The anti-glaucoma drugs function to lower IOP by either reducing the inflow or enhancing the outflow. There are a number of classes of anti-glaucoma drugs available, yet their hypotensive efficacies are varied to different patients. Moreover, “fading of reported effectiveness” of several drugs has been documented (Gehr et al., 2006). A single drug may fail to accomplish sufficient IOP reduction that a combination of drugs may be required. The frequency of dosing and multiple drug administration increase the complexity and hence reduce patient compliance and persistence (Schwartz, 2005). Furthermore, diverse local and systemic side effects are induced by these regimens (Marquis and Whitson, 2005) that reduce patient compliance. These limitations point to the inadequacy of the current anti-glaucoma drugs and the need for development of novel and more potent medications.

1.2 Structures of ciliary body

The ciliary body forms an annulus along the inner border of the globe, and its cross section is triangular in shape. It is anatomically divided into two regions: the anterior pars plicata, which is ridged or plicated and forms radially arrayed processes called ciliary processes; and the posterior pars plana, which is smooth and flat in appearance. The ciliary body is consisted of three major components: a capillary core, a loose stroma, and a bilayered ciliary epithelium. The capillaries of the ciliary processes are fenestrated, which allow macromolecules to transverse rapidly into the loose ciliary stromal tissues. However, the passage of the macromolecules horseradish peroxidase (HRP) into the posterior chamber is blocked by the ciliary epithelium (Smith and Rudt, 1973; Raviola, 1974). Thus the ciliary epithelium contributes to a selective barrier between the ciliary stroma and the AH.

The ciliary epithelium is consisted of an outer pigmented epithelium (PE) and an inner non-pigmented epithelium (NPE). Anatomically, the PE is the anterior continuation of the retinal pigmented epithelium; whereas the NPE is the anterior continuation of the neural layer of the retina. Basal infolding and lateral interdigitation of the plasma membrane are prominent in both the PE and NPE cells (Smith, 1973), which are distinctive features of secretory epithelia. The basolateral membrane of the PE cell layer faces the ciliary stroma, and that of the NPE cell layer faces the posterior chamber of the eye, while the apices of the two cell layers are connected by gap junctions, such that the epithelium is a functional syncytium (Raviola and Raviola, 1978).

1.2.1 Tight junctions

In the ciliary epithelium, tight junctions are localized only on the lateral surface of the NPE cells near the apical regions (Raviola and Raviola, 1978). As in other epithelia, tight junctions encircle the cells at the apical end of the lateral membrane which separate the apical and basolateral surfaces (Dragsten et al., 1981). Tight junctions serve two major functions (Balda and Matter, 1998):

1. a paracellular gate or barrier, which is semi-permeable and regulates the passive diffusion of ions and solutes through intercellular space; and
2. a junctional fence, which maintains the asymmetric distribution of plasma membrane domains on apical and basolateral membranes.

These two functions are important as the formation of diffusion barrier allows the generation and maintenance of compartments with different compositions, and hence cell polarity, for the physiological functioning of secretory epithelia. The paracellular gate function of the tight junctions constitutes to a major component of the blood-aqueous barrier (Cunha-Vaz, 1979). The intact blood-aqueous barrier function is reflected in the low concentration of plasma protein in the AH.

Tight junctional functions are usually analysed by measuring the transepithelial electrical resistance of the epithelium or monitoring the radiolabelled flux of inert solutes such as mannitol and dextran (Madara, 1998). The transmural resistance of ciliary epithelium in different animals are usually low, a value less than 200 Ωcm^2. (Holland and Gipson, 1970; Watanabe and Saito, 1978; Saito and Watanabe, 1979; Kishida et al., 1981; Burstein et al., 1984a; Iizuka et al., 1984; Krupin et al., 1984; Chu et al., 1987; Wiederholt and Zadunaisky, 1987; Do and To, 2000; Wu et al., 2003a; Kong et al., 2006) However, the normalized resistance was calculated according to the area of the chamber cavity, which neglected the highly

convoluted area of the ciliary processes. Correcting for the estimated convoluted area of the ciliary epithelium, the calculated resistance of the flattened epithelium can be up to 1 $k\Omega cm^2$ (Burstein et al., 1984a; Krupin et al., 1984). Furthermore, the measured mannitol flux across the rabbit iris-ciliary body (Chu and Candia, 1987) was comparable to that measured in "tight" epithelia (Dawson, 1977).

In addition to the functions as paracellular gate and junctional fence, tight junctions are considered to involve in the regulation of cell growth and differentiation (Balda and Matter, 1998). Recent observations supported that the multicomponent, multifunctional complex of tight junction may be involved in regulating diverse processes such as cell proliferation, cell polarity, gene transcription and tumour suppression (Schneeberger and Lynch, 2004). Moreover, it is now believed that tight junctions can be regulated by various signalling pathways, including protein kinase C, protein kinase A, myosin light chain kinase, mitogen-activated protein kinases, phosphoinositide 3-kinase and Rho signalling pathways (Gonzalez-Mariscal et al., 2008).

1.2.2 Gap junctions

Gap junctions connect the cells within PE and NPE, and between the two epithelial layers, which provide intercellular communication between the cells within and between the two layers (Raviola and Raviola, 1978). The functional expressions of gap junctions have been demonstrated by dye coupling (Edelman et al., 1994; Oh et al., 1994; Stelling and Jacob, 1997), electrical coupling (Green et al., 1985; Wiederholt and Zadunaisky, 1986; Carre et al., 1992), and similar intracellular ionic contents (Bowler et al., 1996). A recent study has identified the molecular profile of gap junctions that connexin isoforms Cx40 and Cx43 are localized to the PE-NPE interface whereas Cx26 and Cx31 are found between the NPE cells of rat ciliary epithelium (Coffey et al., 2002). The identity of connexins between the PE cells remains unclear. The existence of gap junctions and hence intercellular communication, suggests that the ciliary epithelial layers function as a syncytium. The functional importance of gap junction in ionic transport will be discussed in more detail in the later section.

1.3 Compositions of aqueous humour

1.3.1 Ionic compositions

It is well-recognized that AH is not a simple ultrafiltrate of the blood plasma (Bill, 1975; Krupin and Civan, 1996; To et al., 2002). The concentrations of various ions in the AH are significantly different from that in the blood plasma. For example, rabbit, cat and guinea pig exhibit an excess of HCO_3^- and a deficit of Cl^- in AH comparing to blood plasma, while the converse occurs in the AH of horse, monkey and humans (Davson and Luck, 1956). This dissimilarity is reflected in the pH of AH, which is alkaline in rabbit, but acidic in human relative to blood pH (Krupin and Civan, 1996). A recent study also demonstrated the Cl^- concentration of AH is higher than in blood plasma in ox, pig and sheep, but not in rabbit (Gerometta et al., 2005). These observations imply that there exists active transport of Cl^- from blood stream into the posterior chamber across the human ciliary epithelium, a HCO_3^- transport in the opposite direction, or both. The higher Cl^- concentration of AH in ox, pig, and sheep has supported the use of their isolated ciliary epithelium for the study of AH formation in human, owing to their similarity in ionic composition in AH and hence the transport mechanism across the ciliary epithelium. A more detail ionic transport mechanisms will be discussed in the later sections.

1.3.2 Ascorbic acid

The concentration of ascorbic acid is remarkably higher in AH than in blood plasma. The ascorbic acid level in AH is about 50- to 70-folds higher than that in blood plasma in rabbit and monkey (Davson, 1969; Gaasterland et al., 1979). Moreover, the ascorbic acid levels are substantially high in AH of many other species (Reiss et al., 1986). It is apparent that the high concentration of ascorbic acid is attributed to the active transport processes of ciliary epithelium as demonstrated in rabbit (Chu and Candia, 1988; Mead et al., 1996) and ox (To et al., 1998b).

The high concentration of ascorbic acid in AH is a primary antioxidant in ocular protection from oxidative damage (Rose et al., 1998). The protective function of ascorbic acid is strongly associated with the cataract formation of the crystalline lens. Lens damage and cataract formation appear to be related to the generation of free radicals and other active oxygen species. The abundance of ascorbic acid serves as an antioxidant and free radical scavenger to protect against the oxidative damages in the lens (Varma et al., 1984; Varma et al., 1986; Varma and Richards, 1988). Another function of ascorbic acid is the protection of intraocular structures against ultraviolet (UV) radiation. Spectrophotometry and spectrofluorimetry of bovine AH has revealed that ascorbate contributes to the UV-filtering action in AH, and played a protective role against UV radiation through three mechanisms: absorption, fluorescence quenching and wavelength transformation (Ringvold, 1995; Ringvold, 1996). Ascorbate is dispersed to other anterior ocular tissues by the AH flow. The similar concentration of ascorbate exists in the corneal stroma, corneal endothelium and AH suggested that AH flow aids in the delivery of ascorbate to the anterior inner ocular surfaces (Ringvold et al., 2000). Above all, ascorbic acid has contributed to ~80% of the antioxidant activity of the porcine and bovine AH (Erb et al., 2004).

1.3.3 Proteins

In contrast to high ascorbic acid level in AH, there is extremely low protein content in AH compared to blood plasma. The protein concentration in human AH ranges from 50 to 150 mg/l, whereas that in blood plasma ranges from 60 to 70 g/l (Davson, 1990). Though variation is observed among species, the protein concentration is generally less than 1% compares to that found in blood plasma (Davson, 1990). The extremely low protein content in AH reflects the integrity of the blood- aqueous barrier. It is obvious that trace amount of AH proteins is essential for maintaining optical clarity and prevent light scattering for normal visual functions. Although the protein concentration is very low in AH, all the plasma proteins are present in the AH (Davson, 1990), which suggests that AH proteins are primarily derived from the blood plasma.

Recently, a pathway for plasma protein diffusion via the anterior surface has been proposed (Freddo, 2001; Bert et al., 2006). It has been demonstrated that plasma proteins are diffused from the ciliary capillaries via the iris into the anterior chamber AH, bypassing the posterior chamber in rabbit and monkey by a combination of examinations, including *in vivo* aqueous fluorophotometric, morphology and tracer localization, and computational modelling (Freddo et al., 1990; Barsotti et al., 1992). This protein pathway has been confirmed in rabbit using high resolution, contrast- enhanced, magnetic resonance imaging (Kolodny et al., 1996), that the contrast intensity only appears in the anterior chamber but not in the posterior chamber, indicating that the tracer enters the anterior chamber directly via the iris root. Similar study has conducted in normal human volunteers, confirming the existence of the anterior diffusional pathway of proteins (Bert et al., 2006).

1.4 Mechanisms of aqueous humour formation

Fundamentally, the secretion of AH across the ciliary body involves four steps (Bill, 1975):

1. Blood flows through the microvasculature within the ciliary stroma.
2. An ultrafiltrate is derived from the blood plasma via the fenestrated capillaries into the interstitial space of the ciliary stroma.
3. Solutes in the ultrafiltrate are selectively transported across the ciliary epithelium from the stroma into the posterior chamber.
4. The osmotic gradient created by the solute transferred across the CE drives the passive flow of fluid.

The transport of solutes across the ciliary epithelium is of vital importance in the AH secretion, which can be mediated by three basic mechanisms:

1. diffusion - the passive movement of solutes down the electrochemical gradient across the plasma membrane;
2. ultrafiltration - the passive movement of water and water soluble substances across the plasma membrane under the influence of the differential hydrostatic pressure in the blood and osmotic pressure of the ciliary body; and
3. active secretion - the energy-dependent movement of solutes across the plasma membrane.

In the AH, the concentration of several solutes (such as ascorbate) is remarkably higher than predicted from the equilibrium distribution with the blood plasma, indicating that additional mechanisms are required to drive AH formation (Davson, 1990; Krupin and Civan, 1996).

Ultrafiltration was initially considered to account for a major proportion (~80%) of AH secretion, according to the high hydraulic conductivity of the ciliary processes (Green and Pederson, 1972). However, it was later revealed that the differential hydrostatic pressure was lower than the opposing pressure attributed to oncotic pressure and IOP, indicating that the resulting hydrostatic force virtually favoured reabsorption rather than secretion of AH (Bill, 1973). Moreover, experimental variation of the systemic arterial blood pressure to ~25% lower than its physiological level had little effect on AH formation (Reitsamer and Kiel, 2003). These observations suggested that ultrafiltration has minor effect on the secretion of AH. Furthermore, subsequent studies have demonstrated the secretion of AH can be inhibited by metabolic inhibitors (Becker, 1963; Becker, 1980; Kodama et al., 1985; Shahidullah et al., 2003), hypothermia (Becker, 1960; Cole, 1969), and anoxia (Watanabe and Saito, 1978; Krupin et al., 1984; Chu and Candia, 1988). These findings indicate that the AH secretion must involve active transport process.

The current consensus view of the AH inflow comprises the active transport of solutes, primarily Na^+ and Cl^- across the ciliary epithelium, which drives the fluid flow from stroma into posterior chamber. Recent studies have demonstrated a diffusional pathway of protein from the ciliary stroma directly into the anterior chamber via the iris root (Freddo, 2001; Bert et al., 2006). However, its relative contribution to the AH secretion is still unclear. In addition to its function in secreting AH, the ciliary epithelium has recently been demonstrated to constitute a neuroendocrine system producing peptides that influence both the inflow and outflow of AH in different ways (Coca-Prados and Escribano, 2007).

1.5 Electrophysiology of isolated ciliary epithelium

Transepithelial electrophysiology is the study of the electrical activities across the epithelium, which reflects the ionic transport processes within the epithelium. This concept was first developed by Ussing (Ussing and Zerahn, 1951), who invented a chamber for mounting a frog skin and studied the transepithelial Na^+ flux and electrical parameters across the epithelium under short-circuit condition. This seminal technique was later adopted by Cole (Cole, 1961; Cole, 1962) to study the ion transport activities across the ciliary epithelia .

In brief, the Ussing chamber technique can be conducted by mounting an excised iris-ciliary body between two hemichambers, so that the preparation is bathed with identical physiological Ringer's solution on its two surfaces. By connecting electrodes into the two hemichambers, a number of electrical parameters can be measured, including transepithelial potential difference (PD), short-circuit current (I_{sc}) and tissue resistance (R_t).

The electrophysiological activities of the isolated iris-ciliary body have been broadly investigated in a number of species including rabbit (Kishida et al., 1981; Krupin et al., 1984; Chu et al., 1986; Crook et al., 2000), dog (Iizuka et al., 1984), cat (Holland and Gipson, 1970), shark (Wiederholt and Zadunaisky, 1986; Wiederholt and Zadunaisky, 1987; Wiederholt et al., 1989), ox (To et al., 1998a; Do and To, 2000), pig (Wu et al., 2003a; Wu et al., 2004; Kong et al., 2006; Ni et al., 2006), monkey (Chu et al., 1987), and human (Wu et al., 2003a). In view of the underlying ciliary stroma of the iris-ciliary body, alternative preparation of ciliary epithelial bilayer isolated from the ciliary stroma has been developed for the electrophysiological studies across the ciliary epithelium (Sears et al., 1991). The

viability of this preparation has been verified in several studies (Sears et al., 1991; Crook et al., 2000; Ni et al., 2006).

The magnitude and polarity of the transepithelial PD were initially uncertain in the early experiments. The discrepancy was partly explained in terms of the different experimental animals and different bathing solutions. Initially, the polarity of transmural PD was found to be positive on aqueous side of the iris-ciliary body of the rabbit and ox (Cole, 1962). However, later studies has demonstrated that the polarity of the PD is negative on the aqueous side (NPE) with respect to the stromal side (PE) in many species, including cat (Holland and Gipson, 1970), toad (Watanabe and Saito, 1978), dog (Iizuka et al., 1984), rabbit (Kishida et al., 1981; Krupin et al., 1984; Sears et al., 1991), monkey (Chu et al., 1987), ox (To et al., 1998a; To et al., 1998b; Do and To, 2000) and pig (Wu et al., 2003a; Kong et al., 2006; Ni et al., 2006), which strongly implicates an anionic transport of the ciliary epithelium from the stroma into the AH.

In many cases, the measured PD is eliminated by continuously applying an external current across the preparation, the ciliary epithelium is regarded as short-circuited and the current required to abolish the potential is called the I_{sc}. Under the short-circuit condition, the I_{sc} measures the algebraic sum of ionic movement across the cells (transcellular pathway) but not between the cells (paracellular pathway). Na^+ and Cl^- are the major ions transported by the ciliary epithelium. The I_{sc} exhibits ionic dependence as demonstrated by ion substitution experiments and can be modulated by various transporter inhibitors (Holland, 1970; Watanabe and Saito, 1978; Kishida et al., 1981; Krupin et al., 1984; Do and To, 2000; Kong et al., 2006). Moreover, the R_t can be estimated by passing a fixed current across the

preparation. The R_t reflects the leakiness of the tissue, which represents paracellular gate function of the epithelial tight junctions.

The ionic movement across the ciliary epithelium can be further investigated by transepithelial flux measurements of radioactive tracers (Holland and Gipson, 1970; Saito and Watanabe, 1979; Kishida et al., 1982; Pesin and Candia, 1982; Chu and Candia, 1987; Crook et al., 2000; Do and To, 2000; To et al., 2001; Kong et al., 2006). Radioactive isotope is used to act as a tracer for particular ion. The radioactive compound of known activity is added on one side of the preparation, samples of the solution on the other side are withdrawn at intervals to measure the radioactivity, which represents the unidirectional ion flux across the preparation. The difference between the two opposite directional fluxes is considered as the net flux, which quantifies the net magnitude and direction of ion being transported across the preparation. This technique directly quantifies the particular ion transported by the epithelium.

1.6 Transepithelial ion secretion across ciliary epithelium

The driving force for AH secretion is primarily created by the transepithelial ion transport across the ciliary epithelium which generates an osmotic gradient for fluid movement. Transepithelial ion secretion across the ciliary epithelium can proceed in three sequential steps: (1) uptake of ion by the PE cells, (2) transfer of ion from PE to NPE cells through gap junction, (3) ion release by the NPE cells into the posterior chamber (To et al., 2002). Na^+, Cl^- and HCO_3^- to a lesser extent, are the major ionic constituents in the AH and are considered to participate in the transepithelial ion transport across the ciliary epithelium. Over the past few decades, considerable research has been conducted to elucidate the transport mechanisms across the ciliary epithelium, such that the key transport components have been identified (Do and Civan, 2004). The transepithelial transport of the three major ions across the ciliary epithelium is reviewed below.

1.6.1 Na^+ transport

Active Na^+ transport virtually depends on the enzyme sodium-potassium activated adenosine triphosphatase (Na^+,K^+-ATPase). The Na^+,K^+-ATPase pumps 3 Na^+ ions out of the cell and 2 K^+ ions into the cells and the process is fueled by the hydrolysis of ATP (Glynn, 2002). The Na^+ and K^+ gradients are indispensable for maintaining membrane potentials and hence secondary active transport of other solutes. The presence of this enzyme has been identified in the ciliary epithelium of rabbit (Cole, 1964; Flugel and Lutjen-Drecoll, 1988; Usukura et al., 1988), ox (Ghosh et al., 1990), rat and mouse (Wetzel and Sweadner, 2001), and pig (Shahidullah et al., 2007).

The Na^+,K^+-ATPase is primarily localized at the basolateral infoldings and interdigitation of both PE and NPE cells (Usukura et al., 1988; Mori et al., 1991), with a higher activity expressed in the NPE cells (Riley and Kishida, 1986; Usukura et al., 1988). The ciliary epithelium displays a variation in the regional distribution of the Na^+,K^+-ATPase isoforms (Ghosh et al., 1990). The expression of both α- and β-isoforms are more abundant in the anterior pars plicata region than in the posterior pars plana region (Ghosh et al., 1991), implicating that the AH secretion rate may display regional differences along the ciliary epithelium.

Na^+,K^+-ATPase activity can be specifically inhibited by cardiac glycosides such as ouabain. The functional expression of the enzyme has been established in different animal species, including rabbit (Becker, 1980; Riley and Kishida, 1986), cat (Oppelt and White, 1968), ox (Riley and Kishida, 1986; Helbig et al., 1987), monkey (Becker, 1980) and human (Helbig et al., 1989c). Furthermore, the application of ouabain has been shown to decrease IOP in experimental animals (Becker, 1963; Waitzman and Jackson, 1965), principally by reducing the rate of AH

inflow as revealed in cats (Oppelt and White, 1968; Garg and Oppelt, 1970) and in isolated perfused eye of rabbit (Kodama et al., 1985) and ox (Shahidullah et al., 2003).

Net Na^+ transport across the ciliary epithelium was originally proposed by Cole, who studied the ciliary body preparation of rabbit and ox mounted in the Ussing chamber (Cole, 1961; Cole, 1962). The polarity of the transepithelial PD across the ciliary body was found to be positive on aqueous side in both rabbit and ox. The magnitude of PD was reduced by replacement of Na^+ in the bathing medium (Cole, 1961; Cole, 1962). Based on his findings, he suggested that active Na^+ transport was involved in AH formation. This view was supported by other studies that demonstrated a correlation between Na^+ accession rate and AH formation in dog (Maren, 1976). Moreover, intravenous administration of ouabain reduced both the Na^+ entry into the posterior chamber and AH formation in cat (Garg and Oppelt, 1970), dog (Maren, 1976; Zimmerman et al., 1976) and monkey (Maren, 1977).

The proposition of net Na^+ transport was later challenged by the negative polarity of the transepithelial PD observed in the ciliary body of different species (Holland and Gipson, 1970; Watanabe and Saito, 1978; Kishida et al., 1981; Iizuka et al., 1984; Chu et al., 1987). The negative PD pointed to the primarily dependency of an active anion (HCO_3^- and/or Cl^-) rather than Na^+ transport. Furthermore, no net Na^+ transport was demonstrated across the ciliary body of cat (Holland and Gipson, 1970), toad (Saito and Watanabe, 1979), rabbit (Kishida et al., 1982) and ox (To et al., 1998a). However, ouabain elicited paradoxical effects on the measured Na^+ fluxes across the ciliary epithelium. When applied to one or both sides, ouabain did not reduce but slightly stimulated the unidirectional Na^+ fluxes (Saito and Watanabe, 1979; Pesin and Candia, 1982). It has been demonstrated that the unidirectional Na^+

fluxes were generally high, a relatively small net Na^+ transport may be difficult to detect. This assumption was further explored by measuring the unidirectional Na+ fluxes under reduced Na^+ concentration of bathing solution, so that paracellular diffusional fluxes could be minimised (Candia et al., 1991). At 30 mM of bathing Na^+, significant net Na^+ transport was determined. However, such net Na^+ transport can only account for a small portion of total AH formation *in vivo*.

1.6.2 HCO_3^- transport

HCO_3^- transport has long been regarded as fundamental in the AH secretion because the carbonic anhydrase (CA) inhibitors have been used in anti-glaucoma medication for several decades. CA is the enzyme catalyzing the reversible synthesis of HCO_3^- from CO_2 and water. The presence of CA has been identified in the ciliary epithelium of rabbit, monkey and human histochemically (Lutjen-Drecoll and Lonnerholm, 1981; Lutjen-Drecoll et al., 1983). Moreover, the CA activities in the ciliary epithelium have been demonstrated by biochemical studies (Dobbs et al., 1979; Wistrand and Garg, 1979; Muther and Friedland, 1980; Wu et al., 1997). In the ciliary epithelium, both the cytosolic CA II isoform (Wistrand et al., 1986) and membrane-bound CA IV isoform (Matsui et al., 1996; Wu et al., 1997) have been identified, and these two CA isoforms are considered to facilitate the HCO_3^- transport into the posterior chamber in a synergistic manner (Maren, 1997).

Friedenwald was first to propose that HCO_3^- release into the AH facilitated by CA catalysing the conversion of HCO_3^- from CO_2 and OH^- (Friedenwald, 1949). Additionally, subsequent studies have shown that the CA inhibitor acetazolamide reduced the accession of Na^+ and formation of HCO_3^- in the AH (Maren, 1976). The HCO_3^- transport into the AH has occurred with a concomitant Na^+ accession from the blood plasma (Maren, 1977). These findings are in accordance with the higher HCO_3^- concentration in the AH than in the blood plasma of rabbit and guinea pig (Davson and Luck, 1956). However, in others species such as horse, monkey and human, Cl^- concentration is higher in the AH than in the plasma (Davson and Luck, 1956). Yet, the CA inhibitors are effective in reducing the rate of AH formation and IOP in human (Dailey et al., 1982; Larsson and Alm, 1998). From these observations,

the CA appears to play an important role in the AH secretion, regardless of the level of HCO_3^- or Cl^- in the AH.

In HCO_3^--containing bathing solution, a negative PD has been observed in rabbit ciliary epithelium, whereas a reversed polarity is induce by removing HCO_3^- from the bathing solution (Kishida et al., 1981; Krupin et al., 1984). Contrary to rabbit, HCO_3^- depletion of the bathing solution did not elicit a reversal of polarity, but only reduced the magnitude of PD by 30-40% in bovine ciliary epithelium (Do and To, 2000). Recently, in porcine ciliary epithelium, eliminating HCO_3^- nearly abolished the PD (Kong et al., 2006). Apparently, the *in vitro* ionic transport is HCO_3^--dependent to a certain extent, its relative contribution to AH formation likely varies in different species. It has been demonstrated the presence of Na^+-HCO_3^- symport in the PE cells of ox and rabbit (Helbig et al., 1989b; Butler et al., 1994), which may provide a potential uptake mechanism for HCO_3^- into the PE cells. However, it has recently been shown that no net HCO_3^- transport is detected across the bovine ciliary epithelium (To et al., 2001). Interestingly, the application of acetazolamide inhibits the PD by reducing the net Cl^- secretion but has no direct effect on the net HCO_3^- transport, suggesting that HCO_3^- likely plays an indirect role in AH formation by modulating the net Cl^- secretion (To et al., 2001).

1.6.3 Cl^- transport

Over the past decade, the vital importance of the Cl^- transport in driving the AH secretion has been generally recognized (Civan, 2003) and the transporters involved are largely identified (Do and Civan, 2004; Do and Civan, 2006). In brief, the transepithelial Cl^- transport across the ciliary epithelium has been supported by the Cl^--dependent I_{sc} across the ciliary body demonstrated in cat (Holland, 1970), toad (Watanabe and Saito, 1978), rabbit (Kishida et al., 1981), ox (Do and To, 2000) and pig (Kong et al., 2006). In addition, a net Cl^- secretion across the ciliary epithelium in the direction from stroma to AH has been detected in different species including cat (Holland and Gipson, 1970), toad (Saito and Watanabe, 1979), rabbit (Kishida et al., 1982; Crook et al., 2000), ox (Do and To, 2000) and pig (Kong et al., 2006). Furthermore, the Cl^--dependent I_{sc} and net Cl^- secretion across the ciliary epithelium are inhibited by various transporter inhibitors (Do and To, 2000; Kong et al., 2006). These concomitant findings strongly support the transepithelial Cl^- secretion through different transporters in the ciliary epithelium. An overview of the current consensus model of Cl^- transport is reviewed below.

FIGURE 1.1 An overview of the consensus model of Cl^- transport across the ciliary epithelium. TJ, tight junctions; GJ, gap junctions.

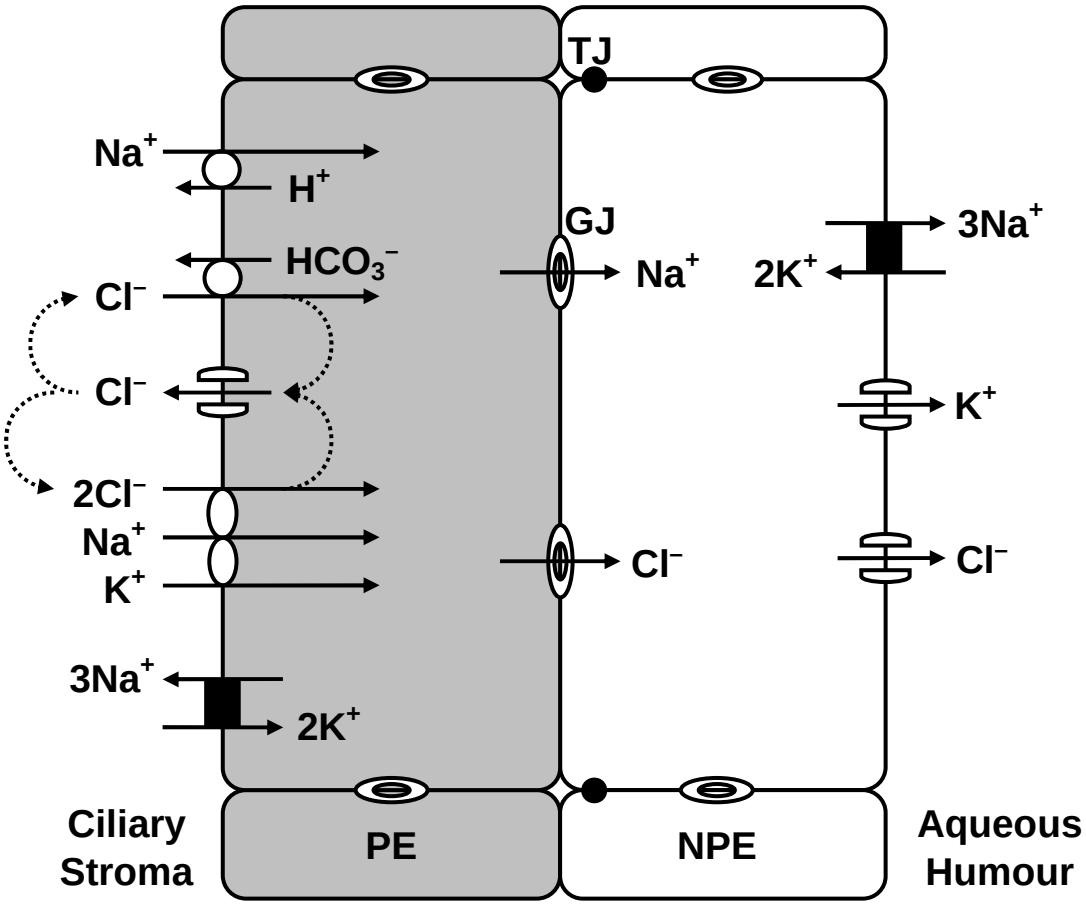

1.6.3.1 Cl^- uptake by PE cells

Several studies have demonstrated that intracellular Cl^- content in the ciliary epithelium is significantly higher than that predicted from electrochemical equilibrium, indicating the existence of Cl^- uptake mechanism in the PE cells (Green et al., 1985; Wiederholt and Zadunaisky, 1986; Bowler et al., 1996). Introduction of furosemide to the bathing solution reduced the intracellular Cl^- activity in the isolated ciliary epithelium of shark, comparable to that predicted from equilibrium (Wiederholt and Zadunaisky, 1986). Moreover, the uptakes of radiolabelled ^{22}Na and ^{36}Cl ions are coupled in cultured bovine PE cells (Helbig et al., 1989a). Based on the measurement of intracellular pH (pH_i) and radiolabelled tracer uptake, two major pathways were proposed for the Cl^- uptake into PE cells (Wiederholt et al., 1991): Na^+-K^+-$2Cl^-$ cotransporter, and paired Cl^-/HCO_3^- and Na^+/H^+ antiporters. Both pathways facilitate the electroneutral uptake of Na^+ and Cl^- into the PE cells simultaneously. Subsequent studies have demonstrated that both pathways are likely functional (Crook et al., 2000; Do and To, 2000; To et al., 2001; Shahidullah et al., 2003; Kong et al., 2006), although their relative contributions may vary with species and with experimental conditions.

(A) Na^+-K^+-$2Cl^-$ cotransporter

The Na^+-K^+-$2Cl^-$ cotransporter transports Na^+, K^+ and Cl^- into the PE cells in an electroneutral manner. The cotransporters are immunolocalized primarily along the basolateral membrane of the PE cells in the anterior pars plicata region (Crook et al., 2000; Dunn et al., 2001). Inhibition of Na^+-K^+-Cl^- cotransporter with the specific inhibitor bumetanide or the non-specific inhibitor furosemide has demonstrated a reduced uptake of Na^+, Cl^- or water by PE cells. Intracellular Cl^- activity was reduced by furosemide in shark ciliary epithelium (Wiederholt and Zadunaisky, 1986). Both ^{22}Na and ^{36}Cl uptakes have been reduced by bumetanide in culture bovine PE cells (Helbig et al., 1989a). Moreover, shrinkage of native bovine PE cells induced by reducing the bathing Na^+, K^+ and Cl^- concentrations was inhibited by bumetanide (Edelman et al., 1994). In addition, blockade of Na^+-K^+-$2Cl^-$ cotransporter with bumetanide has demonstrated a reduction in transepithelial Cl^- transport and AH formation *in vitro*. Stromal bumetanide inhibits both I_{sc} and net Cl^- secretion across the ciliary epithelium in rabbit (Crook et al., 2000), ox (Do and To, 2000) and pig (Kong et al., 2006). In isolated perfused bovine eye, adding bumetanide to the perfusate reduces *in vitro* AH production (Shahidullah et al., 2003). These results indicate the existence of bumetanide-sensitive Na^+-K^+-Cl^- cotransporter in the PE cells and its importance for the Cl^- secretion across the ciliary epithelium.

(B) Cl^-/HCO_3^- and Na^+/H^+ antiporters

Studies have demonstrated that the paired Cl^-/HCO_3^- and Na^+/H^+ antiporters are important in the pH_i regulation as well as the uptake of Cl^- into the PE cells. Both the Cl^-/HCO_3^- and Na^+/H^+ antiporters likely participate in the coupled uptake of Na^+ and Cl^- into the PE cells (Helbig et al., 1989a). Moreover, introduction of HCO_3^--containing solution increases the Cl^- content of both the PE and NPE cells (Bowler et al., 1996; McLaughlin et al., 1998), whereas the Cl^- level was reduced by blocking CA with acetazolamide. These findings indirectly indicate that the paired antiporters are the dominant pathway for the uptake of Cl^- into the PE cells (McLaughlin et al., 1998). It has also demonstrated the parallel antiporters are involved in the uptakes of fluid and ^{22}Na, and pH_i regulation in cultured bovine PE cells (Counillon et al., 2000). The Cl^-/HCO_3^- antiporter has been identified as AE2 isoform by reverse transcriptase polymerase chain reaction (RT-PCR) amplification of RNA from human ciliary body and immunostaining of cultured bovine PE cells (Counillon et al., 2000). The Na^+/H^+ antiporter has displayed pharmacological characteristics of NHE-1 isoform (Counillon et al., 2000).

The paired Cl^-/HCO_3^- and Na^+/H^+ antiporters transport Na^+ and Cl^- into the PE cell in exchange for H^+ and HCO_3^-, which reversibly form water and CO_2 as catalysed by CA. The cytosolic CA II facilitates the delivery of H^+ and HCO_3^- to the antiporters. CA II has been shown to enhance the turnover rate by direct interaction to both NHE-1 (Li et al., 2002) and AE2 exchangers (Sterling et al., 2001). Membrane-bound CA IV catalyses the reversible formation of CO_2 and water from H^+ and HCO_3^- at the stromal border of the NPE cells (Wu et al., 1998). It is possible that CA inhibitors reduce the AH inflow by inhibiting the actions of CA II and CA IV in catalysing the NaCl uptake by the PE cells (To et al., 2001).

1.6.3.2 Cl^- transfer from PE to NPE cells

Intercellular gap junctions provide a route for the transfer of solutes and water between PE and NPE cells, and between the adjacent cells within the same cell layers. These intercellular junctions have been identified by structural study (Raviola and Raviola, 1978), biochemical methods (Coca-Prados et al., 1992; Wolosin et al., 1997b; Coffey et al., 2002) and functional expression (Green et al., 1985; Wiederholt and Zadunaisky, 1986; Edelman et al., 1994; Oh et al., 1994; Bowler et al., 1996; Stelling and Jacob, 1997; Do and To, 2000; McLaughlin et al., 2004; Kong et al., 2006), suggesting that the ciliary epithelium is a functional syncytium (Krupin and Civan, 1996). The communication and transfer between the cell layers can be interrupted by extracellular acidosis (Oh et al., 1994), elevated extracellular Ca^{2+} level (Oh et al., 1994; Stelling and Jacob, 1997), or by the non-selective gap junction inhibitors such as octanol (Stelling and Jacob, 1997; Hirata et al., 1998) and heptanol (Mitchell and Civan, 1997). Heptanol reduces I_{sc} by ~80% across the ciliary epithelium in rabbit, ox and pig (Wolosin et al., 1997a; Do and To, 2000; Kong et al., 2006) and the inhibition of I_{sc} is largely mediated by reduction in net Cl^- transport (Do and To, 2000; Kong et al., 2006).

1.6.3.3 Cl^- release by NPE into AH

Cl^- release likely limits the rate of AH formation under physiological conditions because of several experimental observations (Jacob and Civan, 1996; Civan et al., 1997):

1. the intracellular Cl^- concentration is significantly higher than that predicted from electrochemical equilibrium, indicating that the uptake of Cl^- from the stroma by PE cells is not rate-limiting (Wiederholt and Zadunaisky, 1986; Bowler et al., 1996);
2. the membrane potentials and intracellular ionic contents of the PE and NPE cells are similar, suggesting a free ion transfer between the PE and NPE cells through gap junctions (Wiederholt and Zadunaisky, 1986; Bowler et al., 1996);
3. the activities of Na^+,K^+-ATPase and K^+ channels at the basolateral membrane of NPE cells are high under baseline conditions, indicating that they are not rate-limiting (Yantorno et al., 1992).

In addition, the importance of Cl^- channels in AH formation has been demonstrated by the application of Cl^- channel blocker 5-Nitro-2-(3-phenylpropylamino)-benzoic acid (NPPB), that significantly reduces both net Cl^- secretion (Do and To, 2000) and AH formation (Shahidullah et al., 2003) *in vitro*. Thus, the modulation of the Cl^- channels in NPE cells is of vital importance in regulating the AH secretion.

The Cl^- channel activities of the cells can be stimulated by various perturbations, including hypotonic swelling of NPE cells (Yantorno et al., 1992; Zhang and Jacob, 1997), introduction of cAMP (Chen et al., 1994; Edelman et al.,

1995; Chen and Sears, 1997), inhibition of protein kinase C (PKC) (Civan et al., 1994; Coca-Prados et al., 1995; Shi et al., 2002; Shi et al., 2003), and activation of A_3 adenosine receptors (A_3ARs) (Mitchell et al., 1999; Carre et al., 2000).

The molecular identity of the NPE Cl^- channels is still unclear. Upon hypotonic swelling, two different Cl^- channels are likely expressed in the NPE cells (Zhang and Jacob, 1997), the Cl^- channel regulator pI_{Cln} and swelling-activated ClC-3 are the possible candidates. The pI_{Cln} was initially cloned from the NPE cells of human (Anguita et al., 1995) and rabbit (Wan et al., 1997), and has been identified in the native bovine NPE cells (Chen et al., 1999). The antisense down-regulation of pI_{Cln} reduced the immunofluorescence staining and inhibited the swelling-activated Cl^- current (Chen et al., 1999), suggested the importance of pI_{Cln} in maintaining the swelling-activated Cl^- current. Nevertheless, subsequent work has revealed that pI_{Cln} is mainly localized in the cytoplasm of NPE cells (Sanchez-Torres et al., 1999). Additionally, upon hypotonic swelling, neither a translocation of pI_{Cln} protein from the cytoplasm into the plasma membrane, nor changes in pI_{Cln} protein expression occurred in the NPE cells (Sanchez-Torres et al., 1999). These results suggested that pI_{Cln} may not be the major Cl^- channel in the NPE cells, and its effect on Cl^- channel could be indirectly induced by cytoskeletal restructuring.

Alternatively, the swelling-activated ClC-3 has been suggested as the likely predominant Cl^- channels in NPE cells based on several observations (Coca-Prados et al., 1996; Civan, 2003). NPE cells express both transcripts and protein for ClC-3 (Coca-Prados et al., 1996). The Cl^- channel activities in NPE cells are inhibited by PKC (Civan et al., 1994; Coca-Prados et al., 1995; Coca-Prados et al., 1996), which is a characteristic of ClC-3 associated Cl^- currents (Kawasaki et al., 1994). Moreover, antisense oligonucleotides down-regulate message for ClC-3 and swelling-activated

Cl^- channel activity of NPE cells (Wang et al., 2000). Recently, functional inhibiting antibody specific for ClC-3 (Wang et al., 2003) has been shown to inhibit Cl^- current in cultured rabbit (Vessey et al., 2004) and native bovine (Do et al., 2005) NPE cells. However, the ClC-3 expression is distributed throughout the NPE cells, predominantly within the nucleus (Wang et al., 2000). Furthermore, only a portion of the NPE Cl^- current was attributed to ClC-3 (Wang et al., 2000). Therefore it is still questionable that ClC-3 is the only or major Cl^- channel in the NPE cells.

Regardless of the molecular identity of Cl^- channel, it has been recently demonstrated that the stimulation of swelling-activated Cl^- current in NPE cells increase the I_{sc} across the bovine ciliary epithelium (Do et al., 2006). Additionally, the time-course of the I_{sc} stimulation triggered by hypotonicity is comparable to that of regulatory volume decrease in NPE cells, suggesting the swelling-activated Cl^- channels are primarily localized in the NPE cells and their crucial importance in subserving or enhancing AH secretion (Do et al., 2006).

1.7 Regulation of aqueous humour secretion

In addition to the transport mechanisms of AH secretion, the understanding in the regulation of AH secretion is of equal importance in controlling the AH formation and hence IOP *in vivo*. In the literature, different drugs, hormones and signalling cascades have been suggested to modulate the AH secretion. For example, β-blockers have been used in glaucoma treatment by reducing AH formation for many years. However the precise mechanisms of its action are still unclear, primarily due to the unique structures of the bilayered ciliary epithelium and the complicated transport mechanisms that involve various transporters. Several important signalling cascades of the AH formation are reviewed below.

1.7.1 Cyclic 3′,5′-adenosine monophosphate (cAMP)

The initial identification of β_2-adrenergic-stimulated adenylate cyclase (AC) in the ciliary process of rabbit (Nathanson, 1980) led to the idea that cAMP played an important role in the regulation of IOP by modulating AH secretion. This view was supported by the hypotensive effects of cholera toxin, a specific, irreversible activator of AC. Intra-arterial infusion and intravitreal injection of cholera toxin lowered IOP, and the drug activated both the AC activity and cAMP production from ciliary processes by 2.2-fold and 7.4-fold respectively (Gregory et al., 1981).

The ciliary epithelial cell fraction displayed higher basal and isoproterenol-stimulated AC activities, compared to those in the whole ciliary processes or in the partially de-epithelialised vascular network (Nathanson, 1980). The cyclase activity was coupled to the β-adrenoreceptors, predominantly in the β_2 subtype (Nathanson, 1980; Nathanson, 1981; Elena et al., 1984). The cyclase activity was substantially higher in the NPE cells than in the PE cells in both bovine (Elena et al., 1984) and

rabbit (Mittag et al., 1987). Both VIP (vasoactive intestinal peptide)- sensitive and β-adrenergic-sensitive AC activities have been demonstrated in the NPE cells and they appeared to share components of the AC system in the same membrane (Mittag et al., 1987). Furthermore, the presence of HCO_3^--sensitive AC activity has been demonstrated in the bovine ciliary processes and the introduction of HCO_3^- increased the cAMP level (Mittag et al., 1993).

Forskolin is a diterpene of the labdane family, directly activates the AC without interaction with the cell surface receptors (Seamon and Daly, 1981). The stimulatory effects of forskolin in cAMP production has been demonstrated. A 10-fold increase in cAMP concentration in the AH has been induced following topical admininistration of forskolin in rabbit (Bartels et al., 1987). Moreover, isoproterenol, VIP and forskolin also stimulated the production of cAMP in the ciliary processes of rabbit (Horio et al., 1996), and human (Bausher and Horio, 1995).

In the early studies, cAMP-induced hypotensive effects have been demonstrated *in vivo*. Topical application of forskolin lowers IOP in rabbit, monkey and human (Caprioli and Sears, 1983), as a result of a reduction in aqueous flow (Burstein et al., 1984b; Caprioli et al., 1984; Lee et al., 1984). These findings implicated a central role for cAMP in lowering IOP and hence regulation of AH formation (Caprioli and Sears, 1984). However, subsequent studies have reported contradictory findings, in dispute the hypotensive action elicited by cAMP. For example, intravenous administration of VIP increased the AH flow in monkey (Nilsson et al., 1990). Terbutaline (β-adrenergic agonist) and timolol (β-adrenergic antagonist), but not forskolin or 8-Br-cAMP, cause significant reduction in AH formation measured in the isolated arterially-perfused bovine eye (Shahidullah et al.,

1995). The decline in AH formation did not seem to correlate to intracellular cAMP concentration.

Nevertheless, the modulatory role of cAMP has been supported by the diverse effects elicited by cAMP from *in vitro* studies of isolated ciliary body. In monkey, forskolin stimulated the I_{sc} across the ciliary body when added to either side of the preparation. Isoproterenol-induced stimulation of I_{sc} was completely inhibited by the β-blocker propranolol (Chu et al., 1987). In rabbit, 8-Br-cAMP, a cell permeable cAMP analogue, stimulated the I_{sc} when added to either side of the preparation (Chu and Candia, 1985), whereas forskolin only stimulated the I_{sc} when added to the NPE side (Chu et al., 1986). In a study employing isolated stroma-free rabbit ciliary epithelial bilayer (Horio et al., 1996), application of isoproterenol, forskolin or VIP alone to the PE side induced an increase in I_{sc}, in contrast to a reduction in I_{sc} elicited by isoproterenol applied to the same side reported by others (Chu and Candia, 1985). The isoproterenol-stimulated effects were completely blocked by the pretreatment of a non-selective β-blocker timolol or α-adrenergic agonist p-aminoclonidine (Horio et al., 1996).

Most of the *in vitro* studies of CBE reported a stimulation of I_{sc} induced by cAMP, the associated net Cl^- secretion has been further characterised. In rabbit, the isoproterenol-stimulated I_{sc} was linked to an enhanced net Cl^- secretion, with an increase of blood-to-aqueous Cl^- flux by 75% (Crook et al., 2000). A recent study in bovine CBE revealed that several cAMP-elevating agents including isoproterenol, VIP, forskolin and 8-Br-cAMP reduced the net Cl^- secretion (Do et al., 2004a). While in porcine CBE, aqueous application of 8-Br-cAMP induced stimulation in I_{sc} followed by a sustained plateau, and a concomitant transient increase in Cl^- transport was observed with the peak I_{sc} (Ni et al., 2006). Apparently, the I_{sc} response induced

by cAMP is primarily mediated by the net Cl^- transport. However, the precise transport mechanism that is regulated by cAMP has not been fully understood.

Several transport components are found to be regulated by cAMP *in vitro*. Down-regulation of Na^+,K^+-ATPase activity has been demonstrated by the introduction of cAMP or co-incubation of forskolin and IBMX (Delamere and King, 1992; Nakai et al., 1999). This cAMP-triggered down-regulation is likely mediated through protein kinase A (PKA) (Delamere et al., 1990; Nakai et al., 1999).

Maxi-Cl^- channels have been identified in the bovine PE cells (Mitchell and Jacob, 1996; Mitchell et al., 1997). It has been demonstrated that the maxi-Cl^- channel can be directly activated by cAMP thereby enhancing the Cl^- reabsorption from PE to stroma and reducing the net AH secretion (Do et al., 2004b).

The isoproterenol-stimulated I_{sc} in the isolated rabbit ciliary epithelial bilayer was reduced by bumetanide applied on PE (Crook et al., 2000), suggesting that the Na^+-K^+-$2Cl^-$ cotransporters in PE cells are likely modulated by the β-adrenergic stimulated cAMP production. It has been shown that the basal Na^+-K^+-$2Cl^-$ cotransport activity is stimulated by isoproterenol, forskolin and cAMP in fetal human PE cells (Hochgesand et al., 2001).

In addition, it has been demonstrated that isoproterenol increased, the gap junctional conductance between the PE and NPE cells (Hirata et al., 1998), likely due to the isoproterenol-induced phosphorylation of the gap junction isoform Cx43 (Sears et al., 1998). In contrast, the cAMP-induced reduction in Cl^- secretion in bovine CE was inhibited by the blockade of gap junction with heptanol (Do et al., 2004a). These findings suggested that gap junction was potentially modulated by cAMP.

In isolated NPE cells, cAMP activated the Cl^- channel activities in the basolateral membrane of NPE in dog (Chen et al., 1994), ox (Edelman et al., 1995) and rabbit (Chen and Sears, 1997). Forskolin or cAMP analogue induced a Cl^- current with a concomitant cell shrinkage in isolated dog NPE cells (Chen et al., 1994), which suggested that stimulation of cAMP production enhanced the Cl^- efflux into the AH, resulting in an increased rate of AH formation. Moreover, cAMP and forskolin enhance the cell shrinkage triggered by hypotonic swelling of cloned human NPE cells, and the shrinkage is abolished by the Cl^- channel blocker NPPB (Civan et al., 1994), suggested that cAMP enhances the cell shrinkage by stimulating the Cl^- channel activity.

1.7.2 Nitric oxide (NO) and cyclic 3′,5′-guanosine monophosphate (cGMP)

NO is a crucial mediator that involves in the regulation of diverse physiological processes, including control of platelet aggregation, smooth muscle contractility, central and peripheral neurotransmission, and the cytotoxic actions of immune cells (Hobbs et al., 1999). NO is synthesized by a family of enzymes known as NO synthase (NOS) (Hobbs et al., 1999). The actions of NO are mediated by the activation of soluble guanylate cyclase (sGC) and the increase in intracellular cGMP concentration in target cells (Moro et al., 1996).

The presence of NOS isoforms has been identified in the ciliary epithelium (Meyer et al., 1999), particularly in the NPE layer (Shahidullah et al., 2007). NO donors have been demonstrated to lower IOP in both rabbit (Behar-Cohen et al., 1996; Kotikoski et al., 2002) and human (Chuman et al., 2000). The reduction in IOP was likely attributed to both the inhibited inflow of AH (Millar et al., 2001) and enhanced outflow facility (Kotikoski et al., 2003b). Recently, in the arterially perfused isolated porcine eye, several NO donors have been shown to reduce the AH formation *in vitro*, independent of the vascular effects induced by NO (Shahidullah et al., 2005). Moreover, the effects induced by the NO donors were dependent on the sGC, suggesting the *in vitro* AH formation was modulated by the NO-cGMP pathway (Shahidullah et al., 2005). Consistent with this finding, NO donors have been demonstrated to increase the cGMP concentration via the activation of sGC in the porcine ciliary body (Kotikoski et al., 2003a).

In isolated CBE preparations, applications of NO donors and cGMP to the NPE side transiently stimulated the I_{sc} in porcine CBE via the cGMP-protein kinase G (PKG) pathway (Wu et al., 2004). However, it has been demonstrated that NO donors elicited two opposing effects, a stimulation in I_{sc} and Cl^- secretion via the

cGMP pathway, and a reduction in I_{sc} and Cl^- secretion via the cytochrome P-450 pathway (Kong et al., 2005). In addition, NO has been shown to inhibit the Na^+,K^+-ATPase activity in bovine ciliary processes (Ellis et al., 2001) and native isolated porcine NPE cells (Shahidullah and Delamere, 2006). This NO-cGMP induced Na^+,K^+-ATPase inhibition was mediated by PKG (Shahidullah and Delamere, 2006).

This NO-cGMP pathway was potentially linked to cAMP. It has been demonstrated that NO production in the porcine ciliary epithelium was stimulated by cAMP-elevating agents including isoproterenol, forskolin and 8-Br-cAMP (Liu et al., 1999). The cAMP-stimulated NO production was mediated through the PKA and involved the activation of NOS. Furthermore, the protein expression of NOS I was up-regulated by forskolin in the porcine ciliary processes (Liu et al., 2002). These findings suggested that NO-cGMP pathway may be one of the down-stream pathways of the cAMP-PKA signalling cascade.

1.7.3 Endothelin (ET)

The family of ET vasoactive peptides comprised of three isoforms, ET-1, -2 and -3 (Inoue et al., 1989). There existed a 2 to 3-fold higher concentration of ETs in the AH than in the blood plasma in both bovine and human eyes (Lepple-Wienhues et al., 1992). Furthermore, ET-1 content in AH was higher in primary open angle glaucoma patients (Noske et al., 1997) and in the glaucoma rat model of elevated IOP (Prasanna et al., 2005).

Among the three isoforms, ET-1- and ET-3-like immunoreactivity was found in different ocular tissues, highest in the iris and ciliary body, lower in choroid and retina and lowest in the cornea (MacCumber et al., 1991). The presence of ET-1 has been identified in the ciliary epithelium (Eichhorn and Lutjen-Drecoll, 1993) and NPE layer (Wollensak et al., 1998). The formation of ET-1 was regulated by tumour necrosis factor-alpha (TNF-α) that mediated through the activation of PKC in human NPE cells (Prasanna et al., 1998b). The activation of PKC by TNF-α was attributed to an elevated level in diacylglycerol, but independent of an increase in intracellular Ca^{2+} concentration (Prasanna et al., 1998a). It has been demonstrated that the ET-converting enzyme-1 was localized in the plasma membrane of the human NPE cells (Prasanna et al., 1999). These findings suggested that ET-1 could be synthesized locally in the NPE cells.

The intravitreal injection of ET-1 has been shown to lower IOP in rabbit (MacCumber et al., 1991), with the effect lasting for at least 5 days. The reduction of IOP induced by ET-1 was likely attributed to both a reduction of the AH inflow as well as an increase in the outflow facility (Taniguchi et al., 1994). It has been demonstrated that *in vivo* AH inflow was reduced by ET_A receptor agonists in rabbit (Taniguchi et al., 1996), consistent with the presence of ET_A receptors identified in

the human NPE by RT-PCR (Tao et al., 1998). Moreover, ET-1 has been shown to modulate various cellular events in the NPE. The application of ET-1 increased the intracellular Ca^{2+} concentration in the human NPE (Tao et al., 1998). ET-1 has been shown to inhibit the Na^{+},K^{+}-ATPase activity (Prasanna et al., 2001), as well as increase the expression of Na^{+},K^{+}-ATPase in human NPE cells (Krishnamoorthy et al., 2003). However, the relationship between these *in vitro* findings and the regulation of AH formation *in vivo* is yet to be determined.

The actions of ET-1 may also be associated with other second messengers. It has been demonstrated that ETs inhibited the cAMP production in the ciliary epithelium of rabbit and human (Bausher, 1995). Additionally, ET-1 has been shown to reduce NO production in porcine ciliary processes (Wu et al., 2003b). Furthermore, regulation of ET-1 and ET receptors by dexamethasone have been demonstrated (Zhang et al., 2003), suggesting that ET and its receptors could be a novel mediator of the effects on IOP induced by corticosteroid. In the posterior eye, ET-1 has been shown to produce vasoconstriction at the optic nerve head and reduced ocular blood flow (Pang and Yorio, 1997), such that its presence may potentially contribute to the glaucoma pathophysiology (Yorio et al., 2002).

1.7.4 Adenosine receptors (AR)

Adenosine was detected in the AH of ox, pig and rabbit (Howard et al., 1998; Crosson and Petrovich, 1999). The topical administration of epinephrine induced an increase in the AH adenosine level in rabbit (Crosson and Petrovich, 1999). The ATP release and ecto-ATPase enzymatic conversion of ATP by the NPE facilitated the delivery of adenosine to the NPE cells (Mitchell et al., 1998). The mRNAs for the A_1, A_{2A} and A_{2B} AR subtypes have been identified by in situ hybridisation in the rat ciliary processes (Kvanta et al., 1997), whereas that for the A_3 subtype was demonstrated using RT-PCR in rabbit ciliary processes and immortalised human NPE cells (Mitchell et al., 1999).

The activation of different subtypes of AR elicited distinct effects on IOP. In rabbit, topical application of adenosine analogues triggered a biphasic change in IOP, an initial rise followed by a reduction in IOP (Crosson, 1992). The initial hypertensive effect was mediated by the activation of the A_2AR, while the hypotensive effect was mediated by the A_1AR (Crosson and Gray, 1994). The reduction of IOP induced by the activation of the A_1AR was associated with a decrease in AH inflow (Crosson, 1995). The activation of A_1AR has been shown to inhibit the forskolin-stimulated AC activity in the transformed human NPE and bovine PE cells (Wax et al., 1993), as well as in the rabbit ciliary body (Crosson and Gray, 1994). Moreover, the activation of A_1AR induced an increase in the intracellular Ca^{2+} concentration in the rabbit NPE cells (Farahbakhsh and Cilluffo, 1997). On the contrary, the increase in IOP triggered by the activation of the A_2AR was related to an increase in AH inflow (Crosson and Gray, 1996). The activation of A_2AR has been shown to up-regulate the AC activity in the transformed human NPE

cells and bovine PE cells (Wax et al., 1993), but not in the rabbit ciliary body (Crosson and Gray, 1996).

Adenosine has been shown to activate the Cl^- channels in the native bovine NPE cells, cultured human NPE cells and rabbit ciliary epithelium (Carre et al., 1997). The observations of whole-cell Cl^- current and cell shrinkage have demonstrated that the adenosine-triggered activation of Cl^- channels was mediated by A_3ARs (Mitchell et al., 1999; Carre et al., 2000). This activation was inhibited by selective A_3AR antagonists (Mitchell et al., 1999; Carre et al., 2000). The role of A_3AR in regulating IOP has been studied in the living mouse. The agonists and antagonists of the A_3AR have been demonstrated to increase and decrease the IOP of mouse respectively (Avila et al., 2001; Avila et al., 2002). Knockout mouse lacking A_3AR displayed a lower baseline IOP and reduced effects on IOP elicited by adenosine and selective A_3AR antagonist (Avila et al., 2002). Furthermore, the infusion of adenosine has been shown to induce a small decrease in IOP in healthy humans (Polska et al., 2003). The selective A_3AR antagonist MRS 1292 blocked the adenosine-triggered cell shrinkage of cultured human NPE cells *in vitro* and reduced the IOP of mouse *in vivo* (Yang et al., 2005). However, the invasive method of IOP measurement in mouse has been shown to enhance the effects of A_3AR agonists and antagonists (Wang et al., 2007). Recently, the introduction of novel nucleoside-derived A_3AR antagonist has been shown to inhibit the adenosine-triggered cell shrinkage, and reduce the IOP of mouse measured non-invasively (Wang et al., 2010).

1.7.5 Inositol triphosphate (IP_3) and calcium signalling

IP_3 is a second messenger which regulates the intracellular Ca^{2+} signals (Berridge and Irvine, 1989). This IP_3-mediated Ca^{2+} signalling pathway controls a diversity of cellular processes, including fertilisation, cell growth, transformation, secretion, smooth muscle contraction, sensory perception and neuronal signalling (Berridge, 1993). The IP_3 receptor isoforms have been studied in the rabbit NPE cells. In the absence of type II IP_3 receptors, type I isoform was identified in the basal membrane of the NPE cells, while type III isoform was localized in the apical membrane (Hirata et al., 1999).

The IP_3-Ca^{2+} signalling pathway has been extensively studied in the ciliary epithelial preparations of different species. An elevated intracellular Ca^{2+} level in response to a variety of agents has been found in the cultured human NPE cells (Lee et al., 1989; Ohuchi et al., 1992; Adorante and Cala, 1995; Cullinane et al., 2001b; Cullinane et al., 2001a; Cullinane et al., 2002), cultured rabbit NPE cells (Ohuchi et al., 1992; Botchkin and Matthews, 1995; Hou et al., 2001), isolated ciliary epithelial cells of rabbit (Schutte et al., 1996; Hirata et al., 1999; Cilluffo et al., 2000) and ox (Shahidullah and Wilson, 1997), rabbit ciliary epithelial bilayer (Giovanelli et al., 1996; Hirata et al., 1998), and intact rabbit ciliary processes (Farahbakhsh and Cilluffo, 1994; Yoshimura et al., 1995; Schutte et al., 1996; Schutte and Wolosin, 1996; Farahbakhsh and Cilluffo, 1997; Farahbakhsh and Cilluffo, 2002).

Multiple receptor agonists have been shown to trigger the increase in intracellular Ca^{2+} in the ciliary epithelial cells including histamine H_1, vasopressin V_1 (Lee et al., 1989; Crook and Polansky, 1992; Strauss et al., 1992), muscarinic, α-adrenergic (Ohuchi et al., 1992; Farahbakhsh and Cilluffo, 1994; Yoshimura et al., 1995; Schutte et al., 1996; Schutte and Wolosin, 1996; Suzuki et al., 1997; Hirata et

al., 1998; Cilluffo et al., 2000), somatostatin (Xia et al., 1997), A_1AR (Farahbakhsh and Cilluffo, 1997), $P2Y_2$ (Shahidullah and Wilson, 1997; Cullinane et al., 2001b), and angiotensin (Lee et al., 1989; Cullinane et al., 2002). In addition, mechanical stimuli such as hypotonic swelling has been shown to elicit an increase in intracellular Ca^{2+} in the cultured NPE cells of human (Adorante and Cala, 1995) and rabbit (Botchkin and Matthews, 1995). The two types of ciliary epithelial cells have displayed differential response selective to particular receptor agonists. In the PE cells, the increase in intracellular Ca^{2+} was triggered by the α_1-adrenergic agonists phenylephrine, while in the NPE cells, the increase in intracellular Ca^{2+} was elicited by the muscarinic receptor agonists acetylcholine (Schutte and Wolosin, 1996; Suzuki et al., 1997; Hirata et al., 1998). Both α_1- and β- adrenergic stimulation were essential for the epinephrine-induced increase in intracellular Ca^{2+} in both the PE and NPE layers (Hirata et al., 1998). Moreover, it has been demonstrated that activation of the $P2Y_2$ receptor by adenosine 5′-triphosphate (ATP) mobilised the intracellular Ca^{2+} level in the cultured NPE cells of ox (Shahidullah and Wilson, 1997) and human (Cullinane et al., 2001b).

The rise in intracellular Ca^{2+} level was attributed to both the Ca^{2+} release from intracellular stores as well as an Ca^{2+} influx from extracellular medium (Ohuchi et al., 1992; Farahbakhsh and Cilluffo, 1994). The intracellular Ca^{2+} signal was associated with an increase in IP production as triggered by various receptor agonists (Crook and Polansky, 1992; Cilluffo et al., 2000), mediated through the pertussis toxin-sensitive mechanism and phospholipase C-dependent pathway (Farahbakhsh and Cilluffo, 1997; Shahidullah and Wilson, 1997; Cilluffo et al., 2000). The transfer of Ca^{2+} signal from PE to the NPE was dependent on gap junction conductance and PKA activation (Hirata et al., 1998). Furthermore, ATP induced a reduction in

intracellular Ca^{2+} in the thapsigargin-treated human NPE cells mediated by the Ca^{2+} efflux primarily through the vanadate-sensitive Ca^{2+} ATPase pump, and to a lesser extent, through the Na^{+}/Ca^{2+} exchange (Cullinane et al., 2001b). Following the depletion of intracellular Ca^{2+} stores, capacitative Ca^{2+} entry was observed, potentially mediated by the L-type Ca^{2+} channel (Cullinane et al., 2001b).

Ca^{2+} was important for the phosphorylation of proteins in rabbit ciliary processes (Yoshimura et al., 1989). Moreover, the intracellular Ca^{2+} signal has been demonstrated to modulate various molecular target transporters. It has been shown that elevated intracellular Ca^{2+} level up-regulated the activities of several transporters, including ouabain-sensitive Na^{+},K^{+}-ATPase, bumetanide-sensitive Na^{+}-K^{+}-$2Cl^{-}$ cotransporter, and Ca^{2+}-activated K^{+} channel in the cultured human NPE cells (Mito et al., 1993).

Electrophysiological studies have demonstrated the K^{+} channel activity was stimulated by raising Ca^{2+} level in the PE (Jacob, 1991; Stelling and Jacob, 1996; Ryan et al., 1998) and NPE cells (Helbig et al., 1989d; Barros et al., 1991; Edelman et al., 1995). Furthermore, the elevated intracellular Ca^{2+} stimulated the Ca^{2+}-activated K^{+} current, with concomitant cell shrinkage in NPE cells triggered by hypotonic swelling (Adorante and Cala, 1995) or angiotensin II (Cullinane et al., 2002). However, the effect of the Ca^{2+}-activated K^{+} transport on the overall ion transport mechanisms of AH secretion is still unclear.

In addition, carbachol, which was shown to elevate intracellular Ca^{2+} level in PE cells (Stelling and Jacob, 1996), uncoupled the gap junction connecting the PE-NPE couplet (Stelling and Jacob, 1997). Cholinergic or α_1-adrenergic activation of the PE reduced the I_{sc} across the rabbit CBE, which was mediated by Ca^{2+}-dependent inhibition of PE-NPE gap junction (Shi et al., 1996).

However, the effects of certain receptor agonists on the intracellular Ca^{2+} varied in different preparations of different species. For example, epinephrine and norepinephrine increased the intracellular Ca^{2+} in the cultured NPE cells of rabbit, but not in that of human (Ohuchi et al., 1992). This observation is likely due to the differential distribution of membrane receptors across species, such that particular signalling pathway may induce differential effects in different animal species. Furthermore, it seems that varied signalling cascades are potentially involved in the regulation of the transport processes in the ciliary epithelium, their interactions with each other may complicate the overall effects exerted by a single second messenger.

Although the Cl^- transport mechanisms of the ciliary epithelium are largely understood, the regulation of these transport mechanisms is yet to be elucidated. Currently, there is still no consensus on the precise regulation of ion and fluid transport underlying the AH secretion, due to the unique structures of the bilayered ciliary epithelium, the complicated transport mechanisms that involves a number of transporters, and the complex signalling pathways potentially involved. Thus, a full understanding of the signalling mechanisms regulating the AH secretion in the ciliary epithelia of various animal species is in essence for facilitating the development of novel anti-glaucoma agents.

1.8 The objectives of investigation

The transport mechanisms underlying AH formation have been studied extensively. Transporters and channels have been characterised structurally, biochemically and functionally. Although many of the Cl^- transport mechanisms have been functionally identified in the ciliary epithelium, the relationship between the ion transport process and fluid movement has not been examined. Moreover, the second messenger cAMP has been shown to elicit diverse effects on the ion transport processes in the ciliary epithelium and on the AH formation, its potential role in regulating the AH formation is yet to be elucidated. The major objectives of the present study are:

1. to build a modified Ussing-type chamber system for the simultaneous measurement of fluid flow and electrical parameters across the porcine ciliary body epithelium (CBE);
2. to characterise the relationship between *in vitro* fluid flow and anion transport across the CBE;
3. to examine the effects of different Cl^- transporter inhibitors on the *in vitro* fluid flow and Cl^- transport;
4. to investigate the role of cAMP and its pathways in regulating the *in vitro* fluid flow and Cl^- transport.

These findings provide further information on the Cl^- transport mechanisms underlying AH formation and its regulation by the cAMP pathways, which are indicative of the potential pharmacological agents for reducing AH production *in vivo*.

CHAPTER 2

METHODS

2.1 Isolation of iris-ciliary body (ICB) preparation

Freshly enucleated porcine eyes were collected from a local abattoir in Hong Kong and transported to the laboratory on ice. All extra-ocular tissues and muscles were removed, leaving behind the globe. The cornea was removed by cutting circumferentially ~2 mm anterior to the limbus. The remnant of the cornea at the limbal region was gripped carefully with a forceps, exposing the anterior angle of the eye. The sclera was detached from the iris base by incision at the trabecular meshwork around the anterior angle. The sclera was further separated by cutting along the choroid-scleral interface all the way to the equator of the globe. The eye was then cut into half anterio-posteriorly, leaving behind an intact ring of ICB with choroid that was placed, with ciliary process facing upward, in a Petri dish containing Ringer's solution. Remaining vitreous humour on the ciliary body was removed gently. The posterior lens capsule was incised and lens cortex was removed. The posterior lens capsule was removed by trimming all the way to its lens zonules, leaving behind the anterior lens capsule. The whole annulus of the ICB was placed in Ringer's solution at room temperature.

2.2 Structures of the Ussing-type fluid chamber

The porcine ICB preparation was mounted in an Ussing-type chamber which was similar to the previous chamber systems for the rabbit and bovine ICB preparations (Candia et al., 2005). The detailed structures of the hemi-chambers used presently are described as follows. The cavity within one hemi-chamber comprised of an outer circular trough (16.0 mm in diameter) and an inner central post (12.5 mm in diameter). Both the central post and the circular trough were notched to hold an O-ring in the same plane. A small circular Lucite block (pupil block), with a diameter matching the central post, was machined to hold an O-ring and four pins. The pupil block was screwed into the central post for securing the iris and enclosing the pupil. Upon placement of the paired hemi-chamber, the outer circular troughs within each hemi-chamber were aligned so that only the ciliary processes (area of 1.28 cm^2) were exposed to the chamber cavity and bathing solutions. Because of the anatomical asymmetry of the ciliary processes, which are wider at the temporal region and narrower at the nasal region, the central post was decentred to the outer trough wall to accommodate this asymmetry. Ports were drilled into the sidewalls of the chambers to connect the fluid in the troughs to external vessels.

Minor modifications were made such that electrodes were connected to the chamber to simultaneously monitor the PD across the ciliary body epithelium (CBE) in addition to the FF measurement. In the first configuration (FC1) as illustrated in Figure 2.1, one pair of electrodes were connected to the paired hemi-chambers respectively for monitoring the transepithelial PD. The hemi-chamber on one side had two ports that led to an external bubbling reservoir that enabled drug additions, replacing bath solutions and delivery of gas mixtures to circulate the bathing solution within the trough. A Ag/AgCl cartridge electrode (EKV/EKC; World Precision

Instruments) filled with 154 mM NaCl polyacrylamide gel was also placed in the bathing solution in the bubbling reservoir. On the other side, an upper port on the hemi-chamber was fitted with a connector that fitted a 25 μL capillary with graduations of 0.25 μL, so that changes in fluid volume inside the compartment could be visually detected for the calculation of FF. The capillary was pre-treated with a hydrophobic agent (Rain-X; SOAPUS Products, Houston, TX) to prevent fluid crawl within the capillary. A lower port on this hemi-chamber enabled connection to a second Ag/AgCl electrode, so that the pair of electrodes could be used to measure the PD across the preparation. This arrangement allowed the study of the fundamental properties of FF and the effects of different Cl^- transport inhibitors.

In the second configuration (FC2) as illustrated in Figure 2.2, two pairs of Ag/AgCl electrodes were incorporated into the chamber such that the tissue resistance (R_t) can be estimated by applying an external current (10 μA) across the preparation, in addition to the simultaneous recording of PD and FF. On the bubbling reservoir side, two 3-way connectors were inserted on top and on the bottom of the chamber connecting to the bubbling reservoir; on the capillary side, another 3-way connector was inserted between the chamber and the graduated capillary, such that extra ports were available to fit two pairs of Ag/AgCl electrodes for the application of external current across the preparation.

FIGURE 2.1 A schematic diagram illustrating the configuration of the Ussing-type fluid chamber simultaneously measuring the FF and PD (FC1).

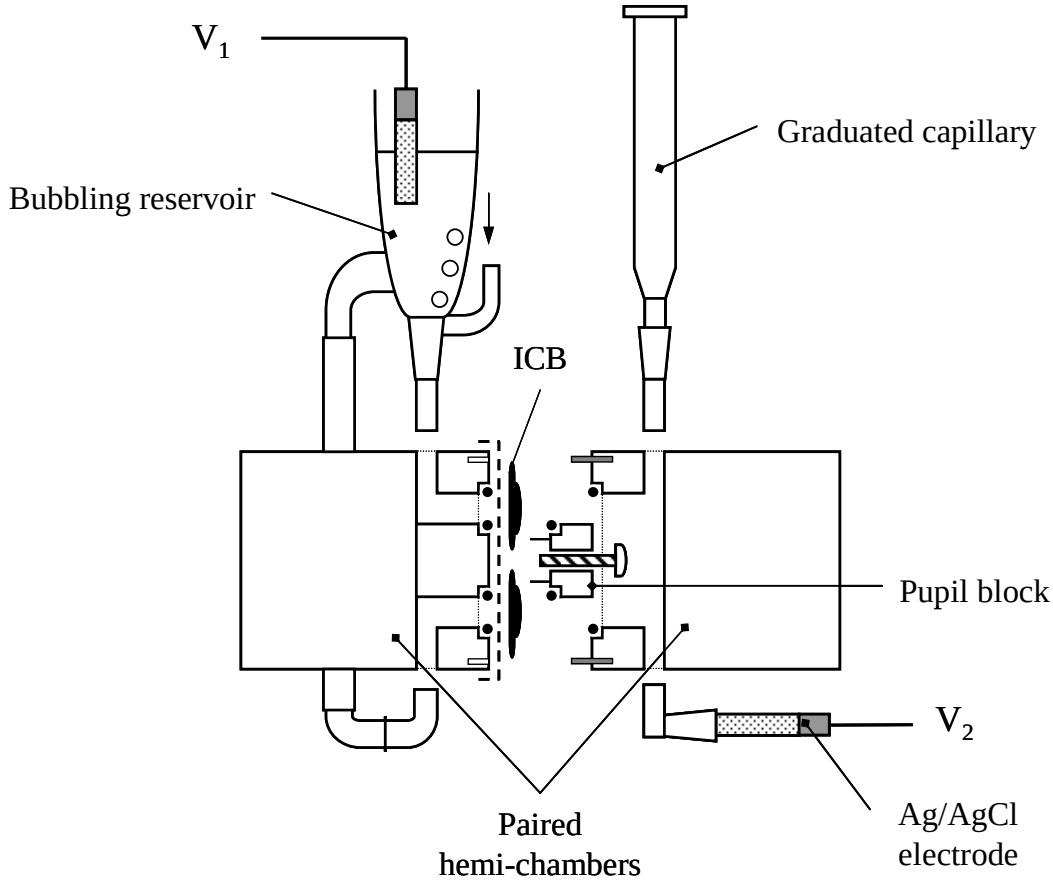

The arrow indicates the passage of gas mixture into the bubbling reservoir. The dashed line represents the nylon mesh. V_1 and V_2 denote the PD-sensing electrodes.

FIGURE 2.2 A schematic diagram illustrating the configuration of the Ussing-type fluid chamber simultaneously measuring the FF, PD and R_t (FC2).

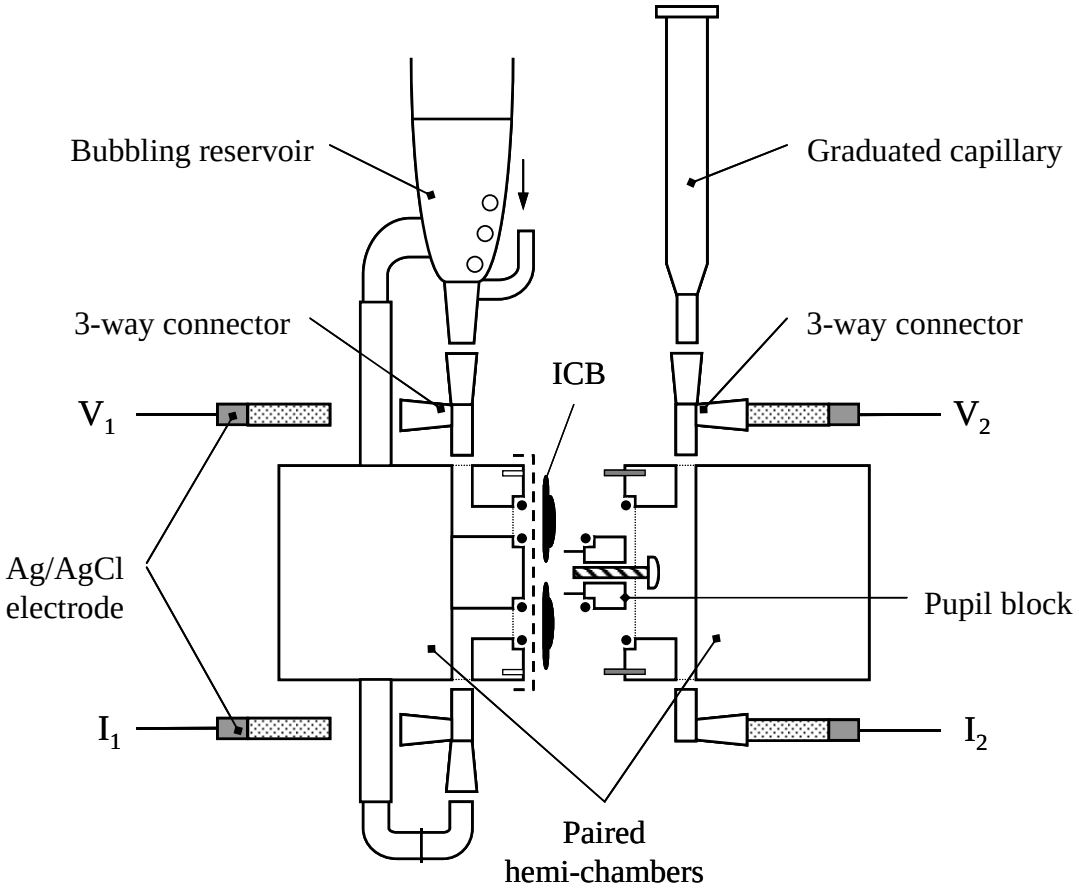

The arrow indicates the passage of gas mixture into the bubbling reservoir. The dashed line represents the nylon mesh. V_1 and V_2 denote the PD-sensing electrodes, while I_1 and I_2, the current applying electrodes.

2.3 Mounting of the ICB onto the Ussing-type fluid chamber

The complete annulus of the ICB preparation was transferred with a flat spatula and placed onto the circular Lucite hemi-chamber covered with tightly stretched nylon. The preparation was carefully aligned to the chamber cavity. Its pupil (with lens capsule) was occluded by the pupil block prior to placing a paired hemi-chamber over the preparation to hold it in place.

After mounting the ICB preparation, a bathing solution that had been pre-equilibrated with 5% CO_2 and 95% O_2 was pipetted into the respective side hemi-chambers through either the bubbling reservoir (8 mL total volume) or through the port and connector (~1 mL total volume). After filling the solution, the graduated capillary was inserted to the connector for measurement. Gas mixture (5% CO_2 and 95% O_2) was delivered through the bubbling reservoir continuously. Experiments were conducted at room temperature maintained at 25 ºC, such that the temperature of Ringer's solution was maintained within 23.5 to 24.5 ºC.

2.4 Measurement of fluid flow

The capillary-containing hemi-chamber was a close compartment, which was maintained unaltered throughout the experiment and enabled the detection of small changes in fluid volume inside the compartment. As such, solution changes and drug additions were made unilaterally on the side of the preparation containing the bubbling reservoir. The changes in capillary volume were recorded in 15-minute intervals and then converted to the rate of FF across the porcine CBE.

As demonstrated in the previous report of FF measurement in rabbit and bovine CBE (Candia et al., 2005), the CBE preparation transported fluid in the direction from blood to aqueous. This directional fluid movement was reflected by a consistent rise in the water level of the capillary when the capillary was placed on the aqueous side of the CBE preparation, and a consistent fall in the capillary level when placed on the blood side. This FF could be maintained for about 4 hours. Throughout the experiment, the capillary level was adjusted so that the difference between the capillary and water levels of the bubbling reservoir was within 5 mm. When the capillary was placed on aqueous side, the spontaneous FF produced a rise in the capillary level which was then manually lowered by withdrawing the fluid. When the capillary was placed on the blood side, the fall in capillary level was compensated by adding fluid into the capillary. This ensured minimal pressure difference across the preparation.

In all experiments, at least 60 minutes was allowed for equilibration after mounting of the preparation. FF was measured for 60 to 90 minutes and it was considered as the baseline data. Then a drug was added unilaterally to the bubbling reservoir to obtain the appropriate concentration. FF was measured thereafter for another 2 hours, the first-hour measurement was regarded as the intermediate period

for the circulation and diffusion of drug, and the FF measurement within the second-hour period was averaged and considered as the drug-treated recording. In separate experiments, the bubbling reservoir and capillary were interchanged so that the blood side or aqueous side of the preparation was facing the chamber containing the capillary. In all experiments, the side of drug addition was opposite to the capillary side.

2.5 Recording of electrical parameters

The PD across the CBE preparation was monitored by two Ag/AgCl electrodes in both FC1 and FC2, which are denoted as V_1 and V_2 in Figures 2.1 and 2.2. This pair of electrodes were connected to a voltage-current clamp unit (DVC-1000; World Precision Instruments, Sarasota, FL) for continuously monitoring of the PD. The signal outputs were fed into a dual-channel chart recorder (BD-12E; Kipp & Zonen Inc., Saskatoon, Saskatchewan, Canada).

In FC2, another pair of Ag/AgCl electrodes (denoted as I_1 and I_2 in Figure 2.2) were connected to the two hemi-chambers respectively for applying an external current (10 μA) across the preparation. Prior to mounting the preparation, the blank resistance of the chamber filled with bathing solution was measured and compensated by the dual-voltage clamp unit. External current was applied across the preparation by switching to the current-clamp function in the dual-voltage clamp unit for a few seconds. This procedure was conducted in 30-minute interval to minimize the interference of ionic distribution induced by the clamping current. R_t was calculated as ΔPD/ΔI, where ΔPD represents the potential change induced by the applied current and ΔI is the magnitude of the applied current.

2.6 Bathing solutions

HEPES-buffered Ringer's solution (NR) was used for dissection and bathing the ICB preparation. It contained the following (in mM): 113.0 NaCl, 4.6 KCl, 21.0 $NaHCO_3$, 0.6 $MgSO_4$, 7.5 D-glucose, 1.0 reduced glutathione, 1.0 Na_2HPO_4, 10.0 HEPES, and 1.4 $CaCl_2$. The pH of the solution was adjusted to 7.4 by pre-equilibrating the solution with 5% CO_2 and 95% O_2. For chloride (Cl^-) substitution experiments, the Cl^- concentration in the Ringer's solution was reduced from 120 mM to 7mM by replacing the NaCl with an equimolar amount of Na-gluconate. The latter compound was also used as a substitute for $NaHCO_3$ in experiments requiring bicarbonate-free conditions with 100% O_2 bubbling.

2.7 Pharmacological agents

Ouabain, bumetanide, niflumic acid, 5-(N,N-dimethyl)amiloride hydrochloride (DMA), 4,4′-diisothiocyanatostilbene-2,2′-disulfonic acid (DIDS), dimethyl sulfoxide (DMSO), forskolin, 8-bromoadenosine 3′,5′-cyclic monophosphate (8-Br-cAMP), 3-isobutyl-1-methylxanthine (IBMX), and H-89 dihydrochloride were all purchased from Sigma-Aldrich (St. Louis, MO). Heptanol was purchased from Fluka Chemie (Buchs, Switzerland). Heptanol was added directly to the bathing solution to obtain the appropriate concentration. Other drugs were dissolved in either water or DMSO prior to the addition to the bathing solution. The final concentrations of the solvents in the bathing solution were not more than 0.2% for DMSO and 0.5% for water.

2.8 Statistical analysis

Data were expressed as mean ± SEM, and statistically analysed with Student's t-test or ANOVA, either as paired or unpaired data, as described in the text. $P < 0.05$ was considered as statistically significant.

CHAPTER 3

RESULTS

We have built a modified Ussing-type fluid chamber to simultaneously measure the FF and transepithelial PD across the isolated porcine CBE. While the intact ICB is mounted within the chamber, the iris is pressed against the chamber walls holding the tissue in place, so that there is no or minimal contact between the iris and the bathing solutions. Under these conditions, the compartmental volume of the blood side gradually decreased, while that of the aqueous side steadily increased. This represented a fluid secretion in the blood-to-aqueous direction across the CBE.

3.1 Baseline values of FF and PD measured using FC1

In FC1, The average changes in the capillary volume of the aqueous side (Figure 3.1A, n = 8) and blood side (Figure 3.2A, n = 8) as a function of time were recorded. The calculated FF rates expressed as µL/h per preparation of the respective time intervals were also plotted (solid squares). The average volumetric increase of the aqueous-side compartment was initially 3.38 µL/h per preparation in the first 15-minute interval, slightly varied throughout the course of experiment, yet maintained the rate of 2.75 µL/h per preparation after 4 hours. Similarly, the average volumetric decrease from the blood-side compartment was initially 2.75 µL/h per preparation and remained stable to 2.63 µl/hr per preparation after 4 hours.

For statistical analysis, the FF data measured over 4 hours were divided into two major time frames i.e., a first and second 2-h period, with each representing about 2 hours. The initial 15-minute value was excluded because of its large variation, which may have reflected a variable equilibration period within the chamber. The remaining FF rates for each major time frame were averaged, and the differences between the two periods were compared. When the capillary tube was connected to the aqueous-side compartment (n = 8), the mean FF was 2.75 ± 0.17 µL/h per preparation during the first 2-h period and 2.61 ± 0.18 µL/h per preparation during the second 2-h period (P = 0.33, as paired data), suggesting that the preparation was physiologically stable for at least 4 hours. With the capillary tube placed in the blood-side compartment (n = 8), the mean FF was 2.63 ± 0.13 and 2.44 ± 0.13 µL/h per preparation for the first and second 2-h periods, respectively (P = 0.16, as paired data). There was no difference in the measured FF rates (P = 0.56, one-way ANOVA, as unpaired data) with the capillary on either the aqueous- or blood-sides of the preparations.

The standing PDs (in mV) across the CBE preparations during these experiments with the capillary connected to the aqueous (Figure 3.1B) and blood sides (Figure 3.2B) are plotted as a function of time. The polarity of the PD was consistently negative on the aqueous side; it declined gradually but slowly with time. From the experiments with the capillary on aqueous side, the PD was initially 1.9 mV and declined to 1.1 mV after 4 hours, while with the capillary on the blood side, the decrease was from 1.04 mV to 0.41 mV.

It was noteworthy that the FF rate was rather constant with time during 4 hours *in vitro*, but the PD declined. This suggests that the integrity of the tight junctions may have been compromised during this time *in vitro* so that an increased movement of counter ions via the paracellular pathway could have shunted the PD while at the same time transcellular fluid transport remained largely unaffected.

FIGURE 3.1 Spontaneous fluid movement across the isolated porcine CBE in the blood-to-aqueous direction and the simultaneously recorded transepithelial PD. (A) Left axis: the calculated FF rate (solid squares), expressed per hour during the course of the experiment. Right axis: the measured change in the capillary level (open circles) on the aqueous side of the preparation plotted as a function of time. Data points are the mean ± SEM of results of 8 control experiments. (B) The value of the PD recorded every 15 minutes simultaneously with the measurement of the capillary levels in (A). Points are the mean ± SEM (n = 8). The polarity of the PD was consistently negative on the aqueous side relative to the blood side.

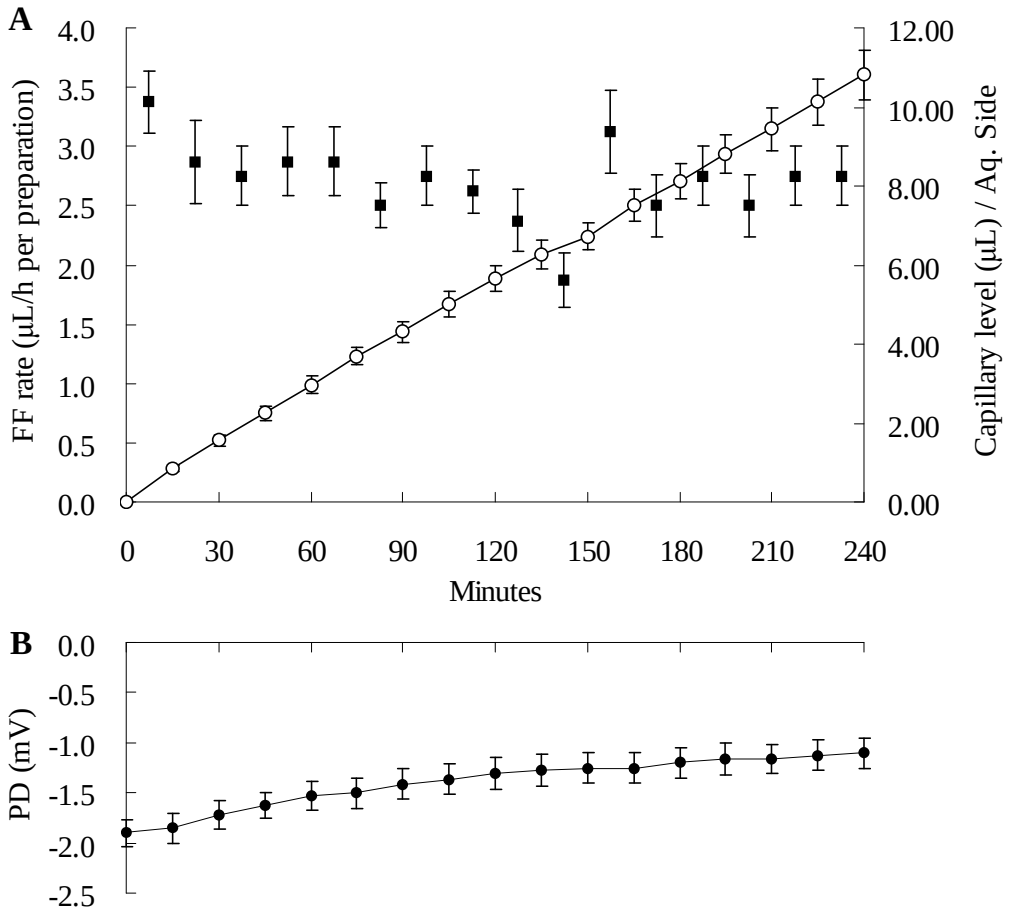

FIGURE 3.2 Spontaneous fluid movement across the isolated porcine CBE measured with the capillary on the blood side of the preparation, and the simultaneously recorded transepithelial PD. (A) Left axis: the calculated FF rate (solid squares), expressed per hour during the course of the experiment. Right axis: the measured change in the capillary level (open circles) on the blood side of the preparation plotted as a function of time. Data points are the mean ± SEM of results in 8 control experiments. (B) PD recorded every 15 minutes simultaneously with the measurement of the capillary levels in (A). Data are the mean ± SEM (n = 8). The polarity of the PD was consistently negative on the aqueous side relative to the blood side.

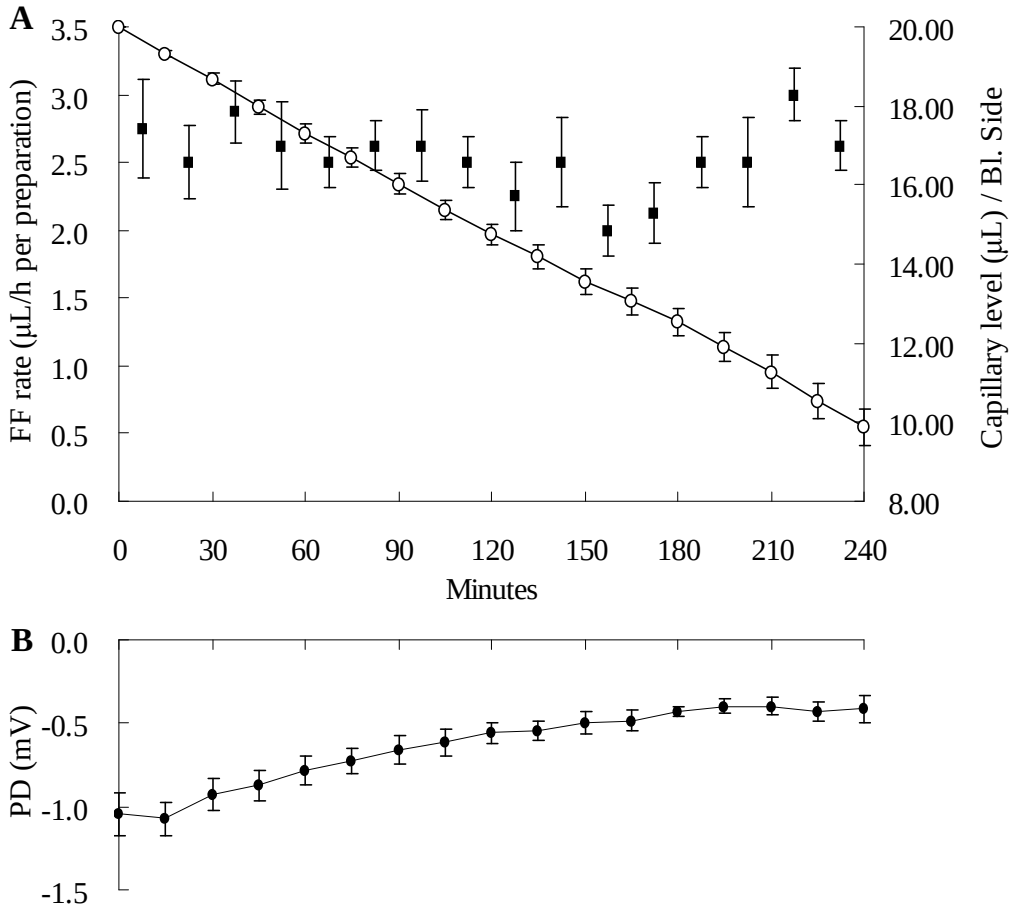

3.2 Preparation selection criteria

It was generally observed that tissue freshness was a critical factor for fluid transport. In approximately one third of the isolated porcine preparations, initial PD was very low or the PD promptly declined to zero, and FF was not detectable. Furthermore, temperature is another crucial factor affecting the success of the experiment. As mentioned in the previous study of porcine CBE, PD declined to zero when the bathing temperature was higher than 30°C (Kong et al., 2006). We also encountered this difficulty in maintaining stable PD and FF at higher temperature. In particular, FF was not steady when the solution was warmed up. We attempted to warm up the solution directly by inserting tubing circulating warm water into the bubbling reservoir, or indirectly by warming up the chamber. However, no satisfactory result was accomplished possibly due to the fluctuating fluid volume as a result of uneven warming. Therefore experiments were conducted at room temperature maintained at 25°C, which showed a more stable FF and PD maintained for at least 4 hours.

The preparations maintained a stable PD with the negative polarity on aqueous side with respect to blood side, and a stable FF value comparable to the control experiment, were included for the data analysis. At the end of each experiment, the responsiveness of PD was confirmed by the addition of heptanol, such that the PD tremendously depolarized. In addition, the viability of FF was examined with the replacement of low Cl^- solution (7 mM Cl^-) on both sides and absence of oxygen supply, such that the FF depleted subsequently.

3.3 Effects of stromal Cl^- substitution

Cl^- substitution experiments were conducted to evaluate the importance of Cl^- in the process of fluid transport across the porcine CBE. With low Cl^- (7 mM Cl^-) solution on the blood-side bath, the FF declined drastically from 2.43 to -1.00 µL/h per preparation (Figure 3.3A), and the PD hyperpolarized tremendously from -1.44 to -5.81 mV. (n = 7, Figure 3.3B). The effects of reducing Cl^- concentration in the blood-side bath on blood-to-aqueous fluid transport of individual experiments are shown in Table 3.1. With the Cl^- concentration reduced, the mean FF rate declined from 2.26 ± 0.15 to -0.57 ± 0.22 µL/h per preparation (n = 7; $P < 0.001$, as paired data), indicating not only a dramatic decrease in FF but also a slight reversal in flow in the aqueous-to-blood direction.

Restoring the Cl^- concentration by re-introducing NR to the blood-side hemi-chamber restored the FF to 1.64 ± 0.09 µL/h per preparation (Figure 3.3A), a rate ≈25% lower than baseline ($P < 0.05$, as paired data). Among the 7 individual experiments, replacing Cl^- in the bathing solution abolished the FF in 2 preparations, while reversing the FF in the remaining 5 preparations (Table 3.1). The marked dependency of FF on blood-side Cl^- level is consistent with the concept that transport of Cl^- ion across the preparation in the aqueous direction underpins the fluid flow.

FIGURE 3.3 Effects of reduced Cl^- concentration of the stromal bath on FF and PD (n = 7). (A) The calculated FF rate in the blood-to-aqueous direction during the course of the experiment. Data points are the mean ± SEM from 7 preparations. (B) PD recorded simultaneously with the measurement of the capillary levels. The polarity of the PD was consistently negative on the aqueous side relative to the blood side. Data are expressed as mean ± SEM. *Arrows:* the points at which Cl^- concentration was reduced and re-introduced in the blood-side bath.

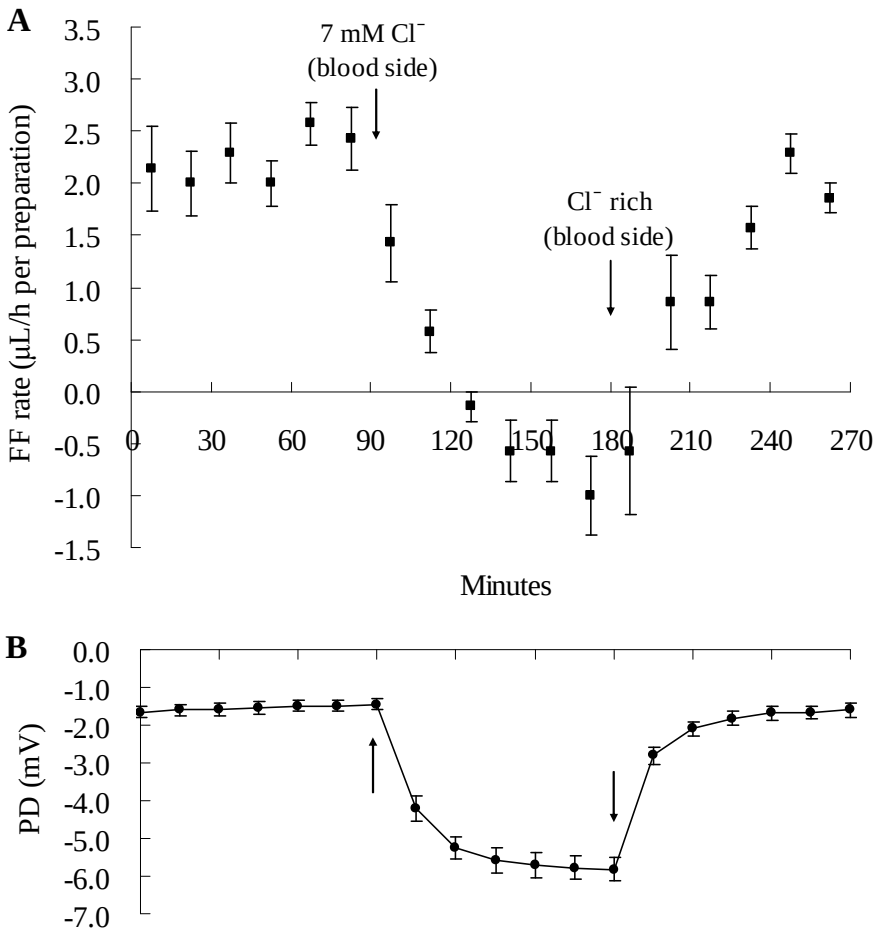

TABLE 3.1 Effects of reduced Cl^- concentration in the stromal bath on FF across the porcine CBE in the blood-to-aqueous direction.

		FF rate	
	Baseline	**Low Cl^-**	**Recovery**
Experiment	**(NR)**	**(7 mM Cl^-)**	**(NR)**
1	2.40	0.00	1.50
2	3.00	-0.25	1.75
3	2.40	-1.25	1.25
4	1.80	-0.25	1.50
5	2.20	-1.25	1.75
6	2.00	-1.00	2.00
7	2.00	0.00	1.75
Mean	**2.26**	**-0.57**§	**1.64**§
SEM	**0.15**	**0.22**	**0.09**

FF rate is expressed as μL/h per preparation and represents the spontaneous volumetric movement of fluid across the epithelium in the blood-to-aqueous direction. A negative value for FF indicates a net fluid flow in the reverse, aqueous-to-blood direction. All tissues were pre-equilibrated and bathed bilaterally in the divided chamber with HEPES-buffered NR solution plus 5% CO_2 bubbling of the blood-side hemi-chamber opposite to the aqueous-side compartment containing the capillary. The FF rate measured during an initial period of 75 minutes was taken as the baseline. Thereafter, the solution on the stromal side of the preparation was replaced with the low Cl^- medium and a stabilization period of 30 minutes was allowed, before measuring of FF for an additional 60 minutes. For the recovery conditions, FF was measured 30 minutes after the reintroduction of NR over a period of an additional hour.

§ Significantly different than respective antecedent, $P < 0.001$, as paired data.

3.4 Effects of stromal HCO_3^- depletion

In addition to a blood-side Cl^- requirement for fluid transport, the *in vitro* FF across the porcine preparation was also linked to the presence of CO_2/HCO_3^- in the stromal bath. Removal and re-introduction of CO_2/HCO_3^- from the blood-side hemichamber (by unilaterally washing out the NR with HCO_3^--free solution at t = 90 minute plus switching to 100% O_2 gas bubbling, followed by restoration of the control conditions at t = 180 minute) elicited a reversible, 52% reduction in FF (Figure 3.4A). In these experiments, the baseline FF was calculated for 75 minutes, thereby obtaining a mean value from 5, 15-min intervals from 5 preparations of 2.20 ± 0.18 µL/h per preparation. Under CO_2/HCO_3^--free conditions, FF declined significantly to 1.05 ± 0.12 µL/h per preparation (mean excludes the first 2 intervals following the solution change; $P < 0.002$), and recovered to 2.00 ± 0.08 µL/h per preparation upon re-introducing the control bathing conditions on the stromal side of the preparation.

Given indications for a linkage between blood-side bicarbonate levels and FF, a second set of experiments was conducted whereby the tissues were bathed bilaterally with the HEPES-buffered, HCO_3^--free medium with 100% O_2 bubbling of the blood-side bath and the capillary on the aqueous-side hemi-chamber (Figure 3.5A). Under these conditions, fluid transport in the blood-to-aqueous direction was 0.38 ± 0.13 µL/h per preparation (n = 4), a relatively low rate, suggesting an important role for bicarbonate in maintaining FF under baseline conditions. The flow immediately increased on replacement of the blood-side bathing medium (aqueous side left unaltered) with NR containing 21 mM HCO_3^- plus 5% CO_2 gas bubbling to 2.20 ± 0.14 µL/h per preparation (n = 4; $P < 0.001$, as paired data), a rate comparable

to that obtained with tissue pre-equilibrated and maintained under CO_2/HCO_3^- -rich conditions (e.g., Figures. 3.1A and 3.2A).

The PD was slightly affected by the unilateral removal and/or addition of bicarbonate (Figures 3.4B and 3.5B). This was not unexpected, given that under open-circuit conditions, changes in the levels in one bath of a charged species that can traverse both transcellular and paracellular pathways, could produce ambiguous and irrelevant PD responses.

FIGURE 3.4 Effects of CO_2/HCO_3^- depletion of the stromal bath on FF and PD (n = 5). (A) The calculated FF rate plotted as squares. Data are the mean ± SEM of results from 5 preparations. (B) PD recorded simultaneously with the measurement of the capillary levels. The polarity of the PD was consistently negative on the aqueous side relative to the blood side. Data points are expressed as mean ± SEM. *Arrows:* the points at which CO_2/HCO_3^- were removed and reintroduced to the blood-side bath.

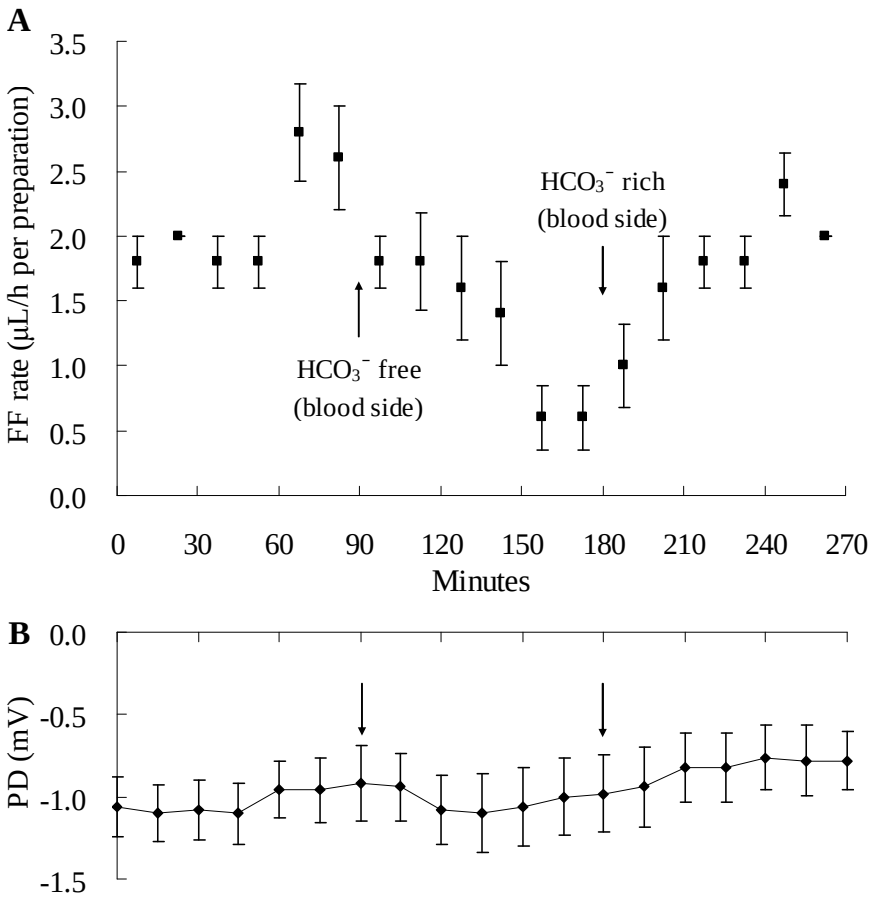

FIGURE 3.5 Effects of restoring CO_2/HCO_3^- concentration of the stromal bath on FF and PD (n = 4). (A) The calculated FF rate in the blood-to-aqueous direction during the course of the experiment. Data from a set of 4 experiments in which the CBE were initially bathed with HEPES-buffered HCO_3^--free medium plus 100% O_2 bubbling of the blood-side bath and the capillary on the aqueous-side hemi-chamber. (B) PD recorded simultaneously with the measurement of the capillary levels. The polarity of the PD was consistently negative on the aqueous side relative to the blood side. Data points are expressed as mean ± SEM. *Arrows:* the point at which CO_2/HCO_3^--rich medium was used to replace the baseline HCO_3^--free medium in the blood-side bath.

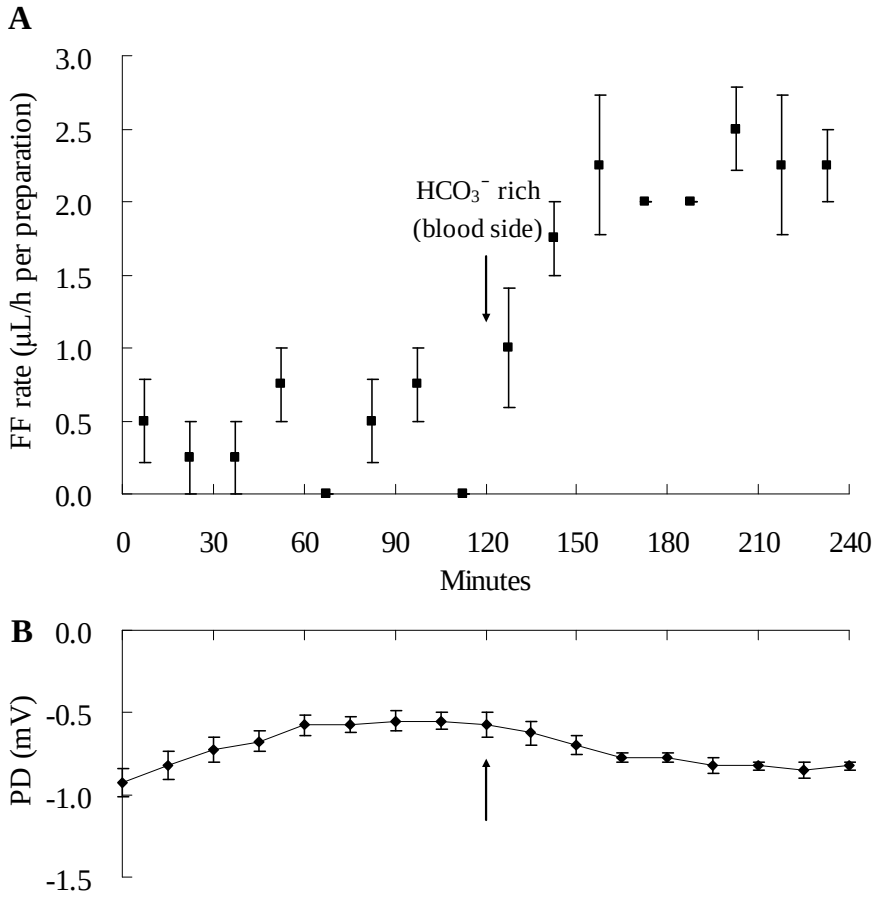

3.5 Inhibition of FF induced by Na^+,K^+-ATPase blockade with ouabain

Ouabain addition at 1 mM to the blood side (n = 6) inhibited the FF by 97% from 2.33 ± 0.19 to 0.08 ± 0.15 µL/h per preparation ($P < 0.001$, as paired data) and elicited a biphasic PD response, i.e. a slight depolarisation that was promptly followed by a more substantial hyperpolarisation lasting for 1 hour, thereafter the PD gradually depolarized (Figure 3.6B). The addition of 1 mM ouabain to the aqueous side (n = 5) also caused a transient hyperpolarisation in PD (Figure 3.7B), along with a 61% reduction in FF, that FF declined from 2.33 ± 0.05 to 0.90 ± 0.13 µL/h per preparation ($P < 0.001$, as paired data). Thus, the effects on PD with ouabain were largely similar when it was applied to either the aqueous or blood sides, however, the effects on FF rates differed significantly. Although the exact explanation of these diverse effects requires further study, it was clear that the driving force for FF was not completely eliminated by aqueous-side ouabain within the 2-h period that the capillary levels were monitored in the presence of the glycoside (Figure 3.7A). It may be due to a time factor and the decay of FF was too slow to be observed completely within the time period.

FIGURE 3.6 Effects of stromal addition of 1 mM ouabain on FF and PD (n = 6). (A) The calculated FF rate in the blood-to-aqueous direction during the course of the experiment. (B) PD recorded simultaneously with the measurement of the capillary levels. The polarity of the PD was consistently negative on the aqueous side relative to the blood side. Data points are expressed as mean ± SEM. *Arrows:* the point at which ouabain was added to the blood-side bath.

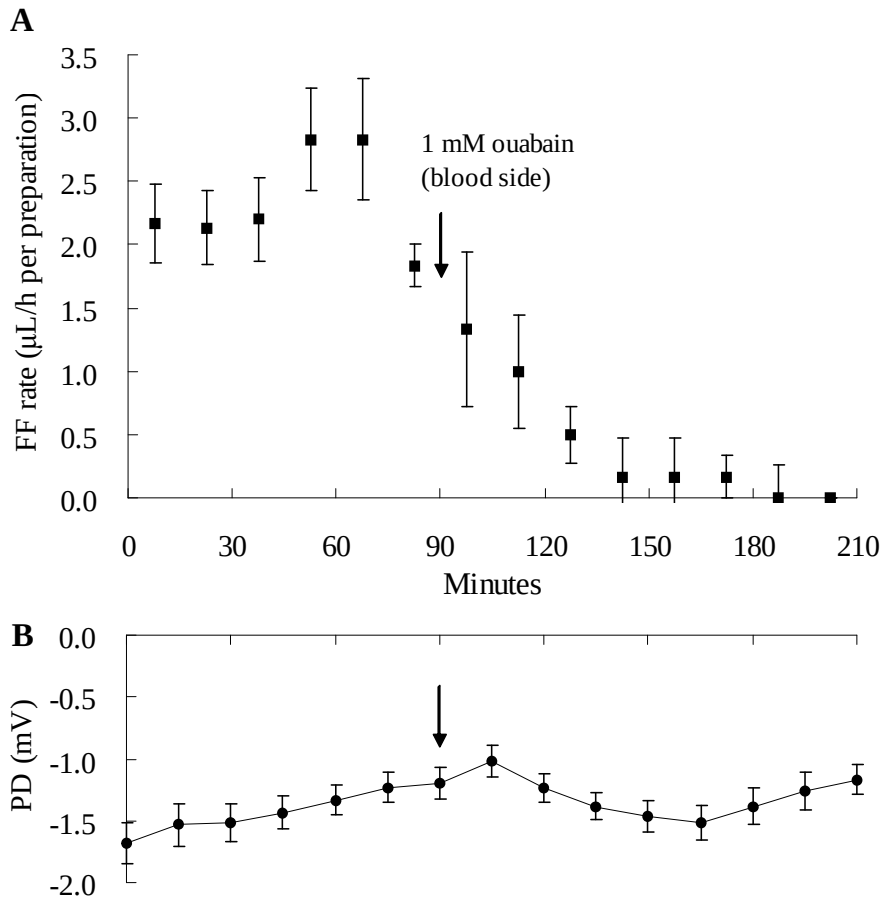

FIGURE 3.7 Effects of aqueous addition of 1 mM ouabain on FF and PD (n = 5). (A) The calculated FF rate in the blood-to-aqueous direction during the course of the experiment. (B) PD recorded simultaneously with the measurement of the capillary levels. The polarity of the PD was consistently negative on the aqueous side relative to the blood side. Data points are expressed as mean ± SEM. *Arrows:* the point at which ouabain was added to the aqueous-side bath.

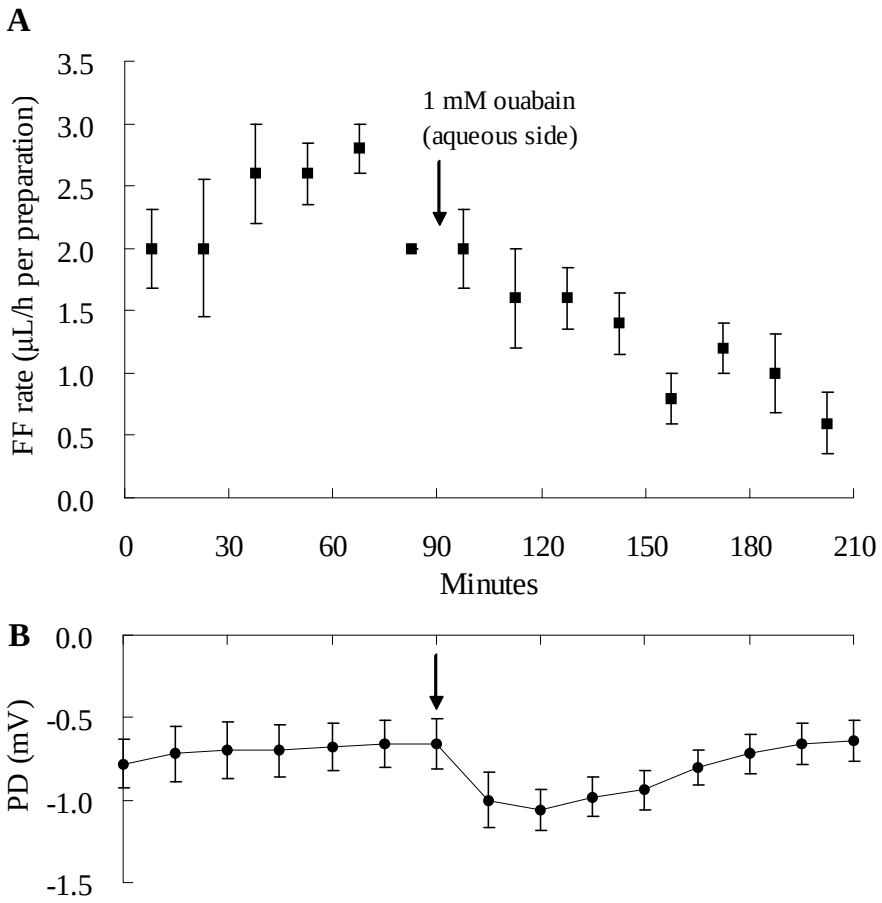

3.6 Inhibition of FF induced by Na^+-K^+-$2Cl^-$ cotransporter blockade with bumetanide

Addition of bumetanide (0.1mM) to the blood-side bath reduced the FF by 46% from 2.50 ± 0.22 to 1.35 ± 0.24 µL/h per preparation (n = 5; P < 0.001, as paired data, Table 3.2). Figure 3.8A shows the calculated FF rates as solid squares between each recorded time interval. It was clear that a steady rate of FF was maintained in the presence of bumetanide for the overall interval 150-210 minutes, suggesting that Na^+-K^+-$2Cl^-$ cotransporter was not completely inhibited in the porcine preparation by the dose of bumetanide applied.

As noted above in the control experiment (Figures 3.1B and 3.2B), the PD during control intervals gradually declined. Similarly, in the case of the bumetanide set of experiments (Fig. 3.8B), the observed PD at t = 90 minute, -1.12 ± 0.24 mV (n = 5), was significantly lower than the value at t = 0 minute, -1.20 ± 0.26 mV (P < 0.02, as paired data). Following the addition of bumetanide, the PD at 210 minute, -0.86 ± 0.25 mV, was also lower than that that at t = 90 minute (P < 0.003, as paired data). However, a dramatic change in PD upon the addition of bumetanide was not observed.

TABLE 3.2 Effect of stromal addition of 0.1 mM bumetanide on FF across the CBE preparation (n = 5).

Experiment	FF Rate		Change (%)
	Baseline	Drug-treated	
1	2.33	1.00	-57.1
2	2.17	1.00	-53.9
3	2.83	1.50	-47.0
4	2.00	1.00	-50.0
5	3.17	2.25	-29.0
Mean	**2.50**	**1.35§**	**-46.0**
SEM	**0.22**	**0.24**	

In each experiment, the FF rate (in μL/h per preparation) measured for 90 minutes prior to the introduction of bumetanide was taken as the baseline. Following the stromal addition of 0.1 mM bumetanide, 60 minutes was allowed for stabilization and the FF rate was measured thereafter for 60 minutes as the drug-treated recording.

§ Significantly lower than the baseline rate, $P < 0.001$, as paired data.

FIGURE 3.8 Effects of stromal addition of 0.1 mM bumetanide on FF and PD (n = 5). (A) The calculated FF rate in the blood-to-aqueous direction during the course of the experiment. (B) PD recorded simultaneously with the measurement of the capillary levels. The polarity of the PD was consistently negative on the aqueous side relative to the blood side. Data points are expressed as mean ± SEM. *Arrows:* the point at which bumetanide was added to the blood-side bath.

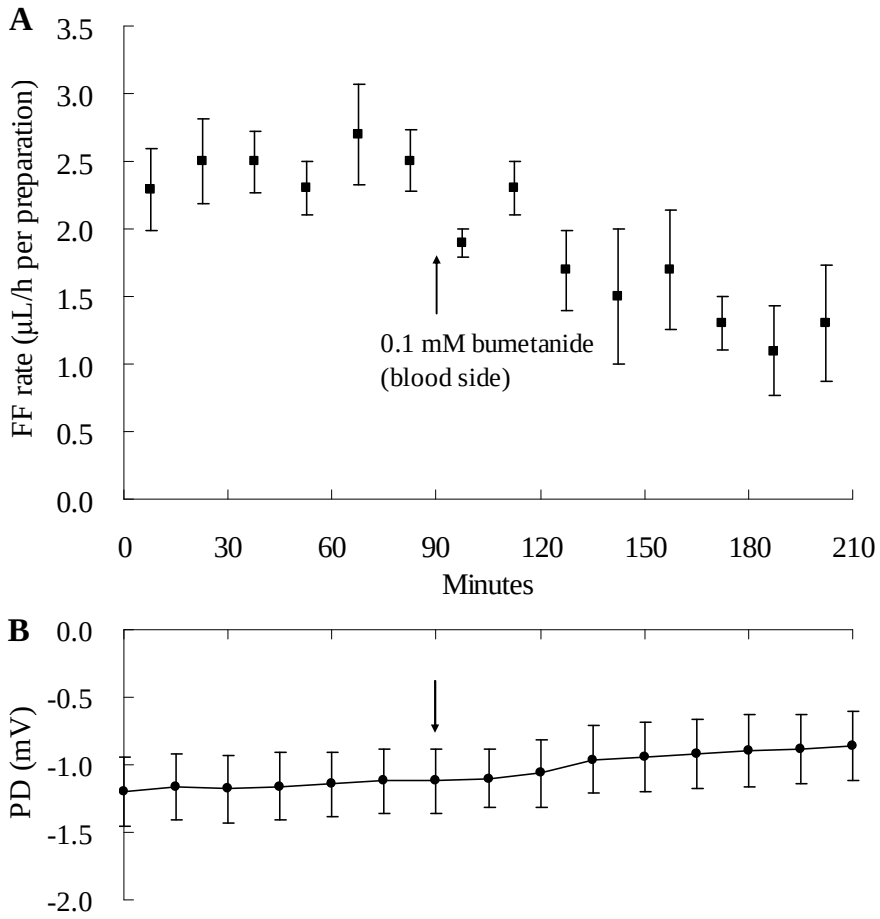

3.7 Effects of Cl^-/HCO_3^- exchanger inhibition with DIDS

Addition of DIDS (0.1 mM) to the blood side of the preparation showed no effect on both the FF and PD (Figure 3.9). The calculated FF prior to the addition of DIDS was 2.43 ± 0.12 µL/h per preparation, and after DIDS addition, it was 2.45 ± 0.09 µL/h per preparation (n = 5; P = 0.83, as paired data, Table 3.3). A greater variation in FF was observed following DIDS addition, however, there was no significant difference between each FF recorded (P > 0.05, repeated ANOVA). A minor decline in PD was observed prior to and subsequent to the addition of DIDS (Figure 3.9B). However, this steady PD drop was similar to that observed in the control experiments (Figures 3.1B and 3.2B).

TABLE 3.3 Effect of stromal addition of 0.1 mM DIDS on FF across the CBE preparation (n = 5).

Experiment	FF Rate		Change (%)
	Baseline	Drug-treated	
1	2.33	2.25	-3.4
2	2.67	2.75	3.0
3	2.50	2.50	0.0
4	2.67	2.50	-6.4
5	2.00	2.25	12.5
Mean	**2.43**	**2.45**	**0.8**
SEM	**0.12**	**0.09**	

In each experiment, the FF rate (in μL/h per preparation) measured for 90 minutes prior to the introduction of DIDS was taken as the baseline. Following the stromal addition of 0.1 mM DIDS, 60 minutes was allowed for stabilization and the FF rate was measured thereafter for 60 minutes as the drug-treated recording.

FIGURE 3.9 Effects of stromal addition of 0.1 mM DIDS on FF and PD (n = 5).

(A) The calculated FF rate in the blood-to-aqueous direction during the course of the experiment. (B) PD recorded simultaneously with the measurement of the capillary levels. The polarity of the PD was consistently negative on the aqueous side relative to the blood side. Data points are expressed as mean ± SEM. *Arrows:* the point at which DIDS was added to the blood-side bath.

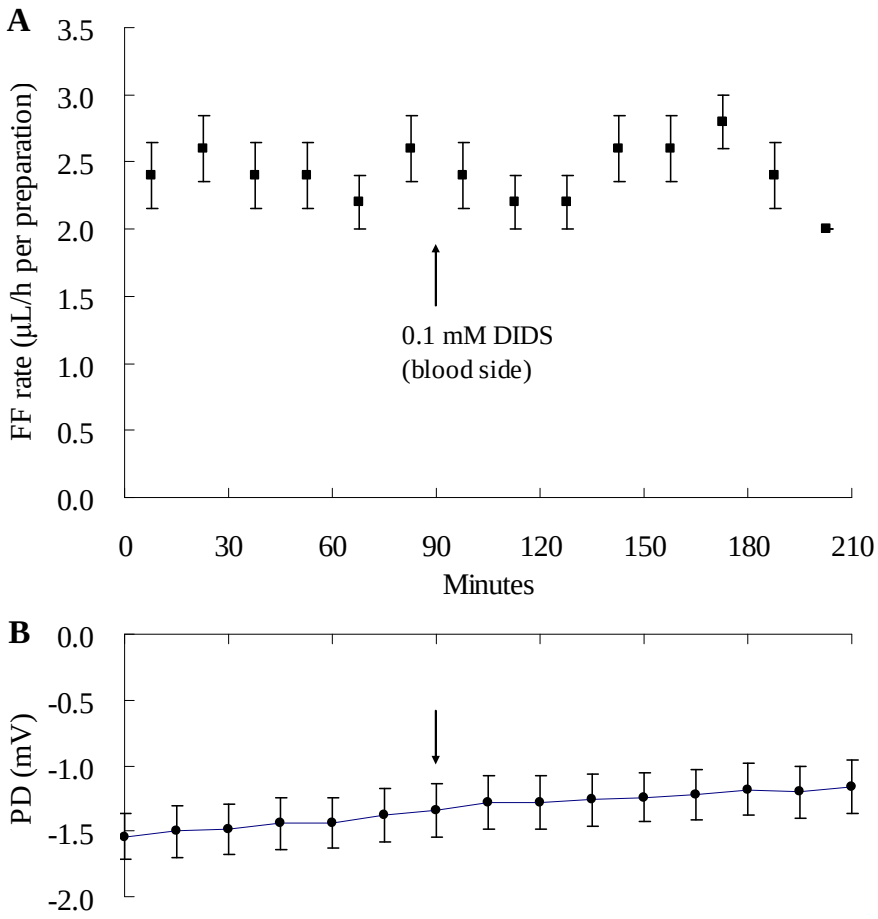

3.8 Effects of Na^+/H^+ exchanger inhibition with DMA

Similar to DIDS, addition of DMA (0.1 mM) to the blood side of the preparation showed no effect on both FF and PD (Figure 3.10). The calculated FF prior to addition of DMA was 2.53 ± 0.15 µL/h per preparation, and that after DMA addition was 2.45 ± 0.15 µL/h per preparation (n = 5; P = 0.53, as paired data, Table 3.4). No significant change in PD was observed prior to and subsequent to the addition of DMA (n = 5; P = 0.53, as paired data, Figure 3.10B).

TABLE 3.4 Effects of stromal addition of 0.1 mM DMA on FF across the CBE preparation (n = 5).

Experiment	FF Rate		Change (%)
	Baseline	Drug-treated	
1	2.83	3.00	6.0
2	2.50	2.25	-10.0
3	2.83	2.50	-11.7
4	2.50	2.25	-10.0
5	2.00	2.25	12.5
Mean	**2.53**	**2.45**	**-3.2**
SEM	**0.15**	**0.15**	

In each experiment, the FF rate (in μL/h per preparation) measured for 90 minutes prior to the introduction of DMA was taken as the baseline. Following the stromal addition of 0.1 mM DMA, 60 minutes was allowed for stabilization and the FF rate was measured thereafter for 60 minutes as the drug-treated recording.

FIGURE 3.10 Effects of stromal addition of 0.1 mM DMA on FF and PD (n = 5). (A) The calculated FF rate in the blood-to-aqueous direction during the course of the experiment. (B) PD recorded every 15 minutes simultaneously with the measurement of the capillary levels. The polarity of the PD was consistently negative on the aqueous side relative to the blood side. Data points are expressed as mean ± SEM. *Arrows:* the point at which DMA was added to the blood-side bath.

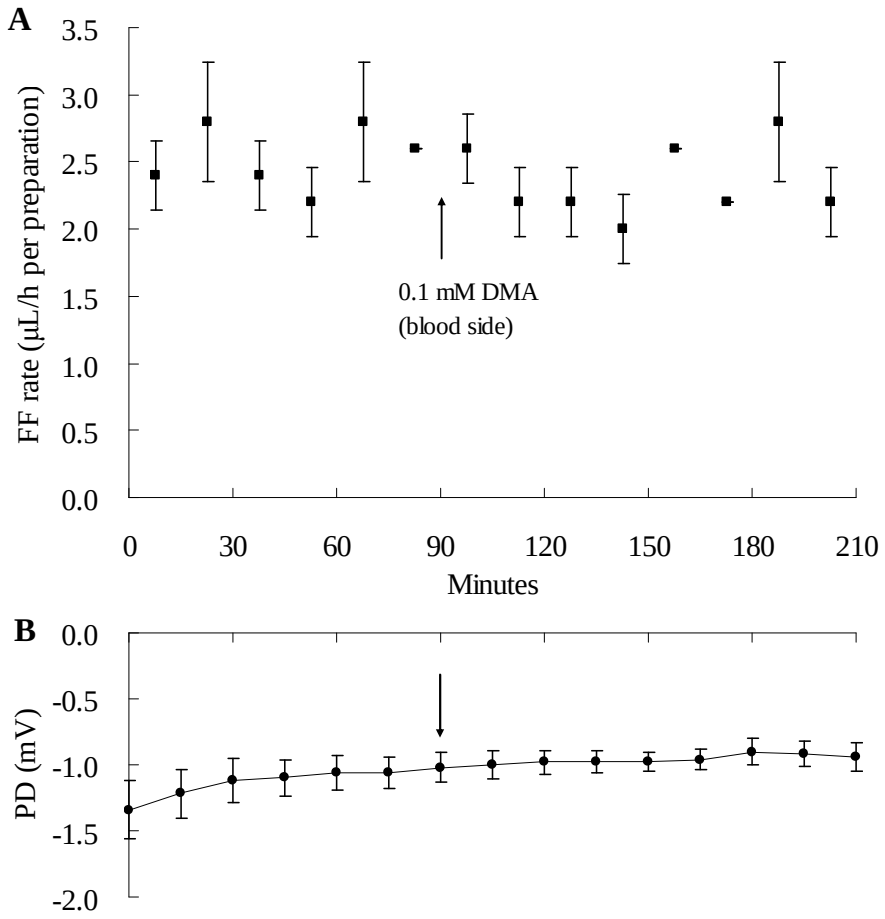

3.9 Inhibition of FF induced by gap junction inhibition with heptanol

Heptanol (3.5 mM) reduced the FF by 45% from 2.50 ± 0.25 to 1.38 ± 0.15 µL/h per preparation when it was applied to the blood side (n = 6; P < 0.007, as paired data, Table 3.5); it induced a greater inhibition of FF by 78% from 2.64 ± 0.21 to 0.58 ± 0.11 µL/h per preparation when it was applied to the aqueous (n = 6; P < 0.001, as paired data, Table 3.6). Simultaneously, it caused a significant depolarisation of the PD when added to either side. (Figures 3.11B and 3.12B). The PD declined by 58% from -1.25 ± 0.15 to -0.52 ± 0.16 mV in the case of stromal addition of heptanol (n = 6), while it depolarized to near zero from -0.90 ± 0.12 to 0.05 ± 0.11 mV in the aqueous addition (n = 6).

The action of heptanol on FF was more drastic when it was added on the aqueous side. A greater inhibition of FF of 78% was elicited by the aqueous-side addition of heptanol, compared to the 45% reduction induced by the blood-side addition (Figures 3.11A and 3.12A). Moreover, the depolarisation of PD was only 58% induced by the stromal addition of heptanol (Figure 3.11B), whereas a much larger depolarisation was caused by the aqueous addition, to the extent that the polarity of PD was subsequently reversed slightly (Figure 3.12B). The response time was also quicker in aqueous heptanol addition. The depolarisation started immediately when heptanol was added on the aqueous side whereas there was approximately a 15 minutes delay for the onset of the depolarisation when heptanol was added to the stromal side (Figures 3.11B and 3.12B).

TABLE 3.5 Effect of stromal addition of 3.5 mM heptanol on FF across the CBE preparation (n = 6).

Experiment	FF Rate		Change (%)
	Baseline	Drug-treated	
1	3.00	2.00	-33.3
2	2.17	1.00	-53.9
3	2.17	1.50	-30.9
4	2.00	1.50	-25.0
5	3.50	1.25	-64.3
6	2.17	1.00	-53.9
Mean	**2.50**	**1.38§**	**-44.8**
SEM	**0.25**	**0.15**	

In each experiment, the FF rate (in μL/h per preparation) measured for 90 minutes before the introduction of heptanol was taken as the baseline. Following the stromal addition of 3.5 mM heptanol, 60 minutes was allowed for stabilization and the FF rate was measured thereafter for 60 minutes as the drug-treated recording.

§ Significantly lower than the baseline rate, $P < 0.001$, as paired data.

TABLE 3.6 Effect of aqueous addition of 3.5 mM heptanol on FF across the CBE preparation (n = 6).

Experiment	FF Rate		Change (%)
	Baseline	Drug-treated	
1	2.67	1.00	-62.5
2	2.33	0.75	-67.8
3	2.17	0.50	-77.0
4	3.33	0.25	-92.5
5	2.17	0.50	-77.0
6	3.17	0.50	-84.2
Mean	**2.64**	**0.58§**	**-78.0**
SEM	**0.21**	**0.11**	

In each experiment, the FF rate (in μL/h per preparation) measured for 90 minutes before the introduction of heptanol was taken as the baseline. Following the aqueous addition of 3.5 mM heptanol, 60 minutes was allowed for stabilization and the FF rate was measured thereafter for 60 minutes as the drug-treated recording.

§ Significantly lower than the baseline rate, $P < 0.001$, as paired data.

FIGURE 3.11 Effects of stromal addition of 3.5 mM heptanol on FF and PD (n = 6). (A) The calculated FF rate in the blood-to-aqueous direction during the course of the experiment. (B) PD recorded simultaneously with the measurement of the capillary levels. The polarity of the PD was consistently negative on the aqueous side relative to the blood side. Data points are expressed as mean ± SEM. *Arrows:* the point at which heptanol was added to the blood-side bath.

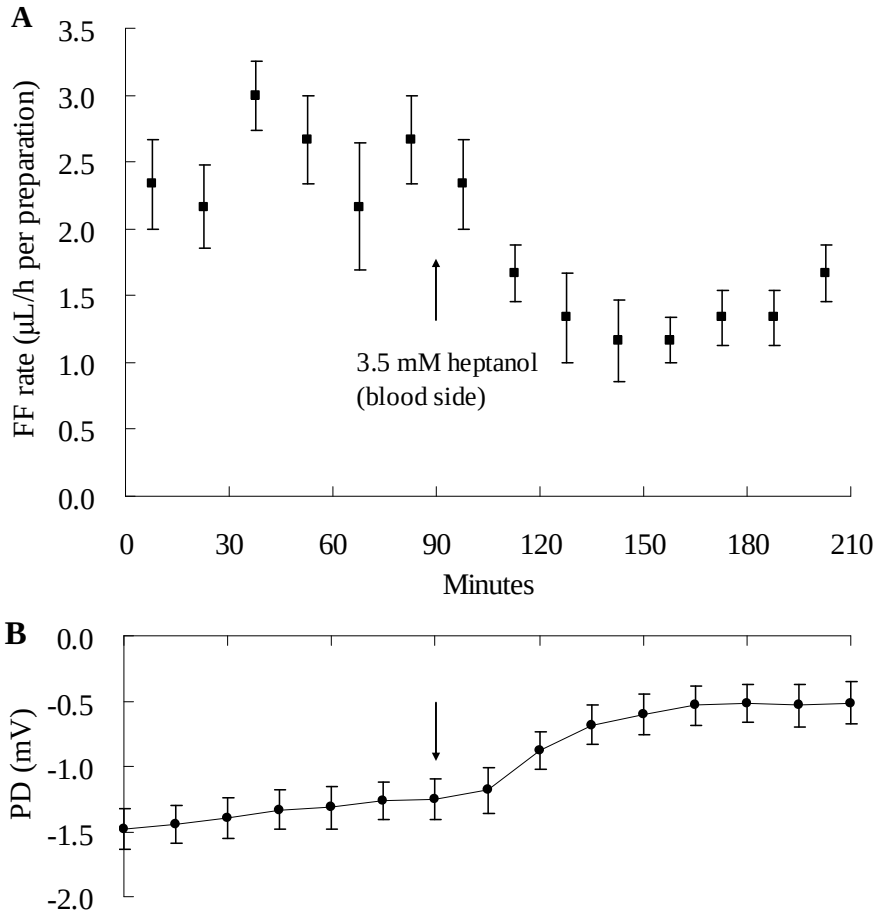

FIGURE 3.12 Effects of aqueous addition of 3.5 mM heptanol on FF and PD (n = 6). (A) The calculated FF rate in the blood-to-aqueous direction during the course of the experiment. (B) PD recorded simultaneously with the measurement of the capillary levels. The polarity of the PD was consistently negative on the aqueous side relative to the blood side. Data points are expressed as mean ± SEM. *Arrows:* the point at which heptanol was added to the aqueous-side bath.

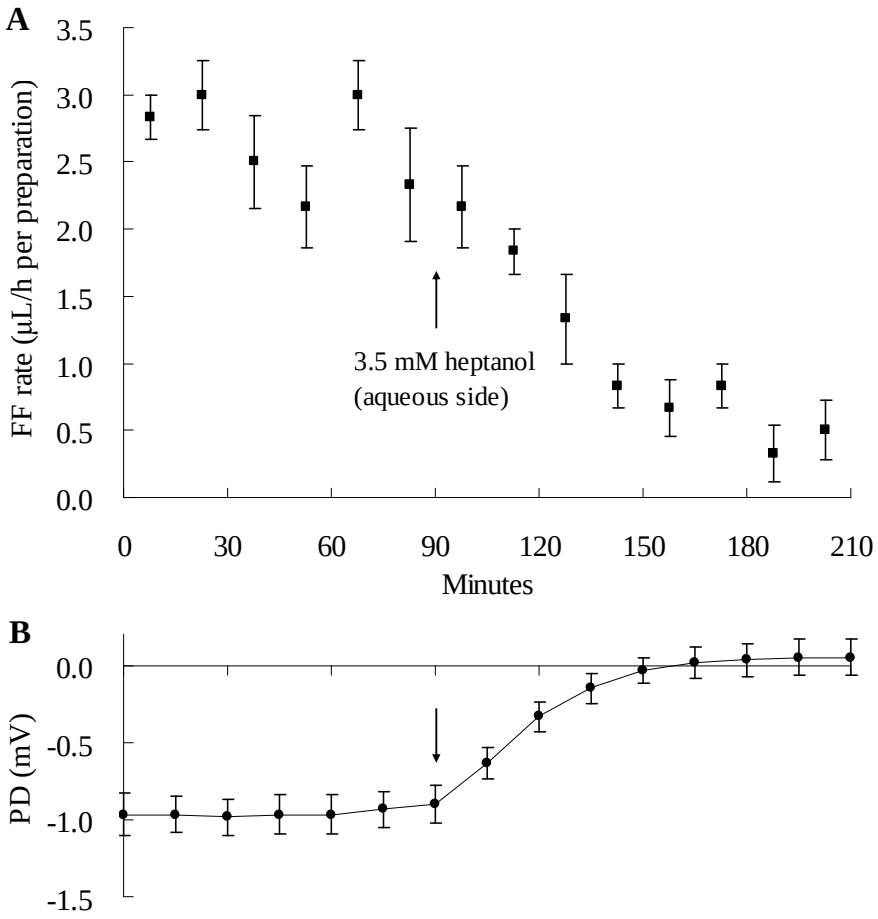

3.10 Inhibition of FF induced by Cl^- channel blockade with niflumic acid

Figure 3.13A shows the time-course of FF upon the aqueous addition of niflumic acid. Addition of niflumic acid (1 mM) in the aqueous-side bath significantly reduced the FF by 61% from 2.69 ± 0.15 to 1.04 ± 0.15 µL/h per preparation (n = 6; P < 0.001, as paired data, Table 3.7) and caused a complete depolarisation of the PD (Figure 3.13B). Upon the addition of niflumic acid at t = 90 minute, the PD depolarized tremendously such that the polarity slightly reserved from -0.78 ± 0.06 to 0.12 ± 0.08 mV in 1 hour and sustained to the end of experiment.

TABLE 3.7 Effect of aqueous addition of 1 mM niflumic acid on FF across the CBE preparation (n = 6).

Experiment	FF Rate		Change (%)
	Baseline	Drug-treated	
1	2.50	0.75	-70.0
2	3.00	1.50	-50.0
3	2.83	0.50	-82.3
4	2.33	1.25	-46.4
5	2.33	1.00	-57.1
6	3.17	1.25	-60.6
Mean	**2.69**	**1.04§**	**-61.3**
SEM	**0.15**	**0.15**	

In each experiment, the FF rate (in μL/h per preparation) measured for 90 minutes before the addition of the drug was taken as the baseline. Following the aqueous addition of 1 mM niflumic acid, 60 minutes was allowed for stabilization, and the FF rate was measured thereafter for 60 minutes as the drug-treated recording.

§ Significantly lower than the baseline rate, $P < 0.001$, as paired data.

FIGURE 3.13 Effects of aqueous addition of 1 mM niflumic acid on FF and PD (n = 6). (A) The calculated FF rate in the blood-to-aqueous direction during the course of the experiment. (B) PD recorded every 15 minutes simultaneously with the measurement of the capillary levels. The polarity of the PD was consistently negative on the aqueous side relative to the blood side. Data points are expressed as mean ± SEM. *Arrows:* the point at which niflumic acid was added to the aqueous-side bath.

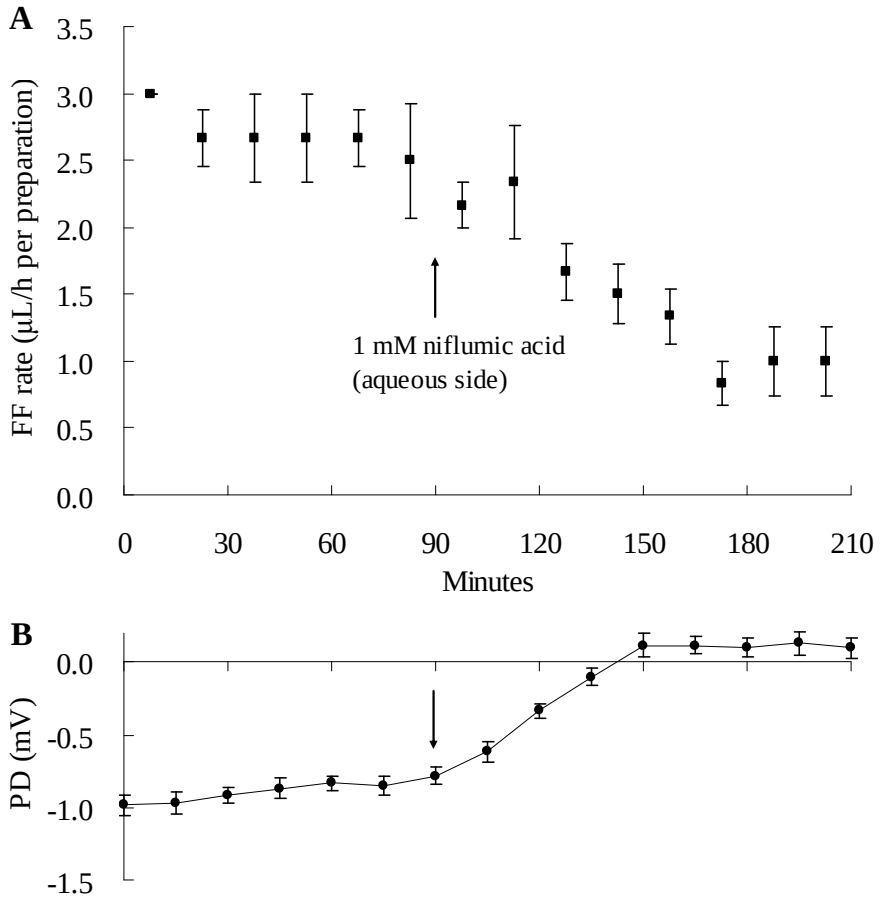

3.11 Baseline values of FF and electrical parameters measured using FC2

In FC2, with the capillary tube placed in the blood-side compartment (n = 8, Figure 3.14A), the mean FF rate was 2.34 ± 0.18 and 2.27 ± 0.20 µL/h per preparation for the first and second 2-h periods, respectively. There was no difference between the two measured FF rates (P = 0.47, as paired data). And the FF rates measured using FC2 was not different from that using FC1 (P = 0.44, one-way ANOVA, as unpaired data).

The PDs across the CBE preparations with the capillary connected to the blood side are plotted as a function of time (Figure 3.14B). The polarity of the PD was consistently negative on the aqueous side. With the capillary placed on blood side, the mean PD was initially -1.03 ± 0.13 mV and slightly declined to -0.91 ± 0.15 mV after 4 hours. There was no difference between the PDs measured at each time point throughout the course of experiment (P = 0.47, one-way ANOVA, as paired data).

The mean R_t was initially 153.8 ± 6.3 Ωcm^2 and maintained at 151.3 ± 6.4 Ωcm^2 after 4 hours (Figure 3.14C). There was no significant difference between the R_t measured at each time point throughout the 4-hour experiment (n = 8; P = 0.57, one-way ANOVA, as paired data).

Comparing to the results obtained with FC1, both the FF and PD measured with FC2 were found to be more stable throughout the course of experiment. This was possibly due to an improvement in the techniques of dissection and mounting, and the careful selection of viable preparations.

FIGURE 3.14 Simultaneous measurement of FF, PD and R_t across the isolated porcine CBE using FC2 (n = 8). (A) The calculated FF rate in the blood-to-aqueous direction during the course of the experiment. (B) PD recorded simultaneously with the measurement of the capillary levels. The polarity of the PD was consistently negative on the aqueous side relative to the blood side. (C) R_t calculated by applying a 10 μA current across the preparation every 30 minutes. Data points are expressed as mean ± SEM.

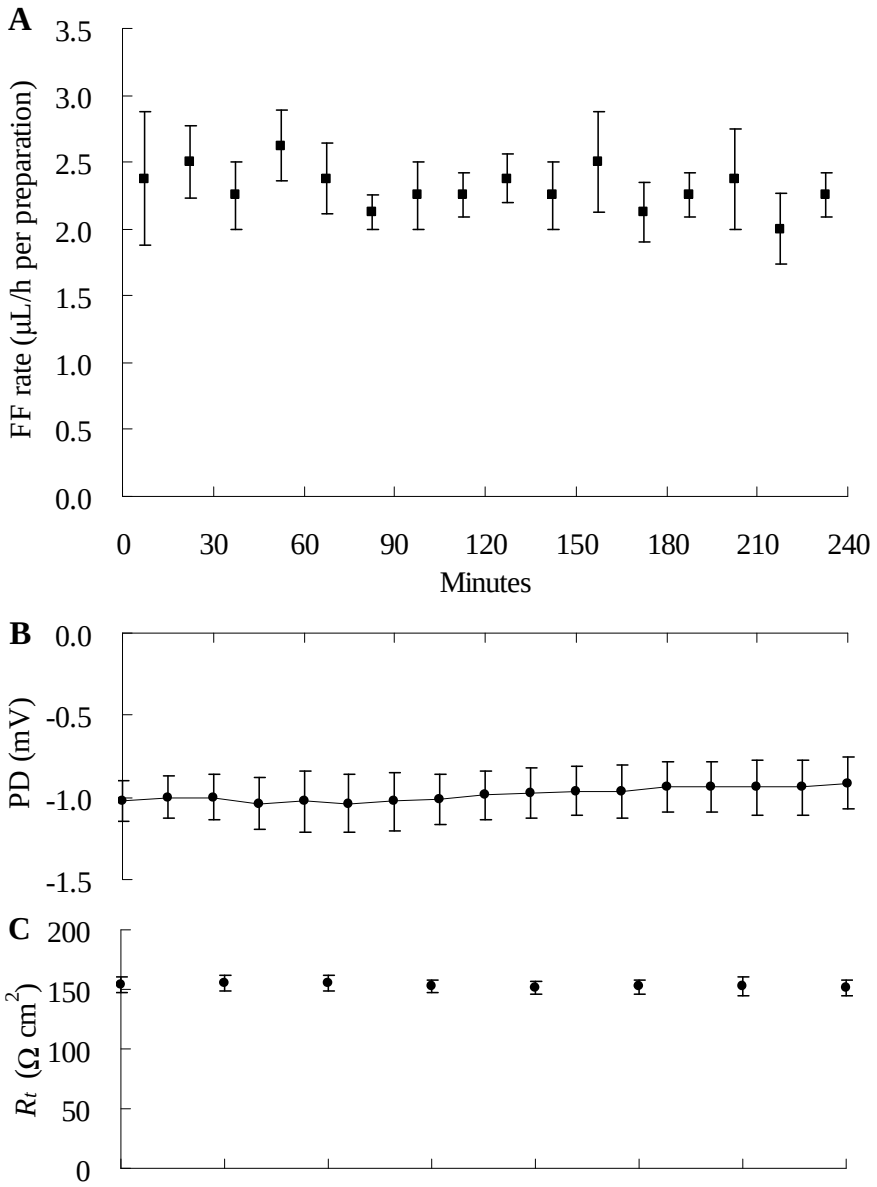

3.12 Stimulation of FF and PD elicited by AC activation with forskolin

In contrast to the inhibitors previously mentioned, forskolin elicited stimulatory effects on both FF and PD. The addition of forskolin at 10 μM to the aqueous side stimulated the FF and caused a hyperpolarisation of the PD. The mean baseline FF was 2.27 ± 0.28 μL/h per preparation (calculated from 90 minutes of 5 experiments), following forskolin addition at t = 90 minute, the FF increased within 45 minutes as shown in Figure 3.15A. The mean FF increased by 21% to 2.73 ± 0.32 μL/h per preparation as calculated within the period 90-135 minutes (n = 5; P < 0.005, as paired data). In individual experiment, since the maximal stimulation of FF occurred at different intervals within the calculated period, averaging the FF in the entire period may underestimate the stimulatory effects. Thus, the maximum FF observed in individual experiment was compared to their respective baseline value, which corresponded to an average stimulation of FF by ~42% (P < 0.005, as paired data) as shown in Table 3.8. Subsequent to the transient increase induced by forskolin, the FF returned to 2.25 ± 0.27 μL/h per preparation (calculated from the last 60 minutes), a level comparable to the baseline value (P = 0.37, as paired data).

In addition to FF increase, the PD was hyperpolarized from -0.74 ± 0.10 to -1.48 ± 0.06 mV (100% increase; P < 0.005, as paired data) at ~30 minutes following forskolin addition (Figure 3.15B). No significant change in the R_t was observed prior to and subsequent to the addition of forskolin (Figure 3.15C). The mean R_t was 143.0 ± 14.9 Ωcm^2 at t = 90 minute, and 138.0 ± 15.2 Ωcm^2 at t = 210 minute (P > 0.05, as paired data).

TABLE 3.8 Effects of aqueous addition of 10 μM forskolin on FF and PD across the CBE preparation (n = 5).

	FF rate			PD		
Experiment	**Baseline**	**Peak FF**	**Change %**	**Control**	**Peak PD**	**Change %**
1	2.83	4.00	41.2	-0.90	-1.40	55.6
2	3.00	4.00	33.3	-0.90	-1.50	66.7
3	1.50	2.00	33.3	-0.60	-1.60	166.7
4	2.00	3.00	50.0	-0.40	-1.30	225.0
5	2.00	3.00	50.0	-0.90	-1.60	77.8
Mean	**2.27**	**3.20‡**	**41.6**	**-0.74**	**-1.48‡**	**100.0**
SEM	**0.28**	**0.37**		**0.10**	**0.06**	

In each experiment, the FF rate (in μL/h per preparation) measured for 90 minutes prior to the introduction of forskolin was taken as the baseline. The PD (in mV) recorded prior to the drug addition was taken as the control. The peak FF and PD represent the maximum stimulation of FF and PD observed respectively following the aqueous addition of forskolin.

‡ $P < 0.005$, significantly different from the baseline value as paired data.

FIGURE 3.15 Effects of aqueous addition of 10 μM forskolin on FF, PD and R_t (n = 5). (A) The calculated FF rate in the blood-to-aqueous direction during the course of the experiment. (B) PD recorded simultaneously with the measurement of the capillary levels. The polarity of the PD was consistently negative on the aqueous side relative to the blood side. (C) R_t calculated by applying a 10 μA current across the preparation every 30 minutes. Data points are expressed as mean ± SEM. *Arrows:* the point at which forskolin was added to the aqueous-side bath.

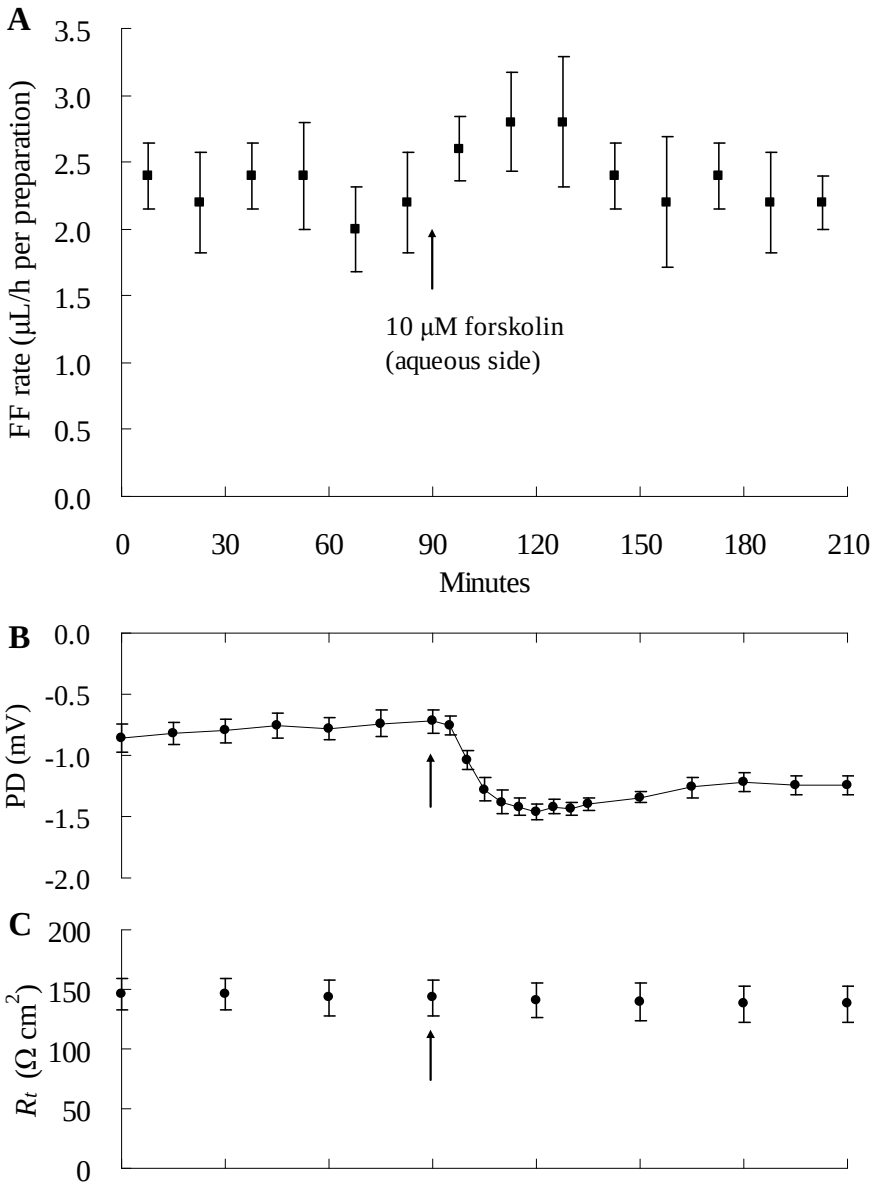

3.13 Stimulation of FF and PD elicited by cAMP analogue 8-Br-cAMP

Similar to forskolin, the addition of cAMP analogue 8-Br-cAMP stimulated both the FF and PD. The mean baseline FF was 2.47 ± 0.15 µL/h per preparation (calculated from 90 minutes of 5 experiments), following 8-Br-cAMP addition at t = 90 minute, the FF increased within 45 minutes as shown in Figure 3.16A. The mean FF increased by 27% to 3.13 ± 0.17 µL/h per preparation in the period 90-135 minutes (n = 5; P < 0.001, as paired data). The maximal stimulation of FF induced by 8-Br-cAMP was ~54% (P < 0.005, as paired data) as shown in Table 3.9. Subsequent to the transient increase induced by 8-Br-cAMP, the FF returned to 2.15 ± 0.13 µL/h per preparation (calculated from the last 60 minutes), a rate not significantly different from the baseline value (P = 0.07, as paired data).

In addition to stimulation in FF, the PD was drastically hyperpolarised from -0.70 ± 0.09 to -1.90 ± 0.14 mV (171% increase; P < 0.001, as paired data) at t = 105 minute, 15 minutes following 8-Br-cAMP addition (Figure 3.16B). No significant change in the R_t was observed prior to and subsequent to the addition of 8-Br-cAMP (Figure 3.16C). The mean R_t was 145.0 ± 9.0 Ωcm^2 at t = 90 minute, and 144.0 ± 8.9 Ωcm^2 at t = 210 minute (P = 0.39, as paired data).

TABLE 3.9 Effects of aqueous addition of 100 μM 8-Br-cAMP on FF and PD across the CBE preparation (n = 5).

	FF rate			PD		
Experiment	**Baseline**	**Peak FF**	**Change %**	**Control**	**Peak PD**	**Change %**
1	3.00	4.00	33.3	-1.00	-2.40	140.0
2	2.17	4.00	84.6	-0.80	-2.00	150.0
3	2.17	3.00	38.5	-0.60	-1.80	200.0
4	2.50	4.00	60.0	-0.60	-1.70	183.3
5	2.50	4.00	60.0	-0.50	-1.60	220.0
Mean	**2.47**	**3.80‡**	**54.1**	**-0.70**	**-1.90§**	**171.4**
SEM	**0.15**	**0.20**		**0.09**	**0.14**	

In each experiment, the FF rate (in μL/h per preparation) measured for 90 minutes prior to the introduction of 8-Br-cAMP was taken as the baseline. The PD (in mV) recorded prior to the drug addition was taken as the control. The peak FF and PD represent the maximum stimulation of FF and PD observed respectively following the aqueous addition of 8-Br-cAMP.

‡ $P < 0.005$; § $P < 0.001$, significantly different from the baseline value as paired data.

FIGURE 3.16 Effects of aqueous addition of 100 μM 8-Br-cAMP on FF, PD and R_t (n = 5). (A) The calculated FF rate in the blood-to-aqueous direction during the course of the experiment. (B) PD recorded simultaneously with the measurement of the capillary levels. The polarity of the PD was consistently negative on the aqueous side relative to the blood side. (C) R_t calculated by applying a 10 μA current across the preparation every 30 minutes. Data points are expressed as mean ± SEM. *Arrows:* the point at which 8-Br-cAMP was added to the aqueous-side bath.

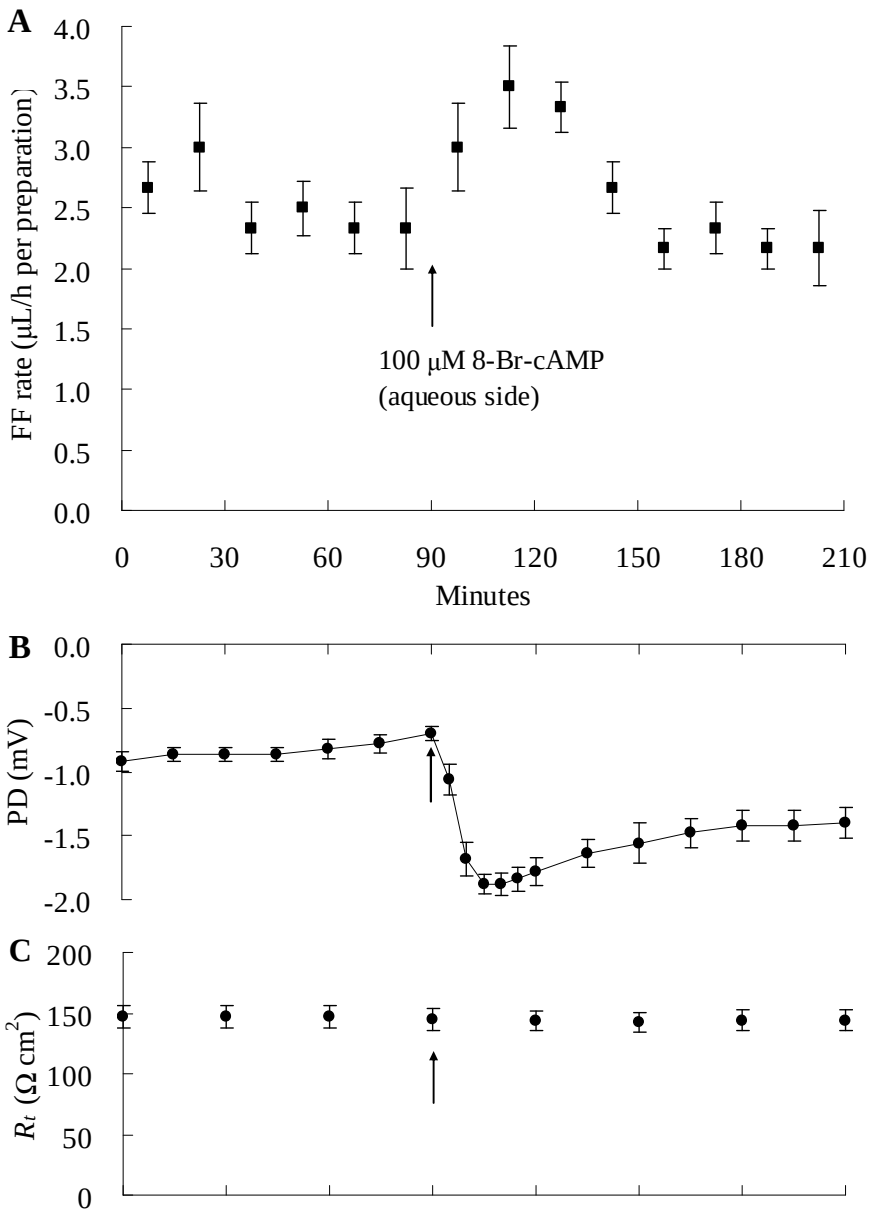

3.14 Effects of phosphodiesterase (PDE) inhibition with IBMX

The addition of IBMX (1 mM) to the aqueous-side bath only slightly stimulated the PD but caused no effects on the FF. The mean baseline FF was 2.71 ± 0.15 µL/h per preparation (calculated from 60 minutes of 6 experiments), following IBMX addition at t = 60 minute, the mean FF maintained at 2.67 ± 0.14 µL/h per preparation in 60-120 minutes (n = 6; P = 0.74, compared to baseline as paired data), and 2.54 ± 0.20 µL/h per preparation in 120-180 minutes (P = 0.17, compared to baseline as paired data, Figure 3.17A).

The PD was slightly hyperpolarized from -0.93 ± 0.10 to -1.13 ± 0.11 mV (22% increase; P < 0.004, as paired data) at 15 minutes following IBMX addition (Figure 3.17B). No significant change in the R_t was observed prior to and subsequent to the addition of IBMX (P = 0.69, as paired data, Figure 3.17C). The mean R_t was 135.0 ± 13.8 Ωcm^2 at t = 60 minute, and 133.3 ± 14.1 Ωcm^2 at t = 180 minute (P = 0.69, as paired data).

FIGURE 3.17 Effects of aqueous addition of 1 mM IBMX on FF, PD and R_t (n = 6). (A) The calculated FF rate in the blood-to-aqueous direction during the course of the experiment. (B) PD recorded simultaneously with the measurement of the capillary levels. The polarity of the PD was consistently negative on the aqueous side relative to the blood side. (C) R_t calculated by applying a 10 μA current across the preparation every 30 minutes. Data points are expressed as mean ± SEM. *Arrows:* the point at which IBMX was added to the aqueous-side bath.

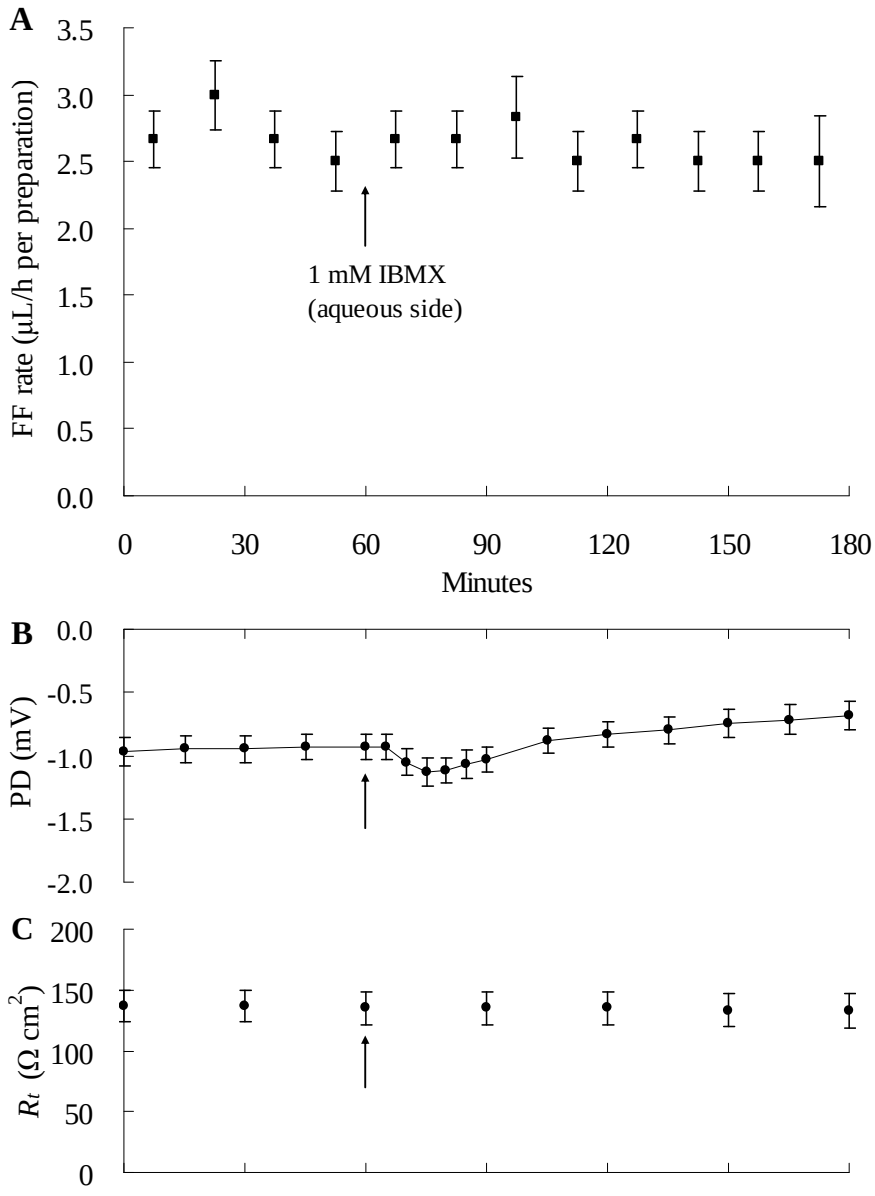

3.15 Effects of protein kinase A (PKA) inhibition with H-89

H-89 is a member of the chemically synthesized H-series protein kinase inhibitors introduced by Hidaka and co-workers (Hidaka et al., 1991; Hidaka and Kobayashi, 1992), having the highest affinity for PKA. The pre-treatment with 10 μM H-89 at the aqueous side was ineffective in preventing the stimulatory effects of 8-Br-cAMP on the FF and PD. Statistical analysis was conducted by comparing the percentage increase of FF and PD as stimulated by 8-Br-cAMP alone (Table 3.9) and with the pre-treatment of 10 μM H-89 as shown in Table 3.10A. There was no statistical significant difference between them ($P > 0.35$, as unpaired data).

However, the pre-exposure of H-89 at 50 μM significantly reduced the 8-Br-cAMP-induced stimulation of FF and PD. With the pre-treatment of H-89 (50 μM) for 60 minutes, stimulation of FF and PD induced by the addition of 8-Br-cAMP (100 μM) was blocked by 65% and 52% respectively. The mean baseline FF was 2.70 ± 0.18 μL/h per preparation (calculated from 60 minutes of 5 experiments), following 8-Br-cAMP addition at t = 90 minute, the mean FF was 3.13 ± 0.27 μL/h per preparation in the period 90-135 minutes, which was not significantly different from the baseline value ($n = 5$; $P = 0.06$, as paired data). The average peak FF was 3.20 ± 0.20 μL/h per preparation (~19% increase, $P < 0.05$, as paired data, Table 3.10B), corresponding to a 65% reduction as compared to the 54% stimulation of FF induced by 8-Br-cAMP ($P < 0.01$, as unpaired data). Subsequently, the FF declined to 2.20 ± 0.14 μL/h per preparation (calculated from the last 60 minutes), a rate of about 19% lower than the baseline level ($P < 0.05$, as paired data, Figure 3.18A).

In addition, the PD was modestly hyperpolarized from -0.82 ± 0.07 to -1.50 ± 0.10 mV (83% increase; $P < 0.001$, as paired data, Table 3.10B) at t = 105 minute

(Figure 3.18B), which was equivalent to 52% inhibition of the expected stimulation by 8-Br-cAMP, considering the average 171% stimulation of PD by 8-Br-cAMP ($P < 0.001$, as unpaired data). No significant change in the R_t was observed prior to and subsequent to the addition of 8-Br-cAMP (Figure 3.18C). The mean R_t was 106.0 ± 6.8 Ω cm^2 at t = 90 minute, declined to 102.0 ± 6.4 Ω cm^2 at t = 210 minute ($P = 0.18$, as paired data).

TABLE 3.10 Effects of pre-treatment of aqueous-side H-89 on 8-Br-cAMP-induced stimulation of FF and PD across the CBE preparation.

(A) 10 μM H-89 (n = 5)

	FF rate			PD		
Experiment	**Baseline**	**Peak FF**	**Change %**	**Control**	**Peak PD**	**Change %**
1	2.00	3.00	50.0	-0.70	-1.30	85.7
2	2.50	4.00	60.0	-0.40	-1.30	225.0
3	2.50	4.00	60.0	-0.60	-2.00	233.3
4	2.25	3.00	33.3	-0.50	-1.30	160.0
5	3.00	4.00	33.3	-1.10	-2.40	118.2
Mean	**2.45**	**3.60‡**	**46.9**	**-0.66**	**-1.66‡**	**151.5**
SEM	**0.17**	**0.24**		**0.12**	**0.23**	

(B) 50 μM H-89 (n = 5)

	FF rate			PD		
Experiment	**Baseline**	**Peak FF**	**Change %**	**Control**	**Peak PD**	**Change %**
1	2.50	3.00	20.0	-0.70	-1.30	85.7
2	3.00	3.00	0.0	-1.00	-1.80	80.0
3	2.25	3.00	33.3	-0.60	-1.30	116.7
4	2.50	3.00	20.0	-0.80	-1.40	75.0
5	3.25	4.00	23.1	-1.00	-1.70	70.0
Mean	**2.70**	**3.20***	**18.5**	**-0.82**	**-1.50§**	**82.9**
SEM	**0.18**	**0.20**		**0.07**	**0.10**	

In each experiment, H-89 was pre-treated on the aqueous side for 60 minutes prior to the introduction of 8-Br-cAMP. The FF rate (in μL/h per preparation) measured for 60 minutes following the addition of H-89 was taken as the baseline. The PD (mV) recorded prior to the addition of 8-Br-cAMP was taken as the control. The peak FF and PD represents the maximum stimulation of FF and PD observed respectively following the aqueous addition of 8-Br-cAMP.

* $P < 0.05$; ‡ $P < 0.005$; § $P < 0.001$, significantly different from the baseline value as paired data.

FIGURE 3.18 Effects of pre-treatment of aqueous-side 50 μM H-89 on the 8-Br-cAMP-induced stimulation of FF and PD (n = 5). (A) The calculated FF rate in the blood-to-aqueous direction during the course of the experiment. (B) PD recorded simultaneously with the measurement of the capillary levels. The polarity of the PD was consistently negative on the aqueous side relative to the blood side. (C) R_t calculated by applying a 10 μA current across the preparation every 30 minutes. Data points are expressed as mean ± SEM. *Arrows:* the points at which H-89 and 8-Br-cAMP were separately added to the aqueous-side bath.

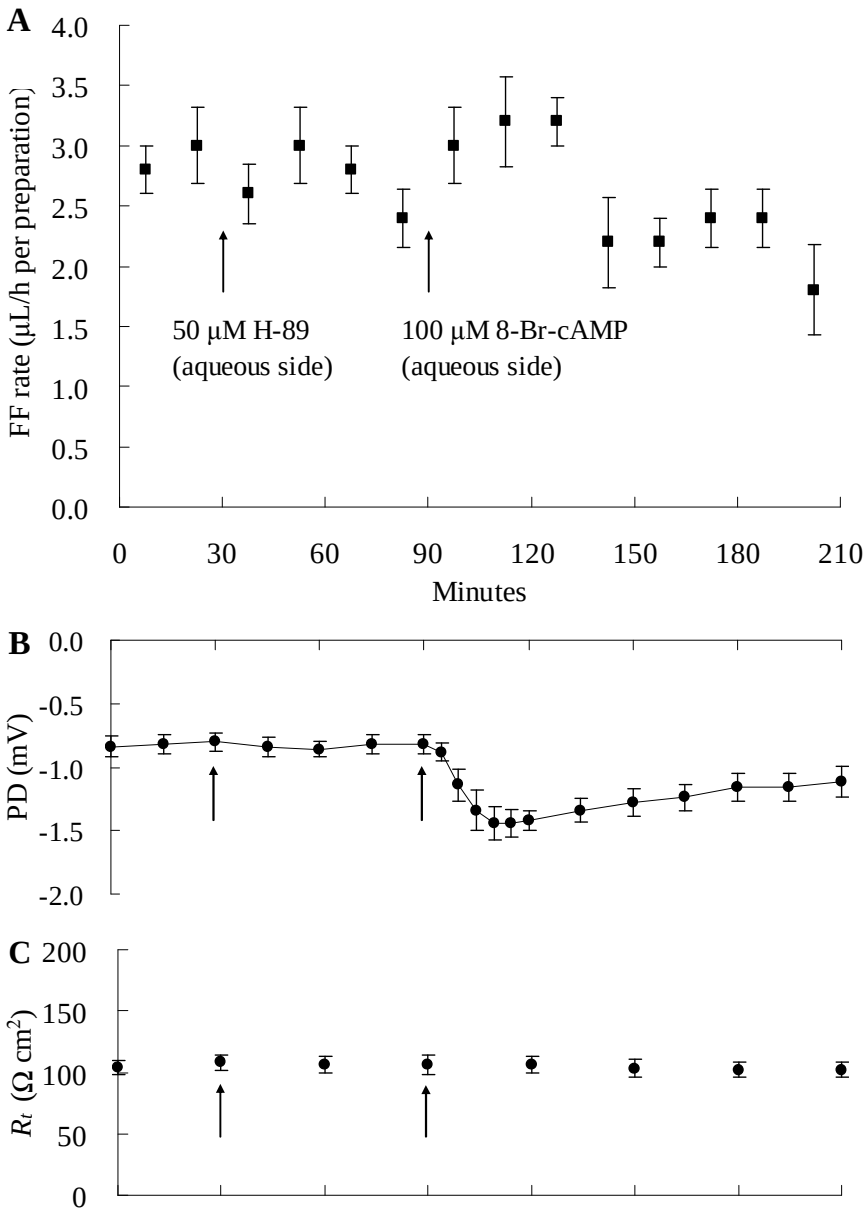

CHAPTER 4

DISCUSSIONS

4.1 Baseline transmural fluid movement in the blood-to-aqueous direction

The present study represents the first report of a simultaneous measurement of spontaneous fluid transport and transepithelial potential difference by the porcine CBE, with a volumetric technique similar to one that previously developed for measurements of spontaneous fluid flows across isolated rabbit and bovine CBE preparations (Candia et al., 2005). The spontaneous fluid movement is readily measurable using a graduated capillary which reflects the volumetric change inside the chamber. A consistent decline of the blood-side fluid volume and a consistent rise in the aqueous-side fluid volume represent a fluid movement in the blood-to-aqueous direction. This fluid movement solely reflects the secretory activity of the isolated ciliary epithelium because the *in vitro* arrangement precludes contributions from ultrafiltration, as well as externally applied osmotic or pressure gradients. One of the main findings of the present study is that the porcine CBE preparation exhibited longer sustained rates of FF than those obtained with CBE preparations of bovine and rabbit (Candia et al., 2005). Although the absolute values for FF among the preparations of the three species were largely similar, the FF across the bovine and rabbit preparations gradually declined within 3 to 4 hours (Candia et al., 2005). In contrast, the porcine preparations were relatively robust in that FF could be maintained *in vitro* for 4 hours under control conditions.

4.2 Baseline transepithelial electrical parameters

The transepithelial electrical parameters of control preparations declined, but subsisted over 3 to 4 hours, suggesting that the driving force for *in vitro* spontaneous fluid transport was not lost within this period. The polarity of the PD was negative on the aqueous side relative to the blood side of the porcine CBE, as reported earlier with isolated ICB preparations of cat (Holland and Gipson, 1970), rabbit (Kishida et al., 1982; Krupin et al., 1984), ox (Do and To, 2000) and pig (Kong et al., 2006). This parameter indicates a net movement of anions across the CBE to the aqueous-side bath. With the exception of the rabbit species (Candia et al., 2005), Cl^- is most likely the predominant anion transported, as a net Cl^- secretion has been demonstrated both in the bovine (Do and To, 2000) and porcine CBE (Kong et al., 2006). There are presently no direct indications of a net transport of other anions or of a net movement of cations in the opposite direction. Consistent with a net flux of Cl^- across the porcine CBE in the blood-to-aqueous direction, the steady state Cl^- level of the porcine AH is higher than that in the plasma (Gerometta et al., 2005).

4.3 Anionic dependent FF (Cl^- and HCO_3^-)

The linkage between FF and the stromal Cl^- concentration is apparent in the data where removing Cl^- drastically reduced the FF. This observation is consistent with a net Cl^- flux in the aqueous direction that was found in isolated porcine CBE preparations in chambers comparable to those used presently (Kong et al., 2006) and also congruent with the inhibitory effects of various Cl^- transport inhibitors on the FF (to be discussed later in this Chapter). As such, the spontaneous, transmural volume change detected under control conditions appears to represent, at least in part, a net fluid transport secondary to active Cl^- transport by the porcine CBE.

In addition, the porcine CBE may also mediate a net HCO_3^- transport in the same direction as that of Cl^-. However, corroborative evidence for this notion is currently lacking and the present data do not substantiate it. Solution changes were made unilaterally, because the chamber design necessary for monitoring FF required a closed capillary-containing compartment. As such, a significant movement of HCO_3^- across both transcellular and paracellular pathways from the HCO_3^--rich bath to the opposite-side solution may have contributed to (1) the reduction in FF obtained on removing CO_2/HCO_3^- from the blood-side hemichamber (Figure 3.4A), and (2) the increase in FF on introducing CO_2/HCO_3^- to the blood-side bath of tissues pre-equilibrated under bicarbonate-free conditions (Figure 3.5A). Either a net bicarbonate transport was indeed present, or the Cl^- fluxes in the aqueous direction was somehow dependent on the presence of cellular H^+ and HCO_3^- (from metabolic CO_2 production and endogenous carbonic anhydrase activity), which are then exchanged with Na^+ and Cl^- via parallel Na^+/H^+ and Cl^-/HCO_3^- antiporters in the PE, as suggested in the case of the rabbit ciliary epithelial cells studied by electron probe X-ray microanalysis (McLaughlin et al., 1998). This possible mechanism would have

been precluded during the initial baseline period with HCO_3^--free solutions with 100% O_2 gassing in the experiments shown in Figure 3.5A, thereby resulting in the markedly lower rate of fluid transport under these conditions.

The PD across the porcine CBE was maintained stable at -0.55 mV with bilateral HCO_3^--free medium, whereas a reversed polarity of PD in rabbit CBE preparation was observed when bathed in HCO_3^--free medium (Kishida et al., 1981; Krupin et al., 1984). Only a minor alteration of PD was observed upon the depletion and restoration of CO_2/HCO_3^- medium in the porcine preparations. Apparently although these maneuvers caused little effects in ionic transport, it induced significant effect in FF.

The drastic hyperpolarisation of PD observed upon the stromal reduction of Cl^- concentration is likely due to an imbalance of Cl^- concentrations between the two sides of the preparation (120 mM on aqueous side versus 7 mM on stromal side). This imbalance led to differential junctional potentials between the sensing electrodes of the two baths. The observed reversed FF may possibly be due to the Cl^- imbalance, which favours the backward diffusion of Cl^- and parallel fluid movement through the paracellular route. Moreover, transcellular reabsorption of Cl^- as postulated by Civan and Macknight (2004) may be activated under this experimental manipulation. Given that the Cl^- concentration was markedly reduced in the stromal bath, the intracellular Cl^- level possibly exceeded the thermodynamic equilibrium of the Na^+-K^+-$2Cl^-$ cotransporter for the uptake of ions into the PE cells. Under this condition, the Na^+-K^+-$2Cl^-$ cotransporter may have been thermodynamically favoured to transport solutes out of the PE cells back to the stroma. However, current findings are inadequate to verify this hypothesis. Further studies are required to investigate the potential contribution of reabsorption in the CBE.

4.4 Active ionic transport mediated fluid movement

The overall effects of ouabain on the PD were largely similar when applied to either the blood- or aqueous-side baths, but its inhibitory effects on FF were more pronounced when it was added to the blood side. It has been demonstrated that the two cell layers possess Na^+,K^+-ATPase transporters (Riley and Kishida, 1986; Flugel and Lutjen-Drecoll, 1988; Ghosh et al., 1990; Mori et al., 1991). In other studies, ouabain elicited a prompt depolarisation of the transmural PD across the CBE at the blood side and triggered a hyperpolarisation when added to the aqueous bath (Burstein et al., 1984a; Krupin et al., 1984). These initial changes commonly reverse as the glycoside diffuses across the preparation and inhibits the pump activity on the opposite-side cell layer. The initial depolarisation obtained on adding ouabain to the blood-side bath (Figure 3.6B) was not as pronounced as reported previously (Burstein et al., 1984a; Krupin et al., 1984). It was rapidly followed by a hyperpolarisation, suggesting that the diffusion of ouabain across the porcine preparation was either quite fast across other preparations, or the levels of ouabain used (1 mM) was high enough to facilitate fast delivery to the opposite-side cell layer. The attenuation of the Na^+ gradient within the bilayered CBE may have occurred faster when ouabain was added to the blood-side bath, so that the inhibitory effects (97% reduction) on FF were more evident (in contrast, there was only a 61% reduction in FF after 2 hours of aqueous-side ouabain exposure). The sidedness of the effectiveness of ouabain is reminiscent of the greater potency of bumetanide when applied from the blood side of the bovine CBE (Do and To, 2000).

4.5 Uptake pathways in the PE

There are two pathways proposed for the uptake of anions into the PE cells: Na^+/H^+ and Cl^-/HCO_3^- parallel antiporters and Na^+-K^+-$2Cl^-$ cotransporter. The importance of the paired Na^+/H^+ and Cl^-/HCO_3^- antiporter system has been shown in rabbit CE, suggested that the paired exchangers play a role in the loading of HCO_3^- ions in the PE cells (Butler et al., 1994). It has been suggested that the paired antiporter system is predominant in rabbit CE, which plays a major role in the HCO_3^- transport across the epithelium (Wolosin et al., 1991; Wolosin et al., 1993; Butler et al., 1994). Moreover, the Na^+/H^+ and Cl^-/HCO_3^- exchangers have been characterized in bovine PE cells (Helbig et al., 1988a; Helbig et al., 1988b). The paired exchangers were proposed as a major uptake pathway of both Na^+ and Cl^- ions in the bovine PE cells. Electron probe X-ray microanalysis of rabbit preparation has supported the idea that the paired antiporters are likely the dominant uptake pathway of NaCl by PE cells (McLaughlin et al., 1998).

However, recent electrophysiological studies showed that the paired exchangers are less likely involved in transepithelial Cl^- secretion (Do and To, 2000; Kong et al., 2006), or only indirectly modulate the transepithelial Cl^- transport (To et al., 2001). In the present study, the lack of effect of DIDS and DMA on both the FF and PD further suggested that the membrane transporters Cl^-/HCO_3^- and Na^+/H^+ exchangers are not functionally important in the *in vitro* transepithelial fluid transport process.

In the literature, little is known about these membrane transporters in the porcine CE, as rabbits or oxen were frequently used as transport models in most studies. A recent study has localized the Cl^-/HCO_3^- antiporter in the NPE cells, and demonstrated its functional importance in regulating the cytoplasmic pH

(Shahidullah et al., 2009). Moreover, addition of DIDS to the NPE side stimulated both the I_{sc} and Cl^- secretion across the porcine CBE (Kong et al., 2006). These findings suggested that the Cl^-/HCO_3^- antiporter on the NPE may be functionally important in maintaining the intracellular pH which indirectly contributes to the modulation of Cl^- transport.

Na^+-K^+-$2Cl^-$ cotransporter is predominantly localized along the PE cells of both the ox and rabbit (Crook et al., 2000; Dunn et al., 2001). The functional importance of Na^+-K^+-$2Cl^-$ cotransporter in bovine and porcine CBE has been demonstrated in isotopic Cl^- flux studies (Do and To, 2000; Kong et al., 2006). Unexpectedly, Kishida et al. (Kishida et al., 1982) and Crook et al. (Crook et al., 2000) have also found that the rabbit CE preparation actively secrets Cl^- which is different from the view that the rabbit CE mainly transports HCO_3^- ions (Wolosin et al., 1991; Wolosin et al., 1993; Butler et al., 1994). In this study, the stromal addition of bumetanide, a specific blocker of Na^+-K^+-$2Cl^-$ cotransporter significantly reduced the FF across the porcine CBE. This observation implies that the Na^+-K^+-$2Cl^-$ cotransporter system is the dominant system for Cl^- uptake and concomitant fluid secretion in the porcine CBE preparation. However, the loop diuretics did not cause a drastic effect on PD. The observation that the PD did not decrease drastically with the fluid flow is indeed very interesting. Similar discrepancy has been observed in previous Cl^- flux and transport experiments (To et al., 1998a; Do and To, 2000; Kong et al., 2006). The main reason for this observation may be due to the electroneutral nature of Na^+-K^+-$2Cl^-$ cotransporter activity. It has previously been proposed that through detailed modelling with all the major transporters and channels, it may be able to correlate the electrical parameters with transport activities among all key protein players (To et al., 2001). The blockade of Na^+-K^+-$2Cl^-$ cotransporter

causes unremarkable effect on both the PD and I_{sc} since both the uptake of cations and anions are reduced. However, the transepithelial Cl^- transport was eventually inhibited as a result of the reduced uptake of Cl^- ions, as shown in previous studies in both the bovine and porcine CBE (To et al., 1998a; Do and To, 2000; Kong et al., 2006). In the present study, although bumetanide did not cause a drastic change in the PD across the CBE, a marked reduction of fluid flow is observed, which could largely be attributed to the Cl^- transporting properties of porcine CBE.

4.6 Intercellular gap junctions

Intercellular gap junctions are located between the PE and NPE cell layers, and between the adjacent cells within the PE and NPE layers (Raviola and Raviola, 1978). This observation has lead to the proposal that the CE is a functional syncytium (Krupin and Civan, 1996). The functional role of gap junctions has been demonstrated in various studies (Stelling and Jacob, 1997; Wolosin et al., 1997a; Do and To, 2000; Kong et al., 2006). In electrophysiological studies, addition of heptanol has been shown to inhibit I_{sc}, and inhibit Cl^- secretion by about 80% across the bovine and porcine CBE (Do and To, 2000; Kong et al., 2006). In the present findings, the application of heptanol to either side of the CBE also depolarized the PD and inhibited the FF across the preparation. The maximum inhibition induced by aqueous addition of heptanol was 78% which is in agreement with previous studies. Thus, the coupling of PE and NPE layers by gap junctions is essential in transepithelial ionic and fluid transport across the CBE.

Since heptanol was able to inhibit the FF up to 78%, a major fraction of the FF measurement is attributed to the transcellular Cl^- secretion across the CBE. This suggested that gap junctions are indispensable in the fluid transport process across the porcine CBE. The actions of heptanol in reducing the fluid flow is likely due to the interruption of intercellular communication between PE and NPE cells and hence the inhibition of the Cl^- secretion across the CE, thereby reducing the solute and osmotic gradient generated as the driving force for fluid transport across the CE.

Furthermore, the functional importance of gap junction is potentially linked to the regulation of the second messenger cAMP, which has been shown to reduce Cl^- secretion in bovine CBE (Do et al., 2004a). However, further experiments are required to elucidate the role of gap junction regulation in the AH formation.

4.7 Cl^- channels in the NPE

The Cl^- release from the NPE cells is the last step in the transepithelial ion transport. The identity of Cl^- channels has been broadly investigated (Jacob and Civan, 1996; Do and Civan, 2006). Recent studies of bovine CBE cells have identified swelling-activated Cl^- channels in both the PE and NPE cells. cAMP-activated maxi-Cl^- channels are localized in the PE cells for recycling Cl^- and A_3 adenosine receptor-activated Cl^- channels in the NPE cells for releasing Cl^- into the AH (Do et al., 2004b; Do and Civan, 2006; Do et al., 2006). The present study revealed that aqueous addition of niflumic acid inhibited FF by 62% and completely depolarized the PD. Compared to a previous study, niflumic acid completely abolished the I_{sc} and Cl^- secretion across the porcine CBE (Kong et al., 2006). Presumably the I_{sc} is directly proportional to the transepithelial PD, our result also indirectly showed the I_{sc} was abolished by niflumic acid. However, if FF is totally dependent on Cl^- secretion, a complete abolishment of FF should be observed in association with a total inhibition of Cl^- secretion. Since this abolition in FF did not occur in our experiments, it indicated that the fraction of FF not inhibited by niflumic acid (~38%) may be associated with other mechanisms of ionic transport.

4.8 Residual FF subsequent to Cl^- transport inhibition

Our findings indicate that *in vitro* FF of porcine CBE is mediated largely by Cl^- secretion but none of the transport inhibitors was able to completely abolish the FF. The exact reason for the residual FF is unclear which could indicate unknown fluid secretion pathway or mechanism. In addition, there are alternative channels or routes that are not inhibited by the above transport inhibitors by which Cl^- can also go through.

Other than Cl^-, HCO_3^- is another candidate ion for the transport mechanism of fluid formation. In the previous sections study, HCO_3^- depletion experiment has shown that FF across the porcine CBE is HCO_3^--dependent to a certain extent. Although the current finding has demonstrated that Cl^-/HCO_3^- exchanger is not active in the PE, there may be unidentified transport mechanism of HCO_3^- present in the porcine CBE which may directly or indirectly drive fluid movement. For example, the recent identification of Cl^-/HCO_3^- antiporter in porcine NPE, and its functional importance in the regulation of intracellular pH (Shahidullah et al., 2009) and stimulation in I_{sc} and Cl^- transport (Kong et al., 2006). Moreover, the Na^+-HCO_3^- cotransporter has been expressed by RT-PCR in the native and cultured porcine NPE cells (Shahidullah et al., 2009). The precise role of these transporters is unclear and requires further investigation.

Nevertheless, it is not surprising that a secretory epithelium transports various ions for secretion of fluid. For instance, the epithelial cells of the choroid plexuses transport a number of ions including Na^+, Cl^-, HCO_3^- from the blood to the ventricles of the brain for the secretion of cerebrospinal fluid (Brown et al., 2004). However, further study is required to reveal the precise role of HCO_3^- or other key ions in the porcine CBE preparation. Although the net Cl^- transport by the porcine

CBE *in vitro* has been demonstrated (Kong et al., 2006) but the net transfer of HCO_3^- ion has yet to be studied so far. In the case of the bovine CBE (To et al., 2001), the unidirectional CO_2/HCO_3^- fluxes across the preparation were measured using a specially designed chamber where the partial pressure of CO_2 was controlled. Similar technique may be employed to study the HCO_3^- transport which may shed light on the roles of CO_2/HCO_3^- in transport physiology across the porcine preparation.

4.9 Regulation of in vitro FF by cAMP

Forskolin is a direct AC activator which stimulates the endogenous production of cAMP without cell surface receptor interaction (Seamon and Daly, 1981). Stimulation of cAMP production has been demonstrated with forskolin in both rabbit and human ciliary processes (Bausher and Horio, 1995; Horio et al., 1996). Topical application of forskolin lowered IOP in rabbit, monkey and human (Caprioli and Sears, 1983), as a result of reduction in the aqueous flow (Burstein et al., 1984b; Caprioli et al., 1984; Lee et al., 1984). However, in vitro study revealed that forskolin stimulated rather than inhibited the I_{sc} across the CBE preparation in both rabbit (Chu et al., 1986) and monkey (Chu et al., 1987).

Similarly, 8-Br-cAMP, a cAMP analogue, elicited a stimulatory effect on I_{sc} in the rabbit (Chu and Candia, 1985) and porcine CBE (Ni et al., 2006). In the porcine CBE (Ni et al., 2006), the effects of I_{sc} stimulation elicited by several cAMP analogues have been compared and 8-Br-cAMP has the strongest effect. The sidedness effects of I_{sc} stimulation induced by cAMP analogues were also examined. Application of cAMP analogues to the NPE side caused stronger effects than when they were applied on the PE side. In addition to a possible barrier effect to the diffusion of drugs from the stromal side, it is consistent with the finding that there is higher AC activity in the NPE cells than in the PE cells (Elena et al., 1984; Mittag et al., 1987).

In the present study, the application of forskolin or 8-Br-cAMP to the aqueous-side bath induced a tremendous hyperpolarisation of PD by 97% and 180% respectively, with a concomitant increase in FF by 42% and 57% respectively. The stimulatory effects of both the PD and FF elicited by the 8-Br-cAMP were larger than that that induced by forskolin. 8-Br-cAMP is a cell permeable analogue of

cAMP more resistant to hydrolysis, whereas forskolin stimulates the endogenous production of cAMP which is more susceptible to the hydrolysis by PDE. This may account for the observation that the effects induced by 8-Br-cAMP are stronger than that induced by forskolin. Since the I_{sc} is directly proportional to the transepithelial PD, our results also indicate the I_{sc} was stimulated by forskolin or 8-Br-cAMP, which is also consistent with the previous findings in both rabbit and monkey (Chu and Candia, 1985; Chu et al., 1986; Chu et al., 1987). In a recent study of porcine CE, aqueous application of 8-Br-cAMP stimulated an increase in I_{sc}, along with a concomitant transient increase in Cl^- transport (Ni et al., 2006). The increase in FF demonstrated in this study is likely attributed to the transient increase in net Cl^- transport across the porcine CE in parallel with changes in the transepithelial electrical parameters.

In contrast, opposite findings have been demonstrated in the bovine CE. Several cAMP-elevating agents including forskolin and 8-Br-cAMP have been shown to reduce the net Cl^- secretion (Do et al., 2004a). Such reduction of Cl^- secretion was likely linked to the maxi-Cl^- channels of the bovine PE cells (Mitchell and Jacob, 1996; Mitchell et al., 1997). It has been suggested that maxi-Cl^- channels in the PE could be activated by cAMP thereby enhancing the Cl^- reabsorption from PE to stroma and reducing the net AH secretion (Do et al., 2004b). Apparently, there is clear species variation in the effects of cAMP on the ion transport in porcine and bovine CE. Therefore, it is important to take species difference into consideration when interpreting and extrapolating data of signalling and regulatory pathways related to ion transport and AH formation in different animals.

Given that cAMP stimulated the ion and fluid transport across the CE, and the HCO_3^--sensitive AC was demonstrated in the bovine CE (Mittag et al., 1993), the

cAMP level could be elevated in the presence of HCO_3^- under the baseline condition. The baseline FF and PD across the CBE could have been under a constant stimulation of elevated cAMP mediated by the HCO_3^--sensitive AC induced by the HCO_3^--rich bathing medium. The depletion of HCO_3^- in the bathing solution could partially reduce cAMP level such that the ion and fluid transport across the CE was declined (as revealed in section 3.4).

The application of IBMX alone merely induced a slight hyperpolarisation of PD, but did not elicit significant effects on FF. IBMX is a non-specific inhibitor of PDE. The blockade of PDE retards the hydrolysis of cAMP, as a result of slower decay in intracellular cAMP level. The lack of effect induced by IBMX is likely due to a low endogenous cAMP level, such that only a slight hyperpolarisation of PD was induced with insignificant effect on the fluid movement.

4.10 PKA as the mediator of cAMP signalling pathway

The second messenger cAMP requires the activation of PKA to modify the state of phosphorylation of specific target proteins to cause various physiological responses. H-89 has been shown to be the most potent and selective inhibitor for PKA among the H-series compounds (Hidaka et al., 1991; Hidaka and Kobayashi, 1992). The introduction of H-89 has no direct influence on the activities of cAMP synthesizing and metabolizing enzymes *in vitro* (Hidaka et al., 1991), which suggests that it acts directly on PKA. However, a limited permeability of H-89 in cell membranes has been observed (Hidaka et al., 1991), such that the effective concentration of H-89 in blocking PKA may be varied in different preparations and systems. H-89 at 10 μM has been demonstrated effective in blocking the forskolin-stimulated Na^+-K^+-Cl^- cotransport activity in the NPE cells (Crook and Polansky, 1994), however, a higher concentration of 70 μM has been required to produce similar inhibitions of Na^+-K^+-Cl^- cotransport stimulated by isoproterenol (Crook and Riese, 1996) or dopamine (Riese et al., 1998).

In the present study, H-89 at 10 μM was ineffective in inhibiting the cAMP-stimulated FF and PD. Yet, at a higher concentration of 50 μM, H-89 markedly eliminated the cAMP-stimulated FF and PD by 62% and 63% respectively, implying that PKA activation is essential, at least in part, for the cAMP-induced stimulation. This result confirmed that cAMP mediates through PKA, which in turn modulate the phosphorylation of the target proteins to induce stimulations in both the ion as well as the fluid transport across the porcine CE.

Although the precise transport component that is stimulated by the cAMP is unclear, consistent with the present findings, both the Na^+-K^+-Cl^- cotransporter and Cl^- channel are plausible targets. Isoproterenol-stimulated I_{sc} in the isolated rabbit

stroma-free ciliary epithelial bilayer was coupled to an increased net Cl^- secretion, with an increase of blood-to-aqueous Cl^- flux by 75% (Crook et al., 2000). This stimulation was reduced by bumetanide applied to the PE, suggested that the Na^+-K^+-$2Cl^-$ cotransporter in PE cells was likely modulated by the β-adrenergic stimulated cAMP production. The stimulation of Na^+-K^+-$2Cl^-$ cotransport activity induced by isoproterenol, forskolin and cAMP was also observed in fetal human PE cells (Hochgesand et al., 2001). A stimulated activity of Na^+-K^+-Cl^- cotransporter in the PE cells may enhance the uptake of Cl^- into the PE cells and facilitate the Cl^- transport across the CE.

Moreover, in isolated cells studied with patch-clamp, cAMP has been shown to activate the Cl^- channel activities in the basolateral membrane of the NPE in dog (Chen et al., 1994), bovine (Edelman et al., 1995) and rabbit (Chen and Sears, 1997). Forskolin or cAMP analogues induced a Cl^- current with a concomitant cell shrinkage in isolated dog NPE cells (Chen et al., 1994), suggested that stimulation of cAMP production enhanced the Cl^- efflux into the AH, resulting in an increase in AH formation. However, further studies are required to verify these hypotheses.

In addition to the ion transporters mentioned above, aquaporin (AQP) may be another potential transporter mediated by the cAMP-PKA signalling pathway. AQPs have been shown to play a role in the transcellular permeability and transport of water. AQP1 and AQP4 have been identified in the NPE cells of rat and human (Nielsen et al., 1993; Hasegawa et al., 1994; Stamer et al., 1994; Patil et al., 1997b; Hamann et al., 1998). The functional expression of AQP1 has been demonstrated in the cultured human NPE cells (Han et al., 2000). Moreover, it has been shown that the *in vitro* cultured NPE layer transported fluid, and the fluid transport was partially blocked by mercuric chloride, a potent nonspecific blocker of AQP, and inhibited by

the AQP1 antisense oligonucleotides (Patil et al., 2001). In the transgenic knockout mice model, the mice lacking AQPs exhibited a reduced baseline IOP compared to the wild type mice (Zhang et al., 2002).

The water permeability mediated by AQP1 could be stimulated by cAMP in the *Xenopus* oocytes (Yool et al., 1996; Patil et al., 1997a). The cAMP-stimulated water permeability of AQP1 was triggered by PKA-dependent phosphorylation (Han and Patil, 2000). Furthermore, cAMP has been shown to stimulate AQPs in other tissues. For example, in the murine lung epithelial cell line, cAMP upregulated the AQP5 mRNA and protein expressions as well as induced the translocation of AQP5 to the apical plasma membrane via the PKA pathway (Yang et al., 2003). Although the current findings are insufficient to substantiate this hypothesis, further investigation on AQP would provide new insight into the transport physiology of the ciliary epithelium.

In the present findings, the inhibition of PKA with H-89 did not completely block the transient stimulation induced by cAMP. Either the concentration of H-89 currently used was insufficient to completely inhibit the PKA, or there is alternative cAMP signalling pathway mediating the transient increase in fluid movement. A possible candidate for such a mediator could be the recently identified cAMP-binding proteins known as Epac (exchange protein directly activated by cAMP). Epac is a guanine-nucleotide-exchange factor for the Ras-like small GTPases Rap1 and Rap2, that is directly activated by cAMP, independent of PKA (de Rooij et al., 1998). It mediates diverse cellular functions including integrin-mediated cell adhesion, vascular endothelial cell barrier formation, and cell-cell junction formation, control of insulin secretion and neurotransmitter release (Bos, 2006; Holz et al., 2006). Moreover, it involves in the regulation of ion channel

functions, intracellular Ca^{2+} signalling and ion transporter activity (Holz et al., 2006). Thus, it is conceivable that this novel signalling transduction mechanism could modulate the ion and fluid transport in the porcine CE.

4.11 Discrepancy between in vitro FF rate and in vivo AH production rate

In the present and previous studies of FF (Candia et al., 2005), the whole CBE preparations from rabbit, ox, and pig secreted only a small quantity of fluid *in vitro*. The isolated rabbit, bovine, and porcine CBE preparations transported fluid at a rate ~3 μL/h per preparation (Candia et al., 2005). Our current findings of FF are also comparable to the previous report. Although we are unaware of measurements for the rate of AH formation in the pig, the reported *in vivo* rate of AH formation in humans, which is similar in size to pig eye, is approximately 165 μL/h (Brubaker, 1991), which is ~60-fold larger than the measured rate of the present study. This large discrepancy is observed in all studies with the *in vitro* preparations from rabbits, cows, and pigs. Several factors may have contributed to this discrepancy. Since there is no blood circulation in the isolated preparation, the ciliary processes are collapsed on one another. This may decrease the effective secretive surface areas of the ciliary body epithelium. The chamber only exposes a fraction of the isolated tissue but not the whole epithelium in the *in vivo* system, therefore the flow may have been underestimated. In other studies in which the I_{sc} and net ion and water fluxes were measured, neither the respective I_{sc} or ion flux (Pesin and Candia, 1982; Krupin et al., 1984; Chu and Candia, 1987; Do and To, 2000; Kong et al., 2006) is large enough to drive the aqueous flow observed *in vivo*, nor is the FF (Burstein et al., 1984a; Candia et al., 2005) of the magnitude measured *in vivo*. Except in the study conducted by Crook and co-workers (Crook et al., 2000), the reported net Cl^- flux appears to be adequate to drive the AH secretion observed *in vivo*.

In addition, a key question in this observed discrepancy between electrical parameters and flux/FF is the relative contributions between active transport of CE and passive processes to AH formation. With the *in vitro* perfused bovine eye model,

at least 60% of the AH secretion was mediated by the active ionic transport, which meant the remaining 40% was contributed by passive processes (Shahidullah et al., 2003). There is evidence suggesting that proteins and AH can be directly transferred into the anterior chamber via the anterior surface of the iris (Freddo, 2001; Candia and Alvarez, 2008). These findings suggested that AH may partly be secreted by an active transport process and the passive process may also play a significant role.

Although our *in vitro* FF of the ciliary body preparation represents only a small fraction of the *in vivo* AH formation rate, our present and previous experiments have shown that the CBE preparation is viable in a similar chamber setting (To et al., 1998b; Do and To, 2000; Kong et al., 2006). The *in vitro* preparation demonstrated typical characteristics of a tight epithelium, with high transepithelial resistance (taking the area folding ratio into consideration) as well as being able to conduct several active transport processes (e.g., ascorbate transport, sodium-pump activities, Cl^- transport) known to occur *in vivo*. In the control experiments of the present study, the control FF was maintained stable for at least 4 hours. No further deterioration was observed within this period.

In addition, the FF measured was abolished by stromal addition of ouabain (1 mM), which strongly suggested that the FF was primarily driven by an active ion transport process. Furthermore, the FF is not only inhibited by agents that act on the transport machinery of the CE, but also stimulated by the second messenger cAMP-elevating agents. The concurrence of both inhibitory and stimulatory responses further support that the preparation is viable and the *in vitro* FF is an active process.

Overall, the present observations indicate that the measurements of volumetric FF across the porcine CBE are suitable for future studies directed towards

the pharmacological control of the secretory activity of the epithelium. It would be important to determine the effects of pharmacological agents on fluid transport to confirm their postulated effect *in vivo*. Drugs which are known to reduce the intraocular pressure, may or may not directly affect fluid transport or AH formation. With an *in vitro* chamber system, one may be able to study the inhibitory effect of novel hypotensive drugs on *in vitro* FF so as to examine whether their action is mediated by inhibition of ionic transport mechanisms of the CE.

4.12 Relationship between short-circuit current (I_{sc}) and FF rate

The precise relationship between the I_{sc} and FF rate is currently unclear. Based on the present findings, the *in vitro* FF is largely dependent on Cl^- transport across the CE as shown in the experiments of Cl^- replacement and Cl^- transporter inhibitors. Moreover, only transepithelial Cl^- secretion has been demonstrated in the porcine CE (Kong et al., 2006), in the absence of Na^+ transport (Ni et al., 2006). Thus, Cl^- is likely the major ion mediating the fluid movement across the CE.

Theoretically, the current attributed to the transport of a specific ion (I_{ion}) can be calculated from the ion flux (J_{net}) detected under short-circuited condition by the following equation:

$$I_{ion} = J_{net} \times z \times F$$

where z is the valence of the ion and F is the Faraday's constant.

Moreover, the fluid secretion rate (F_e) can be estimated from the net ion flux (J_{net}) by the following equation:

$$F_e = J_{net} / C$$

where C is the concentration of Cl^- in the bathing medium (120 mM).

By combining these two equations, the relationship between I_{ion} and F_e is represented by the following calculation:

$$I_{ion} = F_e \times C \times z \times F$$

$$I_{sc} = F_e \times (120 / 1000) \times 1 \times 96485.34 / 3600$$

$$I_{sc} = 3.216\ F_e$$

given that I_{sc} is the algebraic sum of the total current flow, $I_{sc} = I_{ion}$.

This theoretical relationship between the calculated I_{sc} and F_e has been illustrated as the solid line (solid circles) in Figure 4.1.

Experimentally, I_{sc} can be estimated by the measured PD with the relationship I_{sc} = PD / R_t. According to the experimental findings of FF and PD in different drug-treated conditions (including bumetanide, heptanol, niflumic acid, forskolin and 8-Br-cAMP) demonstrated in the present studies, the relationship between I_{sc} and FF revealed in different experimental conditions has been plotted as open circles in Figure 4.1. Based on the scatter plot, a line of best fit is revealed by linear regression (I_{sc} = 3.7162 FF – 1.666, R^2 = 0.558), represented by the dashed line. Correlation coefficient has shown that the I_{sc} is significantly associated with the FF (Pearson correlation r = 0.7475, P < 0.0001). Although there is some discrepancy between the slope of the theoretical plot and that of the experimental plot, the general trends of the two plots are similar that the FF rate increases as the I_{sc} increases. The experimental plot clearly demonstrates that the I_{sc} and FF are linearly correlated, and the FF is likely predictable by the I_{sc}, or vice versa. This implies that the *in vitro* fluid movement is dependent on the transepithelial ion transport across the CE.

FIGURE 4.1 The scatter plot of short-circuit current (I_{sc}) against fluid secretion rate (F_e). The solid line (solid circles) represents the theoretical relationship between the calculated I_{sc} and F_e. The dashed line (open circles) represents the linear relationship between I_{sc} and FF revealed in different experimental conditions.

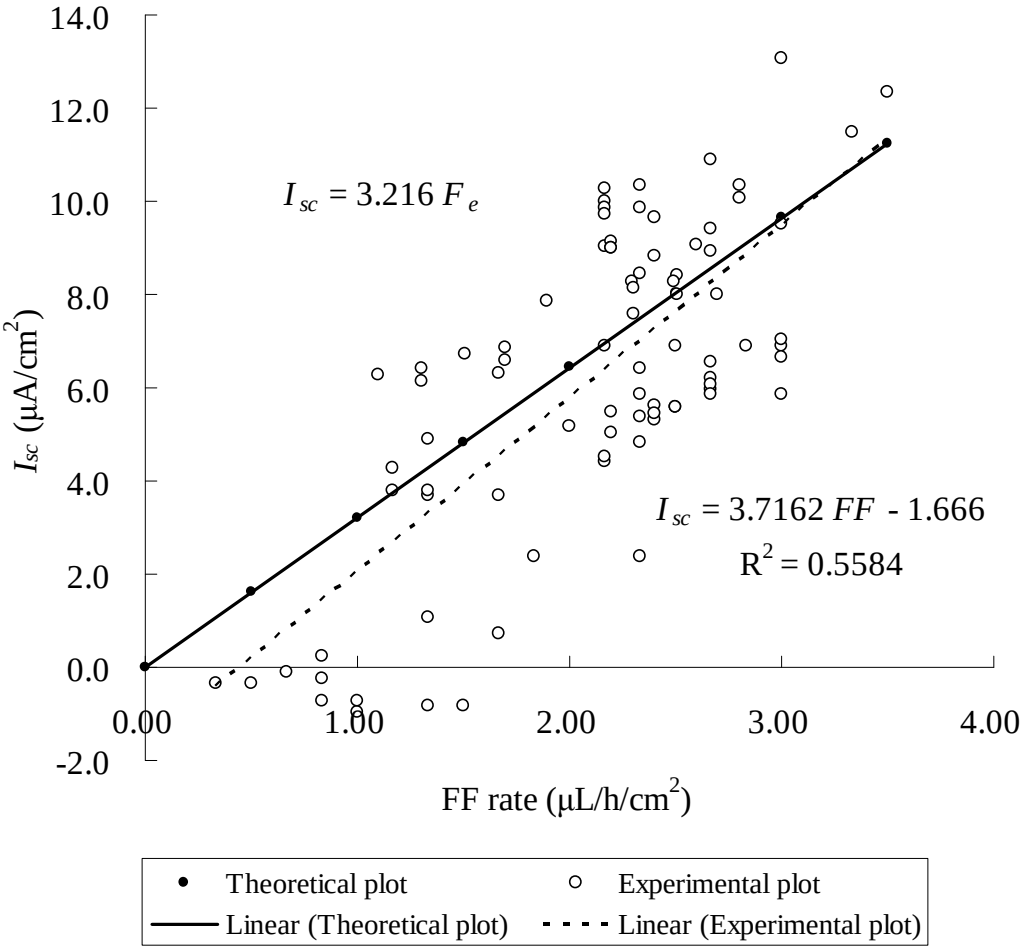

CHAPTER 5

CONCLUSIONS

5.1 Fluid movement measured by Ussing-type fluid chamber

A modified Ussing-type fluid chamber system for the simultaneous measurement of both *in vitro* fluid movement and electrical parameters across the CBE preparation was constructed. In the present chamber system, the porcine CBE preparation transported fluid in the blood-to-aqueous direction at an average rate of ~2.75 µL/h per preparation. The standing transepithelial PD were generally stable for at least 4 hours. The aqueous-negative PD indicated a net anion transport across the CBE from blood to aqueous. The *in vitro* fluid movement was coupled to several physiological relevant events:

1. largely dependent on Cl^- and HCO_3^-, to a lesser extent, indicating that the fluid movement was primarily driven by the transepithelial Cl^- secretion across the preparation; and
2. dependent on the Na^+,K^+-ATPase activity since blocking Na^+,K^+-ATPase with ouabain substantially reduced the FF (stromal ouabain virtually abolished the FF) and elicited a typical biphasic response of PD across the CBE preparation.

These results supported the *in vitro* FF measurement was viable and active. The current modified chamber provides a useful *in vitro* model for the studies directed towards the pharmacological control of the secretory activity of the ciliary epithelium.

5.2 Chloride transport mechanisms underlying in vitro fluid movement

Based on the Cl^--dependent fluid movement *in vitro*, the possibility of Cl^- transport mechanisms underlying the fluid transport has been studied. Inhibitions of several Cl^- transporters and gap junctions have demonstrated the crucial importance of Cl^- transport across the preparation.

1. The paired Cl^-/HCO_3^- and Na^+/H^+ antiporters appeared not directly contribute to the uptake of Cl^- into the PE cells, since their inhibitors DIDS and DMA applied on the PE side did not cause any change in both FF and PD across the CBE.
2. The Na^+-K^+-$2Cl^-$ cotransporter was the predominant Cl^- uptake mechanism into the PE cells, given that its inhibition with stromal bumetanide reduced the FF by 42%, and induced a slight depolarisation of PD across the CBE.
3. A major fraction (~80%) of FF and PD was inhibited by the gap junction blocker, heptanol, indicating that the FF was primarily driven by the transcellular Cl^- transport.
4. The Cl^- release by the NPE cells was mediated by Cl^- channels sensitive to niflumic acid, since aqueous addition of niflumic acid abolished the PD and markedly reduced the FF by 62%.

These results indicated that the *in vitro* fluid movement was primarily driven by the transcellular Cl^- transport across the ciliary epithelium, which is in agreement with the consensus model of Cl^- transport across the ciliary epithelium.

5.3 Regulation of in vitro fluid movement by cAMP-PKA pathway

The potential regulation of AH formation by the second messenger cyclic 3′,5′-adenosine monophosphate (cAMP) were investigated *in vitro*. cAMP-PKA pathway has been demonstrated to modulate the *in vitro* fluid movement concomitant to the ion transport.

1. cAMP was an important modulator of the *in vitro* ion and fluid transport given that cAMP-elevating agents such as forskolin and 8-Br-cAMP have been shown to elicit a tremendous hyperpolarisation of PD and a concomitant increase in FF.
2. Although the PDE inhibitor, IBMX did not cause significant change in FF, it induced a slight hyperpolarisation of PD. The minor effect induced by IBMX was likely due to a low endogenous cAMP level in the CBE preparation.
3. PKA activation was essential, at least in part, for the cAMP-induced stimulation because the pre-treatment of PKA inhibitor H-89 effectively blocked the cAMP-stimulated PD and FF across the CBE preparation.

The demonstration of cAMP-PKA pathway in modulating *in vitro* fluid transport has raised the possibility of regulation of AH formation *in vivo* by cAMP. Further studies are required to elucidate the precise role of cAMP-PKA pathway in regulating the AH formation *in vivo*.

References

Adorante, J. S. and Cala, P. M. (1995). Mechanisms of regulatory volume decrease in nonpigmented human ciliary epithelial cells. *Am J Physiol* 268(3 Pt 1): C721-31.

Anguita, J., Chalfant, M. L., Civan, M. M. and Coca-Prados, M. (1995). Molecular cloning of the human volume-sensitive chloride conductance regulatory protein, pI_{Cln}, from ocular ciliary epithelium. *Biochem Biophys Res Commun* 208(1): 89-95.

Avila, M. Y., Stone, R. A. and Civan, M. M. (2001). A_1-, A_{2A}- and A_3-subtype adenosine receptors modulate intraocular pressure in the mouse. *Br J Pharmacol* 134(2): 241-5.

Avila, M. Y., Stone, R. A. and Civan, M. M. (2002). Knockout of A_3 adenosine receptors reduces mouse intraocular pressure. *Invest Ophthalmol Vis Sci* 43(9): 3021-6.

Balda, M. S. and Matter, K. (1998). Tight junctions. *J Cell Sci* 111 (Pt 5): 541-7.

Barros, F., Lopez-Briones, L. G., Coca-Prados, M. and Belmonte, C. (1991). Detection and characterization of Ca^{2+}-activated K^+ channels in transformed cells of human non-pigmented ciliary epithelium. *Curr Eye Res* 10(8): 731-8.

Barsotti, M. F., Bartels, S. P., Freddo, T. F. and Kamm, R. D. (1992). The source of protein in the aqueous humor of the normal monkey eye. *Invest Ophthalmol Vis Sci* 33(3): 581-95.

Bartels, S. P., Lee, S. R. and Neufeld, A. H. (1987). The effects of forskolin on cyclic AMP, intraocular pressure and aqueous humor formation in rabbits. *Curr Eye Res* 6(2): 307-20.

Bausher, L. P. (1995). Endothelins inhibit cyclic AMP production in rabbit and human ciliary processes. *J Ocul Pharmacol Ther* 11(2): 135-43.

Bausher, L. P. and Horio, B. (1995). Regulation of cyclic AMP production in adult human ciliary processes. *Exp Eye Res* 60(1): 43-8.

Becker, B. (1960). Hypothermia and aqueous humor dynamics of the rabbit eye. *Trans Am Ophthalmol Soc* 58: 337-63.

Becker, B. (1963). Ouabain and Aqueous Humor Dynamics in the Rabbit Eye. *Invest Ophthalmol* 31: 325-31.

Becker, B. (1980). Vanadate and aqueous humor dynamics. Proctor Lecture. *Invest Ophthalmol Vis Sci* 19(10): 1156-65.

Behar-Cohen, F. F., Goureau, O., D'Hermies, F. and Courtois, Y. (1996). Decreased intraocular pressure induced by nitric oxide donors is correlated to nitrite production in the rabbit eye. *Invest Ophthalmol Vis Sci* 37(8): 1711-5.

Berridge, M. J. (1993). Inositol trisphosphate and calcium signalling. *Nature* 361(6410): 315-25.

Berridge, M. J. and Irvine, R. F. (1989). Inositol phosphates and cell signalling. *Nature* 341(6239): 197-205.

Bert, R. J., Caruthers, S. D., Jara, H., Krejza, J., Melhem, E. R., Kolodny, N. H., Patz, S. and Freddo, T. F. (2006). Demonstration of an anterior diffusional pathway for solutes in the normal human eye with high spatial resolution contrast-enhanced dynamic MR imaging. *Invest Ophthalmol Vis Sci* 47(12): 5153-62.

Bill, A. (1973). The role of ciliary blood flow and ultrafiltration in aqueous humor formation. *Exp Eye Res* 16(4): 287-98.

Bill, A. (1975). Blood circulation and fluid dynamics in the eye. *Physiol Rev* 55(3): 383-417.

Bos, J. L. (2006). Epac proteins: multi-purpose cAMP targets. *Trends Biochem Sci* 31(12): 680-6.

Botchkin, L. M. and Matthews, G. (1995). Swelling activates chloride current and increases internal calcium in nonpigmented epithelial cells from the rabbit ciliary body. *J Cell Physiol* 164(2): 286-94.

Bowler, J. M., Peart, D., Purves, R. D., Carre, D. A., Macknight, A. D. and Civan, M. M. (1996). Electron probe X-ray microanalysis of rabbit ciliary epithelium. *Exp Eye Res* 62(2): 131-9.

Brown, P. D., Davies, S. L., Speake, T. and Millar, I. D. (2004). Molecular mechanisms of cerebrospinal fluid production. *Neuroscience* 129(4): 957-70.

Brubaker, R. F. (1991). Flow of aqueous humor in humans [The Friedenwald Lecture]. *Invest Ophthalmol Vis Sci* 32(13): 3145-66.

Brubaker, R. F. (1998). Clinical measurements of aqueous dynamics: implications for addressing glaucoma. *Curr Top Membr* 45: 234-284.

Burstein, N. L., Fischbarg, J., Liebovitch, L. and Cole, D. F. (1984a). Electrical potential, resistance, and fluid secretion across isolated ciliary body. *Exp Eye Res* 39(6): 771-9.

Burstein, N. L., Sears, M. L. and Mead, A. (1984b). Aqueous flow in human eyes is reduced by forskolin, a potent adenylate cyclase activator. *Exp Eye Res* 39(6): 745-9.

Butler, G. A., Chen, M., Stegman, Z. and Wolosin, J. M. (1994). Na^+- Cl^-- and HCO_3^--dependent base uptake in the ciliary body pigment epithelium. *Exp Eye Res* 59(3): 343-9.

Candia, O. A. and Alvarez, L. J. (2008). Fluid transport phenomena in ocular epithelia. *Prog Retin Eye Res* 27(2): 197-212.

Candia, O. A., Shi, X. P. and Chu, T. C. (1991). Ascorbate-stimulated active Na^+ transport in rabbit ciliary epithelium. *Curr Eye Res* 10(3): 197-203.

Candia, O. A., To, C. H., Gerometta, R. M. and Zamudio, A. C. (2005). Spontaneous fluid transport across isolated rabbit and bovine ciliary body preparations. *Invest Ophthalmol Vis Sci* 46(3): 939-47.

Caprioli, J. and Sears, M. (1983). Forskolin lowers intraocular pressure in rabbits, monkeys, and man. *Lancet* 1(8331): 958-60.

Caprioli, J. and Sears, M. (1984). The adenylate cyclase receptor complex and aqueous humor formation. *Yale J Biol Med* 57(3): 283-300.

Caprioli, J., Sears, M., Bausher, L., Gregory, D. and Mead, A. (1984). Forskolin lowers intraocular pressure by reducing aqueous inflow. *Invest Ophthalmol Vis Sci* 25(3): 268-77.

Carre, D. A., Mitchell, C. H., Peterson-Yantorno, K., Coca-Prados, M. and Civan, M. M. (1997). Adenosine stimulates Cl^- channels of nonpigmented ciliary epithelial cells. *Am J Physiol* 273(4 Pt 1): C1354-61.

Carre, D. A., Mitchell, C. H., Peterson-Yantorno, K., Coca-Prados, M. and Civan, M. M. (2000). Similarity of A_3-adenosine and swelling-activated Cl^- channels in nonpigmented ciliary epithelial cells. *Am J Physiol Cell Physiol* 279(2): C440-51.

Carre, D. A., Tang, C. S., Krupin, T. and Civan, M. M. (1992). Effect of bicarbonate on intracellular potential of rabbit ciliary epithelium. *Curr Eye Res* 11(7): 609-24.

Chen, L., Wang, L. and Jacob, T. J. (1999). Association of intrinsic pI_{Cln} with volume-activated Cl^- current and volume regulation in a native epithelial cell. *Am J Physiol* 276(1 Pt 1): C182-92.

Chen, S., Inoue, R., Inomata, H. and Ito, Y. (1994). Role of cyclic AMP-induced Cl conductance in aqueous humour formation by the dog ciliary epithelium. *Br J Pharmacol* 112(4): 1137-45.

Chen, S. and Sears, M. (1997). A low conductance chloride channel in the basolateral membranes of the non-pigmented ciliary epithelium of the rabbit eye. *Curr Eye Res* 16(7): 710-8.

Chu, T. C. and Candia, O. A. (1985). Effects of adrenergic agonists and cyclic AMP on the short-circuit current across the isolated rabbit iris-ciliary body. *Curr Eye Res* 4(4): 523-9.

Chu, T. C. and Candia, O. A. (1987). Electrically silent Na^+ and Cl^- fluxes across the rabbit ciliary epithelium. *Invest Ophthalmol Vis Sci* 28(3): 445-50.

Chu, T. C. and Candia, O. A. (1988). Active transport of ascorbate across the isolated rabbit ciliary epithelium. *Invest Ophthalmol Vis Sci* 29(4): 594-9.

Chu, T. C., Candia, O. A. and Iizuka, S. (1986). Effects of forskolin, prostaglandin F_2 alpha, and Ba^{2+} on the short-circuit current of the isolated rabbit iris-ciliary body. *Curr Eye Res* 5(7): 511-6.

Chu, T. C., Candia, O. A. and Podos, S. M. (1987). Electrical parameters of the isolated monkey ciliary epithelium and effects of pharmacological agents. *Invest Ophthalmol Vis Sci* 28(10): 1644-8.

Chuman, H., Chuman, T., Nao-i, N. and Sawada, A. (2000). The effect of L-arginine on intraocular pressure in the human eye. *Curr Eye Res* 20(6): 511-6.

Cilluffo, M. C., Esqueda, E. and Farahbakhsh, N. A. (2000). Multiple receptor activation elicits synergistic IP formation in nonpigmented ciliary body epithelial cells. *Am J Physiol Cell Physiol* 279(3): C734-43.

Civan, M. M. (1998). Transport components of net secretion of the aqueous humor and their integrated regulation. *Curr Top Membr* 45: 1-24.

Civan, M. M. (2003). The fall and rise of active chloride transport: implications for regulation of intraocular pressure. *J Exp Zoolog Part A Comp Exp Biol* 300(1): 5-13.

Civan, M. M., Coca-Prados, M. and Peterson-Yantorno, K. (1994). Pathways signaling the regulatory volume decrease of cultured nonpigmented ciliary epithelial cells. *Invest Ophthalmol Vis Sci* 35(6): 2876-86.

Civan, M. M. and Macknight, A. D. (2004). The ins and outs of aqueous humour secretion. *Exp Eye Res* 78(3): 625-31.

Civan, M. M., Peterson-Yantorno, K., Sanchez-Torres, J. and Coca-Prados, M. (1997). Potential contribution of epithelial Na^+ channel to net secretion of aqueous humor. *J Exp Zool* 279(5): 498-503.

Coca-Prados, M., Anguita, J., Chalfant, M. L. and Civan, M. M. (1995). PKC-sensitive Cl^- channels associated with ciliary epithelial homologue of pI_{Cln}. *Am J Physiol* 268(3 Pt 1): C572-9.

Coca-Prados, M. and Escribano, J. (2007). New perspectives in aqueous humor secretion and in glaucoma: the ciliary body as a multifunctional neuroendocrine gland. *Prog Retin Eye Res* 26(3): 239-62.

Coca-Prados, M., Ghosh, S., Gilula, N. B. and Kumar, N. M. (1992). Expression and cellular distribution of the alpha 1 gap junction gene product in the ocular pigmented ciliary epithelium. *Curr Eye Res* 11(2): 113-22.

Coca-Prados, M., Sanchez-Torres, J., Peterson-Yantorno, K. and Civan, M. M. (1996). Association of ClC-3 channel with Cl^- transport by human nonpigmented ciliary epithelial cells. *J Membr Biol* 150(2): 197-208.

Coffey, K. L., Krushinsky, A., Green, C. R. and Donaldson, P. J. (2002). Molecular profiling and cellular localization of connexin isoforms in the rat ciliary epithelium. *Exp Eye Res* 75(1): 9-21.

Cole, D. F. (1961). Electrical Potential across the Isolated Ciliary Body Observed in Vitro. *Br J Ophthalmol* 45(10): 641-53.

Cole, D. F. (1962). Transport across the Isolated Ciliary Body of Ox and Rabbit. *Br J Ophthalmol* 46(10): 577-91.

Cole, D. F. (1964). Location of Ouabain-Sensitive Adenosine Triphosphatase in Ciliary Epithelium. *Exp Eye Res* 89: 72-5.

Cole, D. F. (1969). Evidence for active transport of chloride in ciliary epithelium of the rabbit. *Exp Eye Res* 8(1): 5-15.

Coleman, A. L. (1999). Glaucoma. *Lancet* 354(9192): 1803-10.

Collaborative Normal-Tension Glaucoma Study Group (1998a). Comparison of glaucomatous progression between untreated patients with normal-tension glaucoma and patients with therapeutically reduced intraocular pressures. *Am J Ophthalmol* 126(4): 487-97.

Collaborative Normal-Tension Glaucoma Study Group (1998b). The effectiveness of intraocular pressure reduction in the treatment of normal-tension glaucoma. *Am J Ophthalmol* 126(4): 498-505.

Counillon, L., Touret, N., Bidet, M., Peterson-Yantorno, K., Coca-Prados, M., Stuart-Tilley, A., Wilhelm, S., Alper, S. L. and Civan, M. M. (2000). Na^+/H^+ and Cl^-/HCO_3^- antiporters of bovine pigmented ciliary epithelial cells. *Pflugers Arch* 440(5): 667-78.

Crook, R. B. and Polansky, J. R. (1992). Neurotransmitters and neuropeptides stimulate inositol phosphates and intracellular calcium in cultured human nonpigmented ciliary epithelium. *Invest Ophthalmol Vis Sci* 33(5): 1706-16.

Crook, R. B. and Polansky, J. R. (1994). Stimulation of Na^+,K^+,Cl^- cotransport by forskolin-activated adenylyl cyclase in fetal human nonpigmented epithelial cells. *Invest Ophthalmol Vis Sci* 35(9): 3374-83.

Crook, R. B. and Riese, K. (1996). Beta-adrenergic stimulation of Na^+, K^+, Cl^- cotransport in fetal nonpigmented ciliary epithelial cells. *Invest Ophthalmol Vis Sci* 37(6): 1047-57.

Crook, R. B., Takahashi, K., Mead, A., Dunn, J. J. and Sears, M. L. (2000). The role of NaKCl cotransport in blood-to-aqueous chloride fluxes across rabbit ciliary epithelium. *Invest Ophthalmol Vis Sci* 41(9): 2574-83.

Crosson, C. E. (1992). Ocular hypotensive activity of the adenosine agonist (R)-phenylisopropyladenosine in rabbits. *Curr Eye Res* 11(5): 453-8.

Crosson, C. E. (1995). Adenosine receptor activation modulates intraocular pressure in rabbits. *J Pharmacol Exp Ther* 273(1): 320-6.

Crosson, C. E. and Gray, T. (1994). Modulation of intraocular pressure by adenosine agonists. *J Ocul Pharmacol* 10(1): 379-83.

Crosson, C. E. and Gray, T. (1996). Characterization of ocular hypertension induced by adenosine agonists. *Invest Ophthalmol Vis Sci* 37(9): 1833-9.

Crosson, C. E. and Petrovich, M. (1999). Contributions of adenosine receptor activation to the ocular actions of epinephrine. *Invest Ophthalmol Vis Sci* 40(9): 2054-61.

Cullinane, A. B., Coca-Prados, M. and Harvey, B. J. (2001a). Chloride dependent intracellular pH effects of external ATP in cultured human non-pigmented ciliary body epithelium. *Curr Eye Res* 23(6): 443-7.

Cullinane, A. B., Coca-Prados, M. and Harvey, B. J. (2001b). Extracellular ATP effects on calcium signaling in cultured human non-pigmented ciliary body epithelium. *Curr Eye Res* 23(6): 448-54.

Cullinane, A. B., Leung, P. S., Ortego, J., Coca-Prados, M. and Harvey, B. J. (2002). Renin-angiotensin system expression and secretory function in cultured human ciliary body non-pigmented epithelium. *Br J Ophthalmol* 86(6): 676-83.

Cunha-Vaz, J. (1979). The blood-ocular barriers. *Surv Ophthalmol* 23(5): 279-96.

Dailey, R. A., Brubaker, R. F. and Bourne, W. M. (1982). The effects of timolol maleate and acetazolamide on the rate of aqueous formation in normal human subjects. *Am J Ophthalmol* 93(2): 232-7.

Davson, H. (1969). The intra-ocular fluids. *The Eye*. H. Davson. London, Academic Press**:** 67-186.

Davson, H. (1990). The aqueous humor and the intraocular pressure. *Physiology of the Eye*. H. Davson. London, Macmillan Press**:** 3-95.

Davson, H. and Luck, C. P. (1956). A comparative study of the total carbon dioxide in the ocular fluids, cerebrospinal fluid, and plasma of some mammalian species. *J Physiol* 132(2): 454-64.

Dawson, D. C. (1977). Na and Cl transport across the isolated turtle colon: parallel pathways for transmural ion movement. *J Membr Biol* 37(3-4): 213-33.

de Rooij, J., Zwartkruis, F. J., Verheijen, M. H., Cool, R. H., Nijman, S. M., Wittinghofer, A. and Bos, J. L. (1998). Epac is a Rap1 guanine-nucleotide-exchange factor directly activated by cyclic AMP. *Nature* 396(6710): 474-7.

Delamere, N. A. and King, K. L. (1992). The influence of cyclic AMP upon Na,K-ATPase activity in rabbit ciliary epithelium. *Invest Ophthalmol Vis Sci* 33(2): 430-5.

Delamere, N. A., Socci, R. R. and King, K. L. (1990). Alteration of sodium, potassium-adenosine triphosphatase activity in rabbit ciliary processes by cyclic adenosine monophosphate-dependent protein kinase. *Invest Ophthalmol Vis Sci* 31(10): 2164-70.

Do, C. W. and Civan, M. M. (2004). Basis of chloride transport in ciliary epithelium. *J Membr Biol* 200(1): 1-13.

Do, C. W. and Civan, M. M. (2006). Swelling-activated chloride channels in aqueous humour formation: on the one side and the other. *Acta Physiol (Oxf)* 187(1-2): 345-52.

Do, C. W., Kong, C. W. and To, C. H. (2004a). cAMP inhibits transepithelial chloride secretion across bovine ciliary body/epithelium. *Invest Ophthalmol Vis Sci* 45(10): 3638-43.

Do, C. W., Lu, W., Mitchell, C. H. and Civan, M. M. (2005). Inhibition of swelling-activated Cl^- currents by functional anti-ClC-3 antibody in native bovine non-pigmented ciliary epithelial cells. *Invest Ophthalmol Vis Sci* 46(3): 948-55.

Do, C. W., Peterson-Yantorno, K. and Civan, M. M. (2006). Swelling-activated Cl^- channels support Cl^- secretion by bovine ciliary epithelium. *Invest Ophthalmol Vis Sci* 47(6): 2576-82.

Do, C. W., Peterson-Yantorno, K., Mitchell, C. H. and Civan, M. M. (2004b). cAMP-activated maxi-Cl^- channels in native bovine pigmented ciliary epithelial cells. *Am J Physiol Cell Physiol* 287(4): C1003-11.

Do, C. W. and To, C. H. (2000). Chloride secretion by bovine ciliary epithelium: a model of aqueous humor formation. *Invest Ophthalmol Vis Sci* 41(7): 1853-60.

Dobbs, P. C., Epstein, D. L. and Anderson, P. J. (1979). Identification of isoenzyme C as the principal carbonic anhydrase in human ciliary processes. *Invest Ophthalmol Vis Sci* 18(8): 867-70.

Dragsten, P. R., Blumenthal, R. and Handler, J. S. (1981). Membrane asymmetry in epithelia: is the tight junction a barrier to diffusion in the plasma membrane? *Nature* 294(5843): 718-22.

Dunn, J. J., Lytle, C. and Crook, R. B. (2001). Immunolocalization of the Na-K-Cl cotransporter in bovine ciliary epithelium. *Invest Ophthalmol Vis Sci* 42(2): 343-53.

Edelman, J. L., Loo, D. D. and Sachs, G. (1995). Characterization of potassium and chloride channels in the basolateral membrane of bovine nonpigmented ciliary epithelial cells. *Invest Ophthalmol Vis Sci* 36(13): 2706-16.

Edelman, J. L., Sachs, G. and Adorante, J. S. (1994). Ion transport asymmetry and functional coupling in bovine pigmented and nonpigmented ciliary epithelial cells. *Am J Physiol* 266(5 Pt 1): C1210-21.

Eichhorn, M. and Lutjen-Drecoll, E. (1993). Distribution of endothelin-like immunoreactivity in the human ciliary epithelium. *Curr Eye Res* 12(8): 753-7.

Elena, P. P., Fredj-Reygrobellet, D., Moulin, G. and Lapalus, P. (1984). Pharmacological characteristics of beta-adrenergic-sensitive adenylate cyclase in non pigmented and in pigmented cells of bovine ciliary process. *Curr Eye Res* 3(12): 1383-9.

Ellis, D. Z., Nathanson, J. A., Rabe, J. and Sweadner, K. J. (2001). Carbachol and nitric oxide inhibition of Na,K-ATPase activity in bovine ciliary processes. *Invest Ophthalmol Vis Sci* 42(11): 2625-31.

Erb, C., Nau-Staudt, K., Flammer, J. and Nau, W. (2004). Ascorbic acid as a free radical scavenger in porcine and bovine aqueous humour. *Ophthalmic Res* 36(1): 38-42.

Farahbakhsh, N. A. and Cilluffo, M. C. (1994). Synergistic effect of adrenergic and muscarinic receptor activation on $[Ca^{2+}]_i$ in rabbit ciliary body epithelium. *J Physiol* 477 (Pt 2): 215-21.

Farahbakhsh, N. A. and Cilluffo, M. C. (1997). Synergistic increase in Ca^{2+} produced by A1 adenosine and muscarinic receptor activation via a pertussis-toxin-sensitive pathway in epithelial cells of the rabbit ciliary body. *Exp Eye Res* 64(2): 173-9.

Farahbakhsh, N. A. and Cilluffo, M. C. (2002). P2 purinergic receptor-coupled signaling in the rabbit ciliary body epithelium. *Invest Ophthalmol Vis Sci* 43(7): 2317-25.

Flugel, C. and Lutjen-Drecoll, E. (1988). Presence and distribution of Na^+/K^+-ATPase in the ciliary epithelium of the rabbit. *Histochemistry* 88(3-6): 613-21.

Freddo, T. F. (2001). Shifting the paradigm of the blood-aqueous barrier. *Exp Eye Res* 73(5): 581-92.

Freddo, T. F., Bartels, S. P., Barsotti, M. F. and Kamm, R. D. (1990). The source of proteins in the aqueous humor of the normal rabbit. *Invest Ophthalmol Vis Sci* 31(1): 125-37.

Friedenwald, J. S. (1949). The formation of the intraocular fluid. *Am J Ophthalmol* 32 Pt. 2(6): 9-27.

Gaasterland, D. E., Pederson, J. E., MacLellan, H. M. and Reddy, V. N. (1979). Rhesus monkey aqueous humor composition and a primate ocular perfusate. *Invest Ophthalmol Vis Sci* 18(11): 1139-50.

Garg, L. C. and Oppelt, W. W. (1970). The effect of ouabain and acetazolamide on transport of sodium and chloride from plasma to aqueous humor. *J Pharmacol Exp Ther* 175(2): 237-47.

Gehr, B. T., Weiss, C. and Porzsolt, F. (2006). The fading of reported effectiveness. A meta-analysis of randomised controlled trials. *BMC Med Res Methodol* 6: 25.

Gerometta, R. M., Malgor, L. A., Vilalta, E., Leiva, J. and Candia, O. A. (2005). Cl^- concentrations of bovine, porcine and ovine aqueous humor are higher than in plasma. *Exp Eye Res* 80(3): 307-12.

Ghosh, S., Freitag, A. C., Martin-Vasallo, P. and Coca-Prados, M. (1990). Cellular distribution and differential gene expression of the three alpha subunit isoforms of the Na,K-ATPase in the ocular ciliary epithelium. *J Biol Chem* 265(5): 2935-40.

Ghosh, S., Hernando, N., Martin-Alonso, J. M., Martin-Vasallo, P. and Coca-Prados, M. (1991). Expression of multiple Na^+,K^+-ATPase genes reveals a gradient of isoforms along the nonpigmented ciliary epithelium: functional implications in aqueous humor secretion. *J Cell Physiol* 149(2): 184-94.

Giovanelli, A., Fucile, S., Mead, A., Mattei, E., Eusebi, F. and Sears, M. (1996). Spontaneous and evoked oscillations of cytosolic calcium in the freshly prepared ciliary epithelial bilayer of the rabbit eye. *Biochem Biophys Res Commun* 220(2): 472-7.

Glynn, I. M. (2002). A hundred years of sodium pumping. *Annu Rev Physiol* 64: 1-18.

Gonzalez-Mariscal, L., Tapia, R. and Chamorro, D. (2008). Crosstalk of tight junction components with signaling pathways. *Biochim Biophys Acta* 1778(3): 729-56.

Green, K., Bountra, C., Georgiou, P. and House, C. R. (1985). An electrophysiologic study of rabbit ciliary epithelium. *Invest Ophthalmol Vis Sci* 26(3): 371-81.

Green, K. and Pederson, J. E. (1972). Contribution of secretion and filtration to aqueous humor formation. *Am J Physiol* 222(5): 1218-26.

Gregory, D., Sears, M., Bausher, L., Mishima, H. and Mead, A. (1981). Intraocular pressure and aqueous flow are decreased by cholera toxin. *Invest Ophthalmol Vis Sci* 20(3): 371-81.

Hamann, S., Zeuthen, T., La Cour, M., Nagelhus, E. A., Ottersen, O. P., Agre, P. and Nielsen, S. (1998). Aquaporins in complex tissues: distribution of aquaporins 1-5 in human and rat eye. *Am J Physiol* 274(5 Pt 1): C1332-45.

Han, Z. and Patil, R. V. (2000). Protein kinase A-dependent phosphorylation of aquaporin-1. *Biochem Biophys Res Commun* 273(1): 328-32.

Han, Z. B., Yang, J. B., Wax, M. B. and Patil, R. V. (2000). Molecular identification of functional water channel protein in cultured human nonpigmented ciliary epithelial cells. *Curr Eye Res* 20(3): 242-7.

Hasegawa, H., Lian, S. C., Finkbeiner, W. E. and Verkman, A. S. (1994). Extrarenal tissue distribution of CHIP28 water channels by in situ hybridization and antibody staining. *Am J Physiol* 266(4 Pt 1): C893-903.

Helbig, H., Korbmacher, C., Berweck, S., Kuhner, D. and Wiederholt, M. (1988a). Kinetic properties of Na^+/H^+ exchange in cultured bovine pigmented ciliary epithelial cells. *Pflugers Arch* 412(1-2): 80-5.

Helbig, H., Korbmacher, C., Erb, C., Nawrath, M., Knuuttila, K. G., Wistrand, P. and Wiederholt, M. (1989a). Coupling of ^{22}Na and ^{36}Cl uptake in cultured pigmented ciliary epithelial cells: a proposed role for the isoenzymes of carbonic anhydrase. *Curr Eye Res* 8(11): 1111-9.

Helbig, H., Korbmacher, C., Kuhner, D., Berweck, S. and Wiederholt, M. (1988b). Characterization of Cl^-/HCO_3^- exchange in cultured bovine pigmented ciliary epithelium. *Exp Eye Res* 47(4): 515-23.

Helbig, H., Korbmacher, C., Stumpff, F., Coca-Prados, M. and Wiederholt, M. (1989b). Role of HCO_3^- in regulation of cytoplasmic pH in ciliary epithelial cells. *Am J Physiol* 257(4 Pt 1): C696-705.

Helbig, H., Korbmacher, C. and Wiederholt, M. (1987). K^+-conductance and electrogenic Na^+/K^+ transport of cultured bovine pigmented ciliary epithelium. *J Membr Biol* 99(3): 173-86.

Helbig, H., Korbmacher, C., Wohlfarth, J., Coca-Prados, M. and Wiederholt, M. (1989c). Electrical membrane properties of a cell clone derived from human nonpigmented ciliary epithelium. *Invest Ophthalmol Vis Sci* 30(5): 882-9.

Helbig, H., Korbmacher, C., Wohlfarth, J., Coroneo, M. T., Lindschau, C., Quass, P., Haller, H., Coca-Prados, M. and Wiederholt, M. (1989d). Effect of acetylcholine on membrane potential of cultured human nonpigmented ciliary epithelial cells. *Invest Ophthalmol Vis Sci* 30(5): 890-6.

Hidaka, H. and Kobayashi, R. (1992). Pharmacology of protein kinase inhibitors. *Annu Rev Pharmacol Toxicol* 32: 377-97.

Hidaka, H., Watanabe, M. and Kobayashi, R. (1991). Properties and use of H-series compounds as protein kinase inhibitors. *Methods Enzymol* 201: 328-39.

Hirata, K., Nathanson, M. H., Burgstahler, A. D., Okazaki, K., Mattei, E. and Sears, M. L. (1999). Relationship between inositol 1,4,5-trisphosphate receptor isoforms and subcellular Ca^{2+} signaling patterns in nonpigmented ciliary epithelia. *Invest Ophthalmol Vis Sci* 40(9): 2046-53.

Hirata, K., Nathanson, M. H. and Sears, M. L. (1998). Novel paracrine signaling mechanism in the ocular ciliary epithelium. *Proc Natl Acad Sci U S A* 95(14): 8381-6.

Hobbs, A. J., Higgs, A. and Moncada, S. (1999). Inhibition of nitric oxide synthase as a potential therapeutic target. *Annu Rev Pharmacol Toxicol* 39: 191-220.

Hochgesand, D. H., Dunn, J. J. and Crook, R. B. (2001). Catecholaminergic regulation of Na-K-Cl cotransport in pigmented ciliary epithelium: differences between PE and NPE. *Exp Eye Res* 72(1): 1-12.

Holland, M. G. (1970). Chloride ion transport in the isolated ciliary body. II. Ion substitution experiments. *Invest Ophthalmol* 9(1): 30-41.

Holland, M. G. and Gipson, C. C. (1970). Chloride ion transport in the isolated ciliary body. *Invest Ophthalmol* 9(1): 20-9.

Holz, G. G., Kang, G., Harbeck, M., Roe, M. W. and Chepurny, O. G. (2006). Cell physiology of cAMP sensor Epac. *J Physiol* 577(Pt 1): 5-15.

Horio, B., Sears, M., Mead, A., Matsui, H. and Bausher, L. (1996). Regulation and bioelectrical effects of cyclic adenosine monophosphate production in the ciliary epithelial bilayer. *Invest Ophthalmol Vis Sci* 37(4): 607-12.

Hou, Y., Wu, Q. and Delamere, N. A. (2001). H^+-ATPase-mediated cytoplasmic pH-responses associated with elevation of cytoplasmic calcium in cultured rabbit nonpigmented ciliary epithelium. *J Membr Biol* 182(1): 81-90.

Howard, M., Sen, H. A., Capoor, S., Herfel, R., Crooks, P. A. and Jacobson, M. K. (1998). Measurement of adenosine concentration in aqueous and vitreous. *Invest Ophthalmol Vis Sci* 39(10): 1942-6.

Iizuka, S., Kishida, K., Tsuboi, S., Emi, K. and Manabe, R. (1984). Electrical characteristics of the isolated dog ciliary body. *Curr Eye Res* 3(3): 417-21.

Inoue, A., Yanagisawa, M., Kimura, S., Kasuya, Y., Miyauchi, T., Goto, K. and Masaki, T. (1989). The human endothelin family: three structurally and pharmacologically distinct isopeptides predicted by three separate genes. *Proc Natl Acad Sci U S A* 86(8): 2863-7.

Jacob, T. J. (1991). Two outward K^+ currents in bovine pigmented ciliary epithelial cells: IK(Ca) and IK(V). *Am J Physiol* 261(6 Pt 1): C1055-62.

Jacob, T. J. and Civan, M. M. (1996). Role of ion channels in aqueous humor formation. *Am J Physiol* 271(3 Pt 1): C703-20.

Kawasaki, M., Uchida, S., Monkawa, T., Miyawaki, A., Mikoshiba, K., Marumo, F. and Sasaki, S. (1994). Cloning and expression of a protein kinase C-regulated chloride channel abundantly expressed in rat brain neuronal cells. *Neuron* 12(3): 597-604.

Kishida, K., Sasabe, T., Iizuka, S., Manabe, R. and Otori, T. (1982). Sodium and chloride transport across the isolated rabbit ciliary body. *Curr Eye Res* 2(3): 149-52.

Kishida, K., Sasabe, T., Manabe, R. and Otori, T. (1981). Electric characteristics of the isolated rabbit ciliary body. *Jpn J Ophthalmol* 25: 407-416.

Kodama, T., Reddy, V. N. and Macri, F. J. (1985). Pharmacological study on the effects of some ocular hypotensive drugs on aqueous humor formation in the arterially perfused enucleated rabbit eye. *Ophthalmic Res* 17(2): 120-4.

Kolodny, N. H., Freddo, T. F., Lawrence, B. A., Suarez, C. and Bartels, S. P. (1996). Contrast-enhanced magnetic resonance imaging confirmation of an anterior protein pathway in normal rabbit eyes. *Invest Ophthalmol Vis Sci* 37(8): 1602-7.

Kong, C. W., Li, K. K. and To, C. H. (2006). Chloride secretion by porcine ciliary epithelium: new insight into species similarities and differences in aqueous humor formation. *Invest Ophthalmol Vis Sci* 47(12): 5428-36.

Kong, M. C. W., Tse, D. Y. and To, C. H. (2005). Regulation of Nitric Oxide (NO) On the Chloride (Cl^-) Secretion Across the Porcine Ciliary Body Epithelium (CBE) via Both cGMP-Dependent and -Independent Pathway. *Invest Ophthalmol Vis Sci* 46(5): E-Abstract 2414.

Kotikoski, H., Alajuuma, P., Moilanen, E., Salmenpera, P., Oksala, O., Laippala, P. and Vapaatalo, H. (2002). Comparison of nitric oxide donors in lowering intraocular pressure in rabbits: role of cyclic GMP. *J Ocul Pharmacol Ther* 18(1): 11-23.

Kotikoski, H., Kankuri, E. and Vapaatalo, H. (2003a). Incubation of porcine iris-ciliary bodies to study the mechanisms by which nitric oxide donors lower intraocular pressure. *Med Sci Monit* 9(1): BR1-7.

Kotikoski, H., Vapaatalo, H. and Oksala, O. (2003b). Nitric oxide and cyclic GMP enhance aqueous humor outflow facility in rabbits. *Curr Eye Res* 26(2): 119-23.

Krishnamoorthy, R. R., Prasanna, G., Dauphin, R., Hulet, C., Agarwal, N. and Yorio, T. (2003). Regulation of Na,K-ATPase expression by endothelin-1 in transformed human ciliary non-pigmented epithelial (HNPE) cells. *J Ocul Pharmacol Ther* 19(5): 465-81.

Krupin, T. and Civan, M. M. (1996). Physiologic basis of aqueous humor formation. *The Glaucomas: Basic Sciences, vol 1*. R. Ritch, M. B. Shields and T. Krupin. St. Louis, Mosby**:** 251-280.

Krupin, T., Reinach, P. S., Candia, O. A. and Podos, S. M. (1984). Transepithelial electrical measurements on the isolated rabbit iris-ciliary body. *Exp Eye Res* 38(2): 115-23.

Kvanta, A., Seregard, S., Sejersen, S., Kull, B. and Fredholm, B. B. (1997). Localization of adenosine receptor messenger RNAs in the rat eye. *Exp Eye Res* 65(5): 595-602.

Larsson, L. I. and Alm, A. (1998). Aqueous humor flow in human eyes treated with dorzolamide and different doses of acetazolamide. *Arch Ophthalmol* 116(1): 19-24.

Lee, C. H., Reisine, T. D. and Wax, M. B. (1989). Alterations of intracellular calcium in human non-pigmented ciliary epithelial cells of the eye. *Exp Eye Res* 48(6): 733-43.

Lee, P. Y., Podos, S. M., Mittag, T. and Severin, C. (1984). Effect of topically applied forskolin on aqueous humor dynamics in cynomolgus monkey. *Invest Ophthalmol Vis Sci* 25(10): 1206-9.

Lepple-Wienhues, A., Becker, M., Stahl, F., Berweck, S., Hensen, J., Noske, W., Eichhorn, M. and Wiederholt, M. (1992). Endothelin-like immunoreactivity in the aqueous humour and in conditioned medium from cultured ciliary epithelial cells. *Curr Eye Res* 11(11): 1041-6.

Li, X., Alvarez, B., Casey, J. R., Reithmeier, R. A. and Fliegel, L. (2002). Carbonic anhydrase II binds to and enhances activity of the Na^+/H^+ exchanger. *J Biol Chem* 277(39): 36085-91.

Liu, R., Flammer, J. and Haefliger, I. O. (1999). Isoproterenol, forskolin, and cAMP-induced nitric oxide production in pig ciliary processes. *Invest Ophthalmol Vis Sci* 40(8): 1833-7.

Liu, R., Flammer, J. and Haefliger, I. O. (2002). Forskolin upregulation of NOS I protein expression in porcine ciliary processes: a new aspect of aqueous humor regulation. *Klin Monbl Augenheilkd* 219(4): 281-3.

Lutjen-Drecoll, E. and Lonnerholm, G. (1981). Carbonic anhydrase distribution in the rabbit eye by light and electron microscopy. *Invest Ophthalmol Vis Sci* 21(6): 782-97.

Lutjen-Drecoll, E., Lonnerholm, G. and Eichhorn, M. (1983). Carbonic anhydrase distribution in the human and monkey eye by light and electron microscopy. *Graefes Arch Clin Exp Ophthalmol* 220(6): 285-91.

MacCumber, M. W., Jampel, H. D. and Snyder, S. H. (1991). Ocular effects of the endothelins. Abundant peptides in the eye. *Arch Ophthalmol* 109(5): 705-9.

Madara, J. L. (1998). Regulation of the movement of solutes across tight junctions. *Annu Rev Physiol* 60: 143-59.

Maren, T. H. (1976). The rates of movement of Na^+, Cl^-, and HCO_3^- from plasma to posterior chamber: effect of acetazolamide and relation to the treatment of glaucoma. *Invest Ophthalmol* 15(5): 356-64.

Maren, T. H. (1977). Ion secretion into the posterior aqueous humor of dogs and monkeys. *Exp Eye Res* 25 Suppl: 245-7.

Maren, T. H. (1997). Sulfonamides and secretion of aqueous humor. *J Exp Zool* 279(5): 490-7.

Marquis, R. E. and Whitson, J. T. (2005). Management of glaucoma: focus on pharmacological therapy. *Drugs Aging* 22(1): 1-21.

Matsui, H., Murakami, M., Wynns, G. C., Conroy, C. W., Mead, A., Maren, T. H. and Sears, M. L. (1996). Membrane carbonic anhydrase (IV) and ciliary epithelium. Carbonic anhydrase activity is present in the basolateral membranes of the non-pigmented ciliary epithelium of rabbit eyes. *Exp Eye Res* 62(4): 409-17.

McLaughlin, C. W., Peart, D., Purves, R. D., Carre, D. A., Macknight, A. D. and Civan, M. M. (1998). Effects of HCO_3^- on cell composition of rabbit ciliary epithelium: a new model for aqueous humor secretion. *Invest Ophthalmol Vis Sci* 39(9): 1631-41.

McLaughlin, C. W., Zellhuber-McMillan, S., Macknight, A. D. and Civan, M. M. (2004). Electron microprobe analysis of ouabain-exposed ciliary epithelium: PE-NPE cell couplets form the functional units. *Am J Physiol Cell Physiol* 286(6): C1376-89.

Mead, A., Sears, J. and Sears, M. (1996). Transepithelial transport of ascorbic acid by the isolated intact ciliary epithelial bilayer of the rabbit eye. *J Ocul Pharmacol Ther* 12(3): 253-8.

Meyer, P., Champion, C., Schlotzer-Schrehardt, U., Flammer, J. and Haefliger, I. O. (1999). Localization of nitric oxide synthase isoforms in porcine ocular tissues. *Curr Eye Res* 18(5): 375-80.

Millar, J. C., Shahidullah, M. and Wilson, W. S. (2001). Intraocular pressure and vascular effects of sodium azide in bovine perfused eye. *J Ocul Pharmacol Ther* 17(3): 225-34.

Mitchell, C. H., Carre, D. A., McGlinn, A. M., Stone, R. A. and Civan, M. M. (1998). A release mechanism for stored ATP in ocular ciliary epithelial cells. *Proc Natl Acad Sci U S A* 95(12): 7174-8.

Mitchell, C. H. and Civan, M. M. (1997). Effects of uncoupling gap junctions between pairs of bovine NPE-PE ciliary epithelial cells of the eye. *FASEB J*(11): A301.

Mitchell, C. H. and Jacob, T. J. (1996). A nonselective high conductance channel in bovine pigmented ciliary epithelial cells. *J Membr Biol* 150(1): 105-11.

Mitchell, C. H., Peterson-Yantorno, K., Carre, D. A., McGlinn, A. M., Coca-Prados, M., Stone, R. A. and Civan, M. M. (1999). A_3 adenosine receptors regulate Cl^- channels of nonpigmented ciliary epithelial cells. *Am J Physiol* 276(3 Pt 1): C659-66.

Mitchell, C. H., Wang, L. and Jacob, T. J. (1997). A large-conductance chloride channel in pigmented ciliary epithelial cells activated by GTPgammaS. *J Membr Biol* 158(2): 167-75.

Mito, T., Delamere, N. A. and Coca-Prados, M. (1993). Calcium-dependent regulation of cation transport in cultured human nonpigmented ciliary epithelial cells. *Am J Physiol* 264(3 Pt 1): C519-26.

Mittag, T. W., Guo, W. B. and Kobayashi, K. (1993). Bicarbonate-activated adenylyl cyclase in fluid-transporting tissues. *Am J Physiol* 264(6 Pt 2): F1060-4.

Mittag, T. W., Tormay, A. and Podos, S. M. (1987). Vasoactive intestinal peptide and intraocular pressure: adenylate cyclase activation and binding sites for vasoactive intestinal peptide in membranes of ocular ciliary processes. *J Pharmacol Exp Ther* 241(1): 230-5.

Mori, N., Yamada, E. and Sears, M. L. (1991). Immunocytochemical localization of Na/K-ATPase in the isolated ciliary epithelial bilayer of the rabbit. *Arch Histol Cytol* 54(3): 259-65.

Moro, M. A., Russel, R. J., Cellek, S., Lizasoain, I., Su, Y., Darley-Usmar, V. M., Radomski, M. W. and Moncada, S. (1996). cGMP mediates the vascular and platelet actions of nitric oxide: confirmation using an inhibitor of the soluble guanylyl cyclase. *Proc Natl Acad Sci U S A* 93(4): 1480-5.

Muther, T. F. and Friedland, B. R. (1980). Autoradiographic localization of carbonic anhydrase in the rabbit ciliary body. *J Histochem Cytochem* 28(10): 1119-24.

Nakai, Y., Dean, W. L., Hou, Y. and Delamere, N. A. (1999). Genistein inhibits the regulation of active sodium-potassium transport by dopaminergic agonists in nonpigmented ciliary epithelium. *Invest Ophthalmol Vis Sci* 40(7): 1460-6.

Nathanson, J. A. (1980). Adrenergic regulation of intraocular pressure: identification of beta 2-adrenergic-stimulated adenylate cyclase in ciliary process epithelium. *Proc Natl Acad Sci U S A* 77(12): 7420-4.

Nathanson, J. A. (1981). Human ciliary process adrenergic receptor: pharmacological characterization. *Invest Ophthalmol Vis Sci* 21(6): 798-804.

Ni, Y., Wu, R., Xu, W., Maecke, H., Flammer, J. and Haefliger, I. O. (2006). Effect of cAMP on porcine ciliary transepithelial short-circuit current, sodium transport, and chloride transport. *Invest Ophthalmol Vis Sci* 47(5): 2065-74.

Nielsen, S., Smith, B. L., Christensen, E. I. and Agre, P. (1993). Distribution of the aquaporin CHIP in secretory and resorptive epithelia and capillary endothelia. *Proc Natl Acad Sci U S A* 90(15): 7275-9.

Nilsson, S. F., Maepea, O., Samuelsson, M. and Bill, A. (1990). Effects of timolol on terbutaline- and VIP-stimulated aqueous humor flow in the cynomolgus monkey. *Curr Eye Res* 9(9): 863-72.

Noske, W., Hensen, J. and Wiederholt, M. (1997). Endothelin-like immunoreactivity in aqueous humor of patients with primary open-angle glaucoma and cataract. *Graefes Arch Clin Exp Ophthalmol* 235(9): 551-2.

Oh, J., Krupin, T., Tang, L. Q., Sveen, J. and Lahlum, R. A. (1994). Dye coupling of rabbit ciliary epithelial cells in vitro. *Invest Ophthalmol Vis Sci* 35(5): 2509-14.

Ohuchi, T., Yoshimura, N., Tanihara, H., Kuriyama, S., Ito, S. and Honda, Y. (1992). Ca^{2+} mobilization in nontransformed ciliary nonpigmented epithelial cells. *Invest Ophthalmol Vis Sci* 33(5): 1696-705.

Oppelt, W. W. and White, E. D., Jr. (1968). Effect of ouabain on aqueous humor formation rate in cats. *Invest Ophthalmol* 7(3): 328-33.

Pang, I. H. and Yorio, T. (1997). Ocular actions of endothelins. *Proc Soc Exp Biol Med* 215(1): 21-34.

Patil, R. V., Han, Z. and Wax, M. B. (1997a). Regulation of water channel activity of aquaporin 1 by arginine vasopressin and atrial natriuretic peptide. *Biochem Biophys Res Commun* 238(2): 392-6.

Patil, R. V., Han, Z., Yiming, M., Yang, J., Iserovich, P., Wax, M. B. and Fischbarg, J. (2001). Fluid transport by human nonpigmented ciliary epithelial layers in culture: a homeostatic role for aquaporin-1. *Am J Physiol Cell Physiol* 281(4): C1139-45.

Patil, R. V., Saito, I., Yang, X. and Wax, M. B. (1997b). Expression of aquaporins in the rat ocular tissue. *Exp Eye Res* 64(2): 203-9.

Pesin, S. R. and Candia, O. A. (1982). Na^+ and Cl^- fluxes, and effects of pharmacological agents on the short-circuit current of the isolated rabbit iris-ciliary body. *Curr Eye Res* 2(12): 815-27.

Polska, E., Ehrlich, P., Luksch, A., Fuchsjager-Mayrl, G. and Schmetterer, L. (2003). Effects of adenosine on intraocular pressure, optic nerve head blood flow, and choroidal blood flow in healthy humans. *Invest Ophthalmol Vis Sci* 44(7): 3110-4.

Prasanna, G., Dibas, A., Brown, K. and Yorio, T. (1998a). Activation of protein kinase C by tumor necrosis factor-alpha in human non-pigmented ciliary epithelium. *J Ocul Pharmacol Ther* 14(5): 401-12.

Prasanna, G., Dibas, A., Finkley, A. and Yorio, T. (1999). Identification of endothelin converting enzyme-1 in human non-pigmented ciliary epithelial cells. *Exp Eye Res* 69(2): 175-83.

Prasanna, G., Dibas, A., Hulet, C. and Yorio, T. (2001). Inhibition of Na^+/K^+-ATPase by endothelin-1 in human nonpigmented ciliary epithelial cells. *J Pharmacol Exp Ther* 296(3): 966-71.

Prasanna, G., Dibas, A., Tao, W., White, K. and Yorio, T. (1998b). Regulation of endothelin-1 in human non-pigmented ciliary epithelial cells by tumor necrosis factor-alpha. *Exp Eye Res* 66(1): 9-18.

Prasanna, G., Hulet, C., Desai, D., Krishnamoorthy, R. R., Narayan, S., Brun, A. M., Suburo, A. M. and Yorio, T. (2005). Effect of elevated intraocular pressure on endothelin-1 in a rat model of glaucoma. *Pharmacol Res* 51(1): 41-50.

Quigley, H. A. (1996). Number of people with glaucoma worldwide. *Br J Ophthalmol* 80(5): 389-93.

Raviola, G. (1974). Effects of paracentesis on the blood-aqueous barrier: an electron microscope study on Macaca mulatta using horseradish peroxidase as a tracer. *Invest Ophthalmol* 13(11): 828-58.

Raviola, G. and Raviola, E. (1978). Intercellular junctions in the ciliary epithelium. *Invest Ophthalmol Vis Sci* 17(10): 958-81.

Reiss, G. R., Werness, P. G., Zollman, P. E. and Brubaker, R. F. (1986). Ascorbic acid levels in the aqueous humor of nocturnal and diurnal mammals. *Arch Ophthalmol* 104(5): 753-5.

Reitsamer, H. A. and Kiel, J. W. (2003). Relationship between ciliary blood flow and aqueous production in rabbits. *Invest Ophthalmol Vis Sci* 44(9): 3967-71.

Riese, K., Beyer, A. T., Lui, G. M. and Crook, R. B. (1998). Dopamine D1 stimulation of Na^+,K^+,Cl^- cotransport in human NPE cells: effects of multiple hormones. *Invest Ophthalmol Vis Sci* 39(8): 1444-52.

Riley, M. V. and Kishida, K. (1986). ATPases of ciliary epithelium: cellular and subcellular distribution and probable role in secretion of aqueous humor. *Exp Eye Res* 42(6): 559-68.

Ringvold, A. (1995). Quenching of UV-induced fluorescence by ascorbic acid in the aqueous humour. *Acta Ophthalmol Scand* 73(6): 529-33.

Ringvold, A. (1996). The significance of ascorbate in the aqueous humour protection against UV-A and UV-B. *Exp Eye Res* 62(3): 261-4.

Ringvold, A., Anderssen, E. and Kjonniksen, I. (2000). Distribution of ascorbate in the anterior bovine eye. *Invest Ophthalmol Vis Sci* 41(1): 20-3.

Rose, R. C., Richer, S. P. and Bode, A. M. (1998). Ocular oxidants and antioxidant protection. *Proc Soc Exp Biol Med* 217(4): 397-407.

Ryan, J. S., Tao, Q. P. and Kelly, M. E. (1998). Adrenergic regulation of calcium-activated potassium current in cultured rabbit pigmented ciliary epithelial cells. *J Physiol* 511 (Pt 1): 145-57.

Saito, Y. and Watanabe, T. (1979). Relationship between short-circuit current and unidirectional fluxes of Na and Cl across the ciliary epithelium of the toad: demonstration of active Cl transport. *Exp Eye Res* 28(1): 71-9.

Sanchez-Torres, J., Huang, W., Civan, M. M. and Coca-Prados, M. (1999). Effects of hypotonic swelling on the cellular distribution and expression of pI_{Cln} in human nonpigmented ciliary epithelial cells. *Curr Eye Res* 18(6): 408-16.

Schneeberger, E. E. and Lynch, R. D. (2004). The tight junction: a multifunctional complex. *Am J Physiol Cell Physiol* 286(6): C1213-28.

Schutte, M., Diadori, A., Wang, C. and Wolosin, J. M. (1996). Comparative adrenocholinergic control of intracellular Ca^{2+} in the layers of the ciliary body epithelium. *Invest Ophthalmol Vis Sci* 37(1): 212-20.

Schutte, M. and Wolosin, J. M. (1996). Ca^{2+} mobilization and interlayer signal transfer in the heterocellular bilayered epithelium of the rabbit ciliary body. *J Physiol* 496 (Pt 1): 25-37.

Schwartz, G. F. (2005). Compliance and persistency in glaucoma follow-up treatment. *Curr Opin Ophthalmol* 16(2): 114-21.

Seamon, K. B. and Daly, J. W. (1981). Forskolin: a unique diterpene activator of cyclic AMP-generating systems. *J Cyclic Nucleotide Res* 7(4): 201-24.

Sears, J., Nakano, T. and Sears, M. (1998). Adrenergic-mediated connexin43 phosphorylation in the ocular ciliary epithelium. *Curr Eye Res* 17(1): 104-7.

Sears, M. L., Yamada, E., Cummins, D., Mori, N., Mead, A. and Murakami, M. (1991). The isolated ciliary bilayer is useful for studies of aqueous humor formation. *Trans Am Ophthalmol Soc* 89: 131-52; discussion 152-4.

Shahidullah, M. and Delamere, N. A. (2006). NO donors inhibit Na,K-ATPase activity by a protein kinase G-dependent mechanism in the nonpigmented ciliary epithelium of the porcine eye. *Br J Pharmacol* 148(6): 871-80.

Shahidullah, M., Tamiya, S. and Delamere, N. A. (2007). Primary culture of porcine nonpigmented ciliary epithelium. *Curr Eye Res* 32(6): 511-22.

Shahidullah, M., To, C. H., Pelis, R. M. and Delamere, N. A. (2009). Studies on bicarbonate transporters and carbonic anhydrase in porcine nonpigmented ciliary epithelium. *Invest Ophthalmol Vis Sci* 50(4): 1791-800.

Shahidullah, M. and Wilson, W. S. (1997). Mobilisation of intracellular calcium by $P2Y_2$ receptors in cultured, non-transformed bovine ciliary epithelial cells. *Curr Eye Res* 16(10): 1006-16.

Shahidullah, M., Wilson, W. S. and Millar, C. (1995). Effects of timolol, terbutaline and forskolin on IOP, aqueous humour formation and ciliary cyclic AMP levels in the bovine eye. *Curr Eye Res* 14(7): 519-28.

Shahidullah, M., Wilson, W. S., Yap, M. and To, C. H. (2003). Effects of ion transport and channel-blocking drugs on aqueous humor formation in isolated bovine eye. *Invest Ophthalmol Vis Sci* 44(3): 1185-91.

Shahidullah, M., Yap, M. and To, C. H. (2005). Cyclic GMP, sodium nitroprusside and sodium azide reduce aqueous humour formation in the isolated arterially perfused pig eye. *Br J Pharmacol* 145(1): 84-92.

Shi, C., Barnes, S., Coca-Prados, M. and Kelly, M. E. (2002). Protein tyrosine kinase and protein phosphatase signaling pathways regulate volume-sensitive chloride currents in a nonpigmented ciliary epithelial cell line. *Invest Ophthalmol Vis Sci* 43(5): 1525-32.

Shi, C., Szczesniak, A., Mao, L., Jollimore, C., Coca-Prados, M., Hung, O. and Kelly, M. E. (2003). A3 adenosine and CB1 receptors activate a PKC-sensitive Cl^- current in human nonpigmented ciliary epithelial cells *via* a Gβγ-coupled MAPK signaling pathway. *Br J Pharmacol* 139(3): 475-86.

Shi, X. P., Zamudio, A. C., Candia, O. A. and Wolosin, J. M. (1996). Adreno-cholinergic modulation of junctional communications between the pigmented and nonpigmented layers of the ciliary body epithelium. *Invest Ophthalmol Vis Sci* 37(6): 1037-46.

Smith, R. S. (1973). Fine structure and function of ocular tissues. The ciliary body. *Int Ophthalmol Clin* 13(3): 157-67.

Smith, R. S. and Rudt, L. A. (1973). Ultrastructural studies of the blood-aqueous barrier. 2. The barrier to horseradish peroxidase in primates. *Am J Ophthalmol* 76(6): 937-47.

Stamer, W. D., Snyder, R. W., Smith, B. L., Agre, P. and Regan, J. W. (1994). Localization of aquaporin CHIP in the human eye: implications in the pathogenesis of glaucoma and other disorders of ocular fluid balance. *Invest Ophthalmol Vis Sci* 35(11): 3867-72.

Stelling, J. W. and Jacob, T. J. (1996). Transient activation of K^+ channels by carbachol in bovine pigmented ciliary body epithelial cells. *Am J Physiol* 271(1 Pt 1): C203-9.

Stelling, J. W. and Jacob, T. J. (1997). Functional coupling in bovine ciliary epithelial cells is modulated by carbachol. *Am J Physiol* 273(6 Pt 1): C1876-81.

Sterling, D., Reithmeier, R. A. and Casey, J. R. (2001). A transport metabolon. Functional interaction of carbonic anhydrase II and chloride/bicarbonate exchangers. *J Biol Chem* 276(51): 47886-94.

Strauss, O., Stahl, F. and Wiederholt, M. (1992). Elevation of cytosolic free calcium in cultured ciliary epithelial cells by histamine: effects of verapamil and staurosporine. *J Ocul Pharmacol* 8(4): 359-66.

Suzuki, Y., Nakano, T. and Sears, M. (1997). Calcium signals from intact rabbit ciliary epithelium observed with confocal microscopy. *Curr Eye Res* 16(2): 166-75.

Taniguchi, T., Haque, M. S., Sugiyama, K., Okada, K., Nakai, Y. and Kitazawa, Y. (1996). Effects of endothelin A and B receptors on aqueous humor dynamics in the rabbit eye. *J Ocul Pharmacol Ther* 12(2): 123-30.

Taniguchi, T., Okada, K., Haque, M. S., Sugiyama, K. and Kitazawa, Y. (1994). Effects of endothelin-1 on intraocular pressure and aqueous humor dynamics in the rabbit eye. *Curr Eye Res* 13(6): 461-4.

Tao, W., Prasanna, G., Dimitrijevich, S. and Yorio, T. (1998). Endothelin receptor A is expressed and mediates the $[Ca^{2+}]_i$ mobilization of cells in human ciliary smooth muscle, ciliary nonpigmented epithelium, and trabecular meshwork. *Curr Eye Res* 17(1): 31-8.

The AIGS Investigators (2000). The Advanced Glaucoma Intervention Study (AGIS): 7. The relationship between control of intraocular pressure and visual field deterioration.The AGIS Investigators. *Am J Ophthalmol* 130(4): 429-40.

To, C. H., Do, C. W., Zamudio, A. C. and Candia, O. A. (2001). Model of ionic transport for bovine ciliary epithelium: effects of acetazolamide and HCO. *Am J Physiol Cell Physiol* 280(6): C1521-30.

To, C. H., Kong, C. W., Chan, C. Y., Shahidullah, M. and Do, C. W. (2002). The mechanism of aqueous humour formation. *Clin Exp Optom* 85(6): 335-49.

To, C. H., Mok, K. H., Do, C. W., Lee, K. L. and Millodot, M. (1998a). Chloride and sodium transport across bovine ciliary body/epithelium (CBE). *Curr Eye Res* 17(9): 896-902.

To, C. H., Mok, K. H., Tse, S. K., Siu, W. T., Millodot, M., Lee, K. L. and Hodson, S. (1998b). In vitro bovine ciliary body/epithelium in a small continuously perfused Ussing type chamber. *Cell Struct Funct* 23(5): 247-54.

Ussing, H. H. and Zerahn, K. (1951). Active transport of sodium as the source of electric current in the short-circuited isolated frog skin. *Acta Physiol Scand* 23(2-3): 110-27.

Usukura, J., Fain, G. L. and Bok, D. (1988). [^{3}H]ouabain localization of Na-K ATPase in the epithelium of rabbit ciliary body pars plicata. *Invest Ophthalmol Vis Sci* 29(4): 606-14.

Varma, S. D., Chand, D., Sharma, Y. R., Kuck, J. F., Jr. and Richards, R. D. (1984). Oxidative stress on lens and cataract formation: role of light and oxygen. *Curr Eye Res* 3(1): 35-57.

Varma, S. D., Morris, S. M., Bauer, S. A. and Koppenol, W. H. (1986). In vitro damage to rat lens by xanthine-xanthine oxidase: protection by ascorbate. *Exp Eye Res* 43(6): 1067-76.

Varma, S. D. and Richards, R. D. (1988). Ascorbic acid and the eye lens. *Ophthalmic Res* 20(3): 164-73.

Vessey, J. P., Shi, C., Jollimore, C. A., Stevens, K. T., Coca-Prados, M., Barnes, S. and Kelly, M. E. (2004). Hyposmotic activation of $I_{Cl,swell}$ in rabbit nonpigmented ciliary epithelial cells involves increased ClC-3 trafficking to the plasma membrane. *Biochem Cell Biol* 82(6): 708-18.

Waitzman, M. B. and Jackson, R. T. (1965). Effects of topically administered ouabain on aqueous humor dynamics. *Exp Eye Res* 4(3): 135-45.

Wan, X. L., Chen, S. and Sears, M. (1997). Cloning and functional expression of a swelling-induced chloride conductance regulatory protein, pl_{Cln}, from rabbit ocular ciliary epithelium. *Biochem Biophys Res Commun* 239(3): 692-6.

Wang, G. X., Hatton, W. J., Wang, G. L., Zhong, J., Yamboliev, I., Duan, D. and Hume, J. R. (2003). Functional effects of novel anti-ClC-3 antibodies on native volume-sensitive osmolyte and anion channels in cardiac and smooth muscle cells. *Am J Physiol Heart Circ Physiol* 285(4): H1453-63.

Wang, L., Chen, L. and Jacob, T. J. (2000). The role of ClC-3 in volume-activated chloride currents and volume regulation in bovine epithelial cells demonstrated by antisense inhibition. *J Physiol* 524 Pt 1: 63-75.

Wang, Z., Do, C. W., Avila, M. Y., Peterson-Yantorno, K., Stone, R. A., Gao, Z. G., Joshi, B., Besada, P., Jeong, L. S., Jacobson, K. A. and Civan, M. M. (2010).

Nucleoside-derived antagonists to A3 adenosine receptors lower mouse intraocular pressure and act across species. *Exp Eye Res* 90(1): 146-54.

Wang, Z., Do, C. W., Avila, M. Y., Stone, R. A., Jacobson, K. A. and Civan, M. M. (2007). Barrier qualities of the mouse eye to topically applied drugs. *Exp Eye Res* 85(1): 105-12.

Watanabe, T. and Saito, Y. (1978). Characteristics of ion transport across the isolated ciliary epithelium of the toad as studied by electrical measurements. *Exp Eye Res* 27(2): 215-26.

Wax, M., Sanghavi, D. M., Lee, C. H. and Kapadia, M. (1993). Purinergic receptors in ocular ciliary epithelial cells. *Exp Eye Res* 57(1): 89-95.

Wetzel, R. K. and Sweadner, K. J. (2001). Immunocytochemical localization of NaK-ATPase isoforms in the rat and mouse ocular ciliary epithelium. *Invest Ophthalmol Vis Sci* 42(3): 763-9.

Wiederholt, M., Flugel, C., Lutjen-Drecoll, E. and Zadunaisky, J. A. (1989). Mechanically stripped pigmented and non-pigmented epithelium of the shark ciliary body: morphology and transepithelial electrical properties. *Exp Eye Res* 49(6): 1031-43.

Wiederholt, M., Helbig, H. and Korbmacher, C. (1991). Ion transport across the ciliary epithelium: Lessons from cultured cells and proposed role of the carbonic anhydrase. *Carbonic Anhydrase*. F. Botre', G. Gross and B. T. Storey. New York, VCH**:** 232-44.

Wiederholt, M. and Zadunaisky, J. A. (1986). Membrane potentials and intracellular chloride activity in the ciliary body of the shark. *Pflugers Arch* 407 Suppl 2: S112-5.

Wiederholt, M. and Zadunaisky, J. A. (1987). Effects of ouabain and furosemide on transepithelial electrical parameters of the isolated shark ciliary epithelium. *Invest Ophthalmol Vis Sci* 28(8): 1353-6.

Wistrand, P. J. and Garg, L. C. (1979). Evidence of a high-activity C type of carbonic anhydrase in human ciliary processes. *Invest Ophthalmol Vis Sci* 18(8): 802-6.

Wistrand, P. J., Schenholm, M. and Lonnerholm, G. (1986). Carbonic anhydrase isoenzymes CA I and CA II in the human eye. *Invest Ophthalmol Vis Sci* 27(3): 419-28.

Wollensak, G., Schaefer, H. E. and Ihling, C. (1998). An immunohistochemical study of endothelin-1 in the human eye. *Curr Eye Res* 17(5): 541-5.

Wolosin, J. M., Bonanno, J. A., Hanzel, D. and Machen, T. E. (1991). Bicarbonate transport mechanisms in rabbit ciliary body epithelium. *Exp Eye Res* 52(4): 397-407.

Wolosin, J. M., Candia, O. A., Peterson-Yantorno, K., Civan, M. M. and Shi, X. P. (1997a). Effect of heptanol on the short circuit currents of cornea and ciliary body demonstrates rate limiting role of heterocellular gap junctions in active ciliary body transport. *Exp Eye Res* 64(6): 945-52.

Wolosin, J. M., Chen, M., Gordon, R. E., Stegman, Z. and Butler, G. A. (1993). Separation of the rabbit ciliary body epithelial layers in viable form: identification of differences in bicarbonate transport. *Exp Eye Res* 56(4): 401-9.

Wolosin, J. M., Schutte, M. and Chen, S. (1997b). Connexin distribution in the rabbit and rat ciliary body. A case for heterotypic epithelial gap junctions. *Invest Ophthalmol Vis Sci* 38(2): 341-8.

Wu, Q., Delamere, N. A. and Pierce, W., Jr. (1997). Membrane-associated carbonic anhydrase in cultured rabbit nonpigmented ciliary epithelium. *Invest Ophthalmol Vis Sci* 38(10): 2093-102.

Wu, Q., Pierce, W. M., Jr. and Delamere, N. A. (1998). Cytoplasmic pH responses to carbonic anhydrase inhibitors in cultured rabbit nonpigmented ciliary epithelium. *J Membr Biol* 162(1): 31-8.

Wu, R., Flammer, J. and Haefliger, I. (2003a). Transepithelial short circuit currents in human and porcine isolated ciliary bodies: effect of acetazolamide and epinephrine. *Klin Monatsbl Augenheilkd* 220(3): 156-60.

Wu, R., Flammer, J., Yao, K. and Haefliger, I. O. (2003b). Reduction of nitrite production by endothelin-1 in isolated porcine ciliary processes. *Exp Eye Res* 77(2): 189-93.

Wu, R., Yao, K., Flammer, J. and Haefliger, I. O. (2004). Role of anions in nitric oxide-induced short-circuit current increase in isolated porcine ciliary processes. *Invest Ophthalmol Vis Sci* 45(9): 3213-22.

Xia, S. L., Fain, G. L. and Farahbakhsh, N. A. (1997). Synergistic rise in Ca^{2+} produced by somatostatin and acetylcholine in ciliary body epithelial cells. *Exp Eye Res* 64(4): 627-35.

Yang, F., Kawedia, J. D. and Menon, A. G. (2003). Cyclic AMP regulates aquaporin 5 expression at both transcriptional and post-transcriptional levels through a protein kinase A pathway. *J Biol Chem* 278(34): 32173-80.

Yang, H., Avila, M. Y., Peterson-Yantorno, K., Coca-Prados, M., Stone, R. A., Jacobson, K. A. and Civan, M. M. (2005). The cross-species A_3 adenosine-receptor antagonist MRS 1292 inhibits adenosine-triggered human nonpigmented ciliary epithelial cell fluid release and reduces mouse intraocular pressure. *Curr Eye Res* 30(9): 747-54.

Yantorno, R. E., Carre, D. A., Coca-Prados, M., Krupin, T. and Civan, M. M. (1992). Whole cell patch clamping of ciliary epithelial cells during anisosmotic swelling. *Am J Physiol* 262(2 Pt 1): C501-9.

Yool, A. J., Stamer, W. D. and Regan, J. W. (1996). Forskolin stimulation of water and cation permeability in aquaporin 1 water channels. *Science* 273(5279): 1216-8.

Yorio, T., Krishnamoorthy, R. and Prasanna, G. (2002). Endothelin: is it a contributor to glaucoma pathophysiology? *J Glaucoma* 11(3): 259-70.

Yoshimura, N., Mittag, T. W. and Podos, S. M. (1989). Calcium-dependent phosphorylation of proteins in rabbit ciliary processes. *Invest Ophthalmol Vis Sci* 30(4): 723-30.

Yoshimura, N., Tanabe-Ohuchi, T., Takagi, H. and Honda, Y. (1995). Drug-dependent Ca^{2+} mobilization in organ-cultured rabbit ciliary processes. *Curr Eye Res* 14(8): 629-35.

Zhang, D., Vetrivel, L. and Verkman, A. S. (2002). Aquaporin deletion in mice reduces intraocular pressure and aqueous fluid production. *J Gen Physiol* 119(6): 561-9.

Zhang, J. J. and Jacob, T. J. (1997). Three different Cl^- channels in the bovine ciliary epithelium activated by hypotonic stress. *J Physiol* 499 (Pt 2): 379-89.

Zhang, X., Krishnamoorthy, R. R., Prasanna, G., Narayan, S., Clark, A. and Yorio, T. (2003). Dexamethasone regulates endothelin-1 and endothelin receptors in human non-pigmented ciliary epithelial (HNPE) cells. *Exp Eye Res* 76(3): 261-72.

Zimmerman, T. J., Garg, L. C., Vogh, B. P. and Maren, T. H. (1976). The effect of acetazolamide on the movement of sodium into the posterior chamber of the dog eye. *J Pharmacol Exp Ther* 199(3): 510-7.